

ADVANCED LECTURES 1986

DYNAMICAL PROCESSES

IN

METEOROLOGY

DR G J SHUTTS

PERMISSION TO QUOTE FROM THIS DOCUMENT MUST BE OBTAINED FROM  
THE PRINCIPAL, METEOROLOGICAL OFFICE COLLEGE, SHINFIELD PARK,  
READING, RG2 9AU.



1) Linear models of stationary planetary waves forced by orography and thermal contrast

(a) Quasi-geostrophic theory

By studying the dynamics of large-scale motion systems using linear theory one can effectively regard the weather chart (eg. 500 mb contour height map) as an interference pattern (as in wave optics) formed by the superposition of waves of different dynamical origin. Ultra-long wave motion (wavelengths greater than ~ 6000 km) is particularly amenable to this type of representation since global fields are readily expanded into complete sets of orthogonal functions (eg sines/cosines, Legendre functions and Hough functions). The linear approach ignores interactions between waves or between waves and zonally-averaged flow and so must be regarded as a gross approximation. Nevertheless, linearized solutions reveal much about the wave character of dynamical systems and provide a dynamically consistent model against which real data can be interpreted.

We begin by considering the Rossby wave as a three-dimensional motion system capable of transmitting energy and momentum over great distances in the atmosphere.

The quasi-geostrophic vorticity equation on a mid-latitude beta-plane may be written as:

$$\frac{D\zeta_g}{Dt_H} + \beta v_g = \frac{f_0}{\rho_0} \frac{\partial}{\partial z} (\rho_0 w) \quad - (1)$$



where  $\zeta_g$  is the vertical component of the geostrophic vorticity vector,  $\beta$  is the meridional gradient of the Coriolis parameter,  $\rho_0(z)$  is the basic state density field and  $W$  is the vertical velocity. Also, the substantial derivative  $\frac{D}{Dt_H}$  is given by:

$$\frac{D}{Dt_H} = \frac{\partial}{\partial t} + u_g \frac{\partial}{\partial x} + v_g \frac{\partial}{\partial y}$$

where  $(u_g, v_g)$  is the geostrophic velocity vector. Note, furthermore that the geostrophic wind and vorticity are related to the pressure field by:

$$\left. \begin{aligned} (u_g, v_g) &= \frac{1}{f_0} \left( -\frac{\partial}{\partial y} \left( \frac{P'}{\rho_0} \right), \frac{\partial}{\partial x} \left( \frac{P'}{\rho_0} \right) \right) \\ \text{and } \zeta_g &= \nabla_H^2 \left( \frac{P'}{\rho_0 f_0} \right) = \left( \frac{\partial^2}{\partial x^2} + \frac{\partial^2}{\partial y^2} \right) \frac{P'}{\rho_0 f_0} \end{aligned} \right\} \quad (2)$$

The geostrophic wind is approximated by its non-divergent, f-plane equivalent (based on  $f_0$ ) in quasi-geostrophic theory.

Equation (1) tells us that the relative vorticity  $\zeta_g$  can be changed following the geostrophic wind by meridional advection ( $\beta v_g$  term) and by the stretching of planetary vorticity.

The thermodynamic equation may be expressed as:

$$\frac{D}{Dt_H} \left( \frac{\theta'}{\theta_0} \right) + wB = S \quad - (3)$$



where  $\theta'$  is the perturbation of the potential temperature from its horizontally stratified basic state  $\theta_0(z)$ ,  $B$  is the static stability,  $\frac{1}{\theta_0} \frac{d\theta_0}{dz}$  and  $S$  is some unspecified diabatic heat source. Using the hydrostatic equation:

$$\frac{\partial}{\partial z} \left( \frac{p'}{\rho_0} \right) = g \frac{\theta'}{\theta_0}$$

eq. (3) may be written as:

$$\frac{D}{Dt_H} \left\{ \frac{\partial}{\partial z} \left( \frac{p'}{\rho_0} \right) \right\} + N^2 w = g S \quad - (4)$$

where  $N$  is the Brunt-Vaisala frequency ( $= \sqrt{gB'}$ ). Eliminating  $w$  from eqs. (1) and (4) and substituting  $(u_g, v_g)$  and  $\int_g$  using the expressions (2) gives:

$$\frac{D}{Dt_H} \left[ \nabla_H^2 p' + \frac{\partial}{\partial z} \left\{ \frac{\rho_0 f_0^2}{N^2} \frac{\partial}{\partial z} \left( \frac{p'}{\rho_0} \right) \right\} \right] + \beta \frac{\partial p'}{\partial x} = f_0^2 g \frac{\partial}{\partial z} \left( \frac{\rho_0 S}{N^2} \right) \quad - (5)$$

with

$$\frac{D}{Dt_H} = \frac{\partial}{\partial t} + \frac{1}{f_0 \rho_0} \left( \frac{\partial p'}{\partial x} \frac{\partial}{\partial y} - \frac{\partial p'}{\partial y} \frac{\partial}{\partial x} \right)$$

(c.f. Gill (1982), pg. 530, eq. (12.8.7) - the adiabatic case).

#### (b) Free Rossby waves solutions

Consider now the special case of eq. (5) where  $N^2 = \text{constant}$ ,  $S=0$ , ( $H_0$  is the density scale height) and linearize the equation about an atmosphere with uniform zonal wind  $U$ . This involves the substitution of  $p' = -\rho_0 f_0 u_y + \delta p$  and the neglect of terms quadratic in  $\delta p$  so that:

$$\left( \frac{\partial}{\partial t} + U \frac{\partial}{\partial x} \right) \left[ \nabla_H^2 \delta p + \left( \frac{f_0}{N} \right)^2 \frac{\partial}{\partial z} \left\{ \rho_0 \frac{\partial}{\partial z} \left( \frac{\delta p}{\rho_0} \right) \right\} \right] + \beta \frac{\partial \delta p}{\partial x} = 0 \quad - (6)$$



Looking for solutions to eq. (6) of the form:

$$\delta p = F(z) \exp[i(kx \pm \mu y - \sigma t)]$$

gives:

$$(-i\sigma + 4ik) \left[ -K^2 F + \left( \frac{f_0}{N} \right)^2 \frac{d}{dz} \left\{ \rho_0 \frac{d}{dz} \left( \frac{F}{\rho_0} \right) \right\} \right] + \beta ik F = 0$$

where  $K^2 = k^2 + \mu^2$  . This further simplifies to:

$$\frac{d^2 F}{dz^2} + \frac{1}{H_0} \frac{dF}{dz} + \left[ \left( \frac{N}{f_0} \right)^2 \frac{\beta}{4-c} - K^2 \right] F = 0 \quad -(7)$$

where  $c = \sigma/k$  (the phase speed). It is easily verified that  $F(z)$  has solutions:

$$F(z) = \exp(i\gamma z - \frac{z}{2H_0})$$

where 
$$\gamma^2 + \frac{1}{4H_0^2} = \left( \frac{N}{f_0} \right)^2 \left( \frac{\beta}{4-c} - K^2 \right) \quad -(8)$$

and so that any linear combination of solutions

$$\delta p = \exp[i(kx \pm \mu y \pm \gamma z - \sigma t) - \frac{z}{2H_0}]$$



will satisfy eq. (6). Since  $V_g = \frac{ik}{f_0} \frac{\delta p}{\rho_0}$  it is clear that if  $\nabla^2 > 0$ , then the amplitude of the wind increases exponentially with height as  $e^{z/2H_0}$  though the specific kinetic energy  $\frac{1}{2}\rho_0(u_g^2 + v_g^2)$  is constant with height. This condition may be re-stated as:

$$K^2 < \frac{\beta}{U-c} - \frac{f_0^2}{4H_0^2 N^2} \quad - (A)$$

or

$$U-c < \frac{\beta}{K^2 + \left(\frac{f_0}{N}\right)^2 \cdot \frac{1}{4H_0^2}} \quad - (B)$$

and was first put forward by Charney and Drazin (1961). It can be shown that wave solutions of the form:

$$\delta p \propto \exp\left[i(kx + \nabla z - \sigma t) - \frac{z}{2H_0}\right] \quad - (9)$$

(setting  $\mu=0$  for convenience)

transmit disturbance energy upwards and since their lines of constant phase are given by

$$kx + \nabla z - \sigma t = \text{constant}$$

they tilt upstream with height. In fact it is this type of solution which is most relevant to the real atmosphere since the principal energy sources for these waves are found in the lower troposphere and their upward propagation is unimpeded - even by the sudden change static stability at the tropopause.

The dispersion relation eq. (8) can be re-expressed in terms of  $\sigma$  yielding:

$$\sigma = Uk - \frac{\beta k}{K^2 + \left(\frac{f_0}{N}\right)^2 \left(\nabla^2 + \frac{1}{4H_0^2}\right)}$$



and the vertical component of the group velocity can be obtained by differentiating with respect to  $\gamma$  giving:

$$C_{gz} = \frac{\partial \sigma}{\partial \gamma} = \frac{2\beta k \left(\frac{f_0}{N}\right)^2 \gamma}{\left\{ K^2 + \left(\frac{f_0}{N}\right)^2 \left( \gamma^2 + \frac{1}{4H_0^2} \right) \right\}^2} \quad - (10)$$

Upward energy propagation ( $C_{gz} > 0$ ) is then associated with  $\gamma > 0$  as selected in eq. (9). Alternatively, eq. (10) can be written as:

$$C_{gz} = \frac{2\beta k \left(\frac{f_0}{N}\right)^2 \gamma}{\left( \frac{\beta}{U-c} - K^2 \right)^2}$$

and if  $K^2 \ll \beta / U - c$  then (provided  $\frac{1}{4H_0^2} \ll \gamma^2$  )

$$\gamma^2 \sim \left( \frac{N}{f_0} \right)^2 \frac{\beta}{U - c}$$

and

$$C_{gz} \simeq \frac{2f_0 k (U - c)^{3/2}}{N \beta^{1/2}} \quad - (11)$$

Substituting typical values, eg.  $f = 10^{-4} \text{ s}^{-1}$ ,  $k = 2\pi / (30,000 \text{ km})$ ,  $N = 10^{-2} \text{ s}^{-1}$ ,  $U - c = 10 \text{ ms}^{-1}$  and  $\beta = 1.6 \times 10^{-11} \text{ m}^{-1} \text{ s}^{-1}$  gives  $C_{gz} \sim 3 \text{ km/day}$  suggesting a time scale of about one week for long waves disturbances forced near the surface to reach the stratosphere.



Conditions (A) and (B) suggest that only the largest horizontal scales of wave motion will be capable of propagating vertically and that strong westerly winds may act as a barrier to Rossby wave energy. Note also that for stationary waves ( $c=0$ ) vertical energy propagation is impossible in easterly winds. Figs. 1 and 2 show winter and summer northern hemispheric geopotential height and isotherm maps of the 10 mb pressure surface. The westerly zonal circulation in winter allows planetary wave energy (typically only wavenumbers 1 and 2) to propagate from the troposphere up to the mesosphere so that the time-averaged stratospheric circulation exhibits persistent features such as the Aleutian High. In contrast, the easterly summertime regime of the stratosphere is opaque to upward propagating stationary planetary waves and the flow is extremely zonal.

(c) Stationary forced wave solutions

Differences in thermal energy budgets over land and sea lead to large zonal asymmetries in the diabatic heating rate averaged over, say, one month. In the Northern Hemisphere winter slow radiative cooling ( $\sim 1^\circ\text{K/day}$ ) dominates over continental interiors (eg. Siberia) in marked contrast to flow over the oceans which experiences rapid heating ( $\sim 5^\circ\text{K/day}$ ) due to the vigorous transfer of sensible and latent heat from the sea (Fig. 3). Linear theory can be used to get some idea of the large-scale stationary wave response to zonally-asymmetric, time-averaged heat sources. Again, linearizing about an atmosphere of uniform static stability and zonal wind eq. (5) gives:

$$U \frac{\partial}{\partial x} \left[ \nabla_H^2 \delta p + \frac{\partial}{\partial z} \left\{ \rho_0 \left( \frac{f_0}{N} \right)^2 \frac{\partial (\delta p)}{\partial z} \right\} \right] + \beta \frac{\partial \delta p}{\partial x} = f_0^2 g \frac{\partial}{\partial z} \left( \frac{\rho_0 S}{N^2} \right) \quad (12)$$



We shall require the response  $\delta p$  to a sinusoidal distribution of heating which decays exponentially with height ie.

$$S = a \sin kx \cos \mu y \exp(-bz)$$

or 
$$= \underline{\text{Real}} \left\{ -ia \exp(ikx - bz) \cos \mu y \right\} \quad - (13)$$

which suggests solutions of the form:

$$\delta p = \underline{\text{Real}} \left\{ F(z) e^{ikx} \cos \mu y \right\} \quad - (14)$$

where we expect  $F(z)$  to be a complex function of  $z$ .

Substituting eqs. (13) and (14) into eq. (12) leads to an ordinary differential equation for  $F(z)$ :

$$\frac{d}{dz} \left[ \rho_0 \frac{d}{dz} \left( \frac{F}{\rho_0} \right) \right] + \frac{N^2}{f_0^2} \left( \frac{\beta}{U} - K^2 \right) F = \frac{\rho_s a g (b + \frac{1}{H_0})}{Uk} e^{-(b + \frac{1}{H_0})z} \quad - (15)$$

(NB:  $\rho_s = \rho_0(z=0)$ )  
Particular integrals of eq. (15) will be of the form  $C e^{-(b + \frac{1}{H_0})z}$

and it can be shown that:

$$C = \frac{\rho_s a g (b + \frac{1}{H_0})}{Uk \left[ b(b + \frac{1}{H_0}) + \left( \frac{N}{f_0} \right)^2 \left( \frac{\beta}{U} - K^2 \right) \right]}$$

The full solution will be of the form:

$$\delta p = \underline{\text{Real}} \left\{ \left[ C \exp[-(b + \frac{1}{H_0})z] + \text{complementary function} \right] e^{ikx} \cos \mu y \right\} \quad - (16)$$



and must satisfy boundary conditions at  $z=0$  and  $\infty$ . As for the free solutions discussed earlier the physically relevant complementary function is  $A \exp \left( i\gamma z - \frac{z}{2H_0} \right)$  (consistent with upward energy propagation) where  $A$  remains to be determined by the lower boundary condition. With a plane horizontal surface at  $z=0$ , we require the vertical velocity to vanish there. This condition can be enforced through the linearized form of the thermodynamic equation (4) ie.

$$U \frac{\partial^2}{\partial x \partial z} \left( \frac{\delta p}{\rho_0} \right) + N^2 w = g S \quad - (17)$$

The lower boundary condition is then:

$$U \frac{\partial^2}{\partial x \partial z} \left( \frac{\delta p}{\rho_0} \right) \Big|_{z=0} = -i a g e^{i k x} \cos \mu y$$

which can then be shown, using eq. (16) and the expression for  $C$ , implies that:

$$A = \frac{\frac{\rho_s a g}{U k} \left( i\gamma - \frac{1}{2H_0} \right)}{\left[ b \left( b + \frac{1}{H_0} \right) + \gamma^2 + \frac{1}{4H_0^2} \right]}$$

(also the dispersion relation eq. (8), with  $c=0$ , has been used).



The full solution is therefore given by:

$$\delta p = \text{Real} \left\{ \frac{\frac{\rho_s a g \cos \mu y}{U k} \left\{ \left( b + \frac{1}{H_0} \right) e^{-(b + \frac{1}{H_0})z} + \left( i\gamma - \frac{1}{2H_0} \right) e^{(i\gamma - \frac{1}{2H_0})z} \right\} e^{ikx}}{\left[ b \left( b + \frac{1}{H_0} \right) + \gamma^2 + \frac{1}{4H_0^2} \right]} \right\} \quad (18)$$

where

$$\gamma^2 = \left( \frac{N}{f_0} \right)^2 \left( \frac{\beta}{U} - (k^2 + \mu^2) \right) - \frac{1}{4H_0^2}$$

Notice that if the Charney/Drazin criterion (A) is not satisfied  $\gamma$  is imaginary and the disturbance energy decays with height. Eq. (18) also implies that the response is inversely proportional to the basic state wind speed  $U$ . This is because air parcels spend a time  $\propto \frac{1}{U}$  in, say, the heating region of  $S$  and so the longer the time they are there, the bigger the response. Fig. 4 shows some typical amplitude and phase plots of the geopotential height and temperature for wave numbers 1, 2 and 3 derived from the solution. Note that the geopotential height amplitude is given by  $\delta p / \rho_0 g$ ,  $a = 3^\circ\text{K/day}/260^\circ\text{K}$ ,  $b = 1/(4 \text{ km})$ ,  $U = 10 \text{ ms}^{-1}$  and  $B = 3 \times 10^{-5} \text{ m}^{-1}$ . Characteristic features of these energy radiating solutions are:

- (i) a strong surface pressure response ( $\sim 10 \text{ mb}$ ).
- (ii) mid-troposphere minimum amplitude (at about 3 or 4 km)
- (iii) amplitude increase at  $e^{z/2H_0}$  as  $z \rightarrow \infty$  (specific kinetic energy,  $\frac{1}{2}(u_y^2 + v_y^2) = \text{const}$ ).
- (iv) strong westward tilt with height particularly in heating region.



- (v) Since the maximum cooling rate occurs at a phase angle of  $90^\circ$  then the maximum surface pressure occurs about  $50^\circ$  downstream of this. ( $90^\circ$  downstream for evanescent waves which have  $\sqrt{z} < 0$ ) This implies that surface anticyclones will be found on the eastern side of continental land masses, eg. Siberian High.

Waves which tilt to the west with height and which are geostrophic and hydrostatically balanced, transport heat polewards in the sense that  $\overline{v_g \theta} > 0$  where the overbar denotes the zonal average. To show this, let the geopotential height perturbation, associated with any wave field be given by:

$$h = \frac{\delta p}{\rho_0 g} = H(z) \cos[kx + \epsilon(z)]$$

where  $H(z)$  is the amplitude and  $\epsilon(z)$  the phase.

The hydrostatic equation can then be used to find  $\theta'$  so that:

$$\frac{\theta'}{\theta_0} = \frac{\partial h}{\partial z} = \frac{dH}{dz} \cos(kx + \epsilon) - H \sin(kx + \epsilon) \frac{d\epsilon}{dz}$$

Also the geostrophic wind relation gives:

$$v_g = \frac{g}{f} \frac{\partial h}{\partial x} = -\frac{g}{f} H(z) k \sin(kx + \epsilon)$$

so that:

$$\overline{\frac{\theta' v_g}{\theta_0}} = \frac{1}{2} \frac{gk}{f} H^2 \frac{d\epsilon}{dz}$$



Since westward phase tilt with height implies  $\frac{d\epsilon}{dz} > 0$  then heat transport is poleward. It is then clear that our radiating wave solutions have  $\overline{\rho_0 v_y \theta'} > 0$  which turns out to be a maximum at the surface. For reasons beyond the scope of this lecture one should be cautious before equating  $\overline{\rho_0 v_y \theta'}$  to any real tendency of stationary waves to transport heat. In the adiabatic regions of the model flow, parcels return from high latitudes with the same potential temperature as they began with so that no real transport is achieved. This is not true of parcels in the lower tropospheric heating region which experience heating (on average) as they travel poleward and cooling as they travel equatorward, thereby achieving real heat transport.

(d) Comparison with observations

Figure 5 shows the observed, time-averaged wintertime amplitude and phase of wavenumber one as a function of height and latitude. There are many interesting points of agreement with the highly idealized solutions presented here including rapid phase tilt westward with height, amplification with height, and even the suggestion of an amplitude minimum near 3 km. Observations of the amplitude of wavenumbers one and two up to a height of 100 km have been collated by Green (1972) and plotted on a logarithmic scale (Fig. 6). The specific kinetic energy is found to be roughly constant with height up to 40 or 50 km above which it falls off. The accompanying phase diagram shows rapid phase tilt westward with height.



The linear solution eq. (18) must break down at some height since the pressure perturbation amplitude falls off as  $e^{-\frac{z}{2H_0}}$  compared to  $e^{-z/H_0}$  for the basic state pressure so that at some height the total pressure would become negative. In practice wave breakdown occurs long before this as a nonlinear advection process. The absorption of disturbance energy in the stratosphere through the breakdown process is probably the dominant mechanism for the tail-off of the specific kinetic energy.

Figure 7 shows the observed poleward heat transport due to stationary waves in the admittedly rather anomalous January 1963. The low-level maximum and 'whip-lash' amplification effect in the stratosphere are both in agreement with the solution. Since the stationary wave heat transport (primarily wavenumbers one, two and three) constitutes about 50% of the total atmospheric poleward heat transport in winter, vertically propagating ultra-long waves probably play an important role in the global heat budget. Further solutions for more realistic distributions of  $N^2$  and  $U$  (with height) can be found in Shutts (1978).

(e) Orographic planetary waves

Stationary solutions to eq. (12) with  $S=0$  are easily obtainable for flow over a sinusoidal 'mountain' whose height  $h(x,y)$  is given by:

$$\begin{aligned} h(x,y) &= h_m \sin kx \cos my \\ &= h_m \text{Real} \left\{ -i e^{ikx} \cos my \right\} \end{aligned} \quad - (19)$$

Linearizing the interface condition  $w = \frac{Dh}{Dt}$  at  $z = h$  gives:

$$w = U \frac{\partial h}{\partial x} \quad \text{at} \quad z = 0$$



which may be substituted into the thermodynamic equation (17) yielding:

$$U \frac{\partial^2}{\partial x \partial z} \left( \frac{\delta P}{\rho_0} \right) + N^2 U \frac{\partial h}{\partial x} = 0$$

$$\text{or } \frac{\partial}{\partial z} \left( \frac{\delta P}{\rho_0} \right) = -N^2 h(x, y) \quad \text{at } z=0 \quad - (20)$$

Choosing upward propagating stationary solutions with:

$$\frac{\delta P}{\rho_0} = D e^{(i\gamma z + \frac{z}{2H_0} + ikx)} \cos \mu y$$

then the lower boundary condition (eq. 20) implies that:

$$D \left( i\gamma + \frac{1}{2H_0} \right) = i N^2 h_m$$

or

$$D = \frac{N^2 h_m \left( \gamma + \frac{i}{2H_0} \right)}{\gamma^2 + \frac{1}{4H_0^2}}$$

so that:

$$\frac{\delta P}{\rho_0} = \text{Real} \left\{ \frac{N^2 h_m \left( \gamma + \frac{i}{2H_0} \right) e^{i(\gamma z + kx) + \frac{z}{2H_0}}}{\gamma^2 + \frac{1}{4H_0^2}} \right\} \cos \mu y$$

or

$$\frac{\delta P}{\rho_0} = \frac{-h_m N^2 \sin(kx + \gamma z - \delta) e^{\frac{z}{2H_0}} \cos \mu y}{\left( \gamma^2 + \frac{1}{4H_0^2} \right)^{1/2}}$$



where

$$\delta = \tan^{-1}(2H_0\gamma)$$

The phase difference between  $P/\rho_0$  and  $h(x,y)$  at  $z=0$  implies that the planetary wave is exerting a drag force on the orography. This can be calculated as a second-order quantity (like heat flux) giving:

$$\overline{\delta P \frac{\partial h}{\partial x}} = \frac{\frac{1}{2} h_m^2 N^2 \rho_s k \gamma \cos My}{\gamma^2 + \frac{1}{4H_0^2}}$$

If  $\gamma^2 \gg \frac{1}{4H_0^2}$  then the drag is of the order of  $\frac{1}{2} \rho_s h_m^2 N^2 k / \gamma$

which substituting typical values of  $h_m \sim 400$  m,  $N \sim 10^{-2} \text{s}^{-1}$ ,  $\rho_s \sim 1 \text{kgm}^{-3}$ ,  $k = 2\pi/20,000$  km and  $\gamma^{-1} \sim 5$  km gives

$$\overline{\delta P \frac{\partial h}{\partial x}} \sim 0.01 \text{ Nm}^{-1}$$

which is  $1/10$  of that due to surface frictional stresses. Since most of the terrain height variation is due to mountain ranges which are smaller in scale than the continental scale relevant to planetary Rossby waves, the relevance of these solutions to reality is a little more tenuous. In fact there still remains great debate as to whether thermal or orographic forcing dominates the production of stationary long waves.



## Legends

- Fig. 1      Geopotential height (left) and temperature (right) contours for the northern hemisphere averaged over several winters at the 10 mb level.
- Fig. 2      Same as Fig. 1 except for summer.
- Fig. 3.      Diabatic heating computed for the 700 mb level in winter (for details see Lau (1979)).
- Fig. 4      Amplitude and phase plots of the geopotential height (a) and temperature (b) for wavenumbers 1, 2 and 3 derived from eq (18).
- Fig. 5      Long term January mean amplitude and phase of wavenumber one plotted as a function of height and latitude (van Loon et al, 1973). Units: amplitude in metres; phase in degrees longitude.
- Fig. 6      Variation with height of (a) geopotential height amplitude and (b) phase of the January mean eddy motion at 50°N.  
(a) Amplitude, defined as the difference between maximum and minimum contour height is plotted on a logarithmic scale. Where the specific kinetic energy is constant with height the curve is parallel to the dashed line. The thick line is for wavenumber 1, the thin line is for wavenumber 2.  
(b) Phase is defined as the longitude of the trough. For origin of data see Green (1972).
- Fig. 7      Latitudinally-averaged poleward temperature flux due to stationary waves for January 1963. The data was obtained from Oort and Rasmusson.



## References

- Charney, J G and (1961) 'Propagation of planetary scale  
Drazin, P G disturbances from the lower into the  
upper atmosphere'.  
J. Geophys. Res., 66, 83-109.
- Gill, A E (1982) 'Atmosphere-Ocean Dynamics'.  
Academic Press, International Geophysics  
Series, Vol. 30.
- Green, J S A (1972) 'Large-scale motion in upper  
stratosphere and mesosphere: an  
evaluation of data and theories'.  
Phil. Trans. R. Soc. Lond. A, 271,  
557-583.
- Shutts, G J (1978) 'Quasi-geostrophic planetary wave  
forcing'.  
Quart. J. Roy. Met. Soc., 104, 331-350.
- van Loon, H, Jenne, R and (1973) 'Zonal harmonic standing waves'.  
Labitzke, K J. Geophys. Res., 78, 4463-4471.
- Lau, N-C (1979) 'The observed structure of tropospheric  
stationary waves and the local balances  
of vorticity and heat'.  
J. Atmos. Sci., 36, 996-1016.



Fig. 1

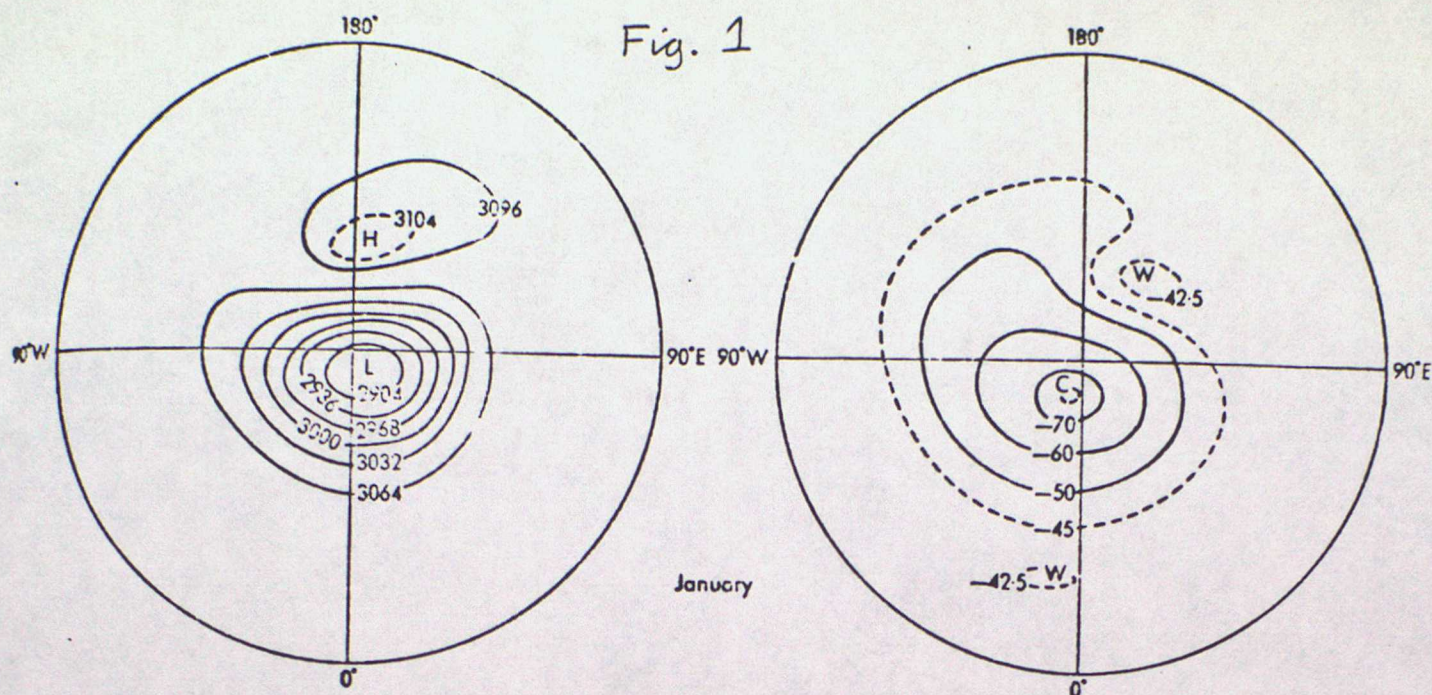
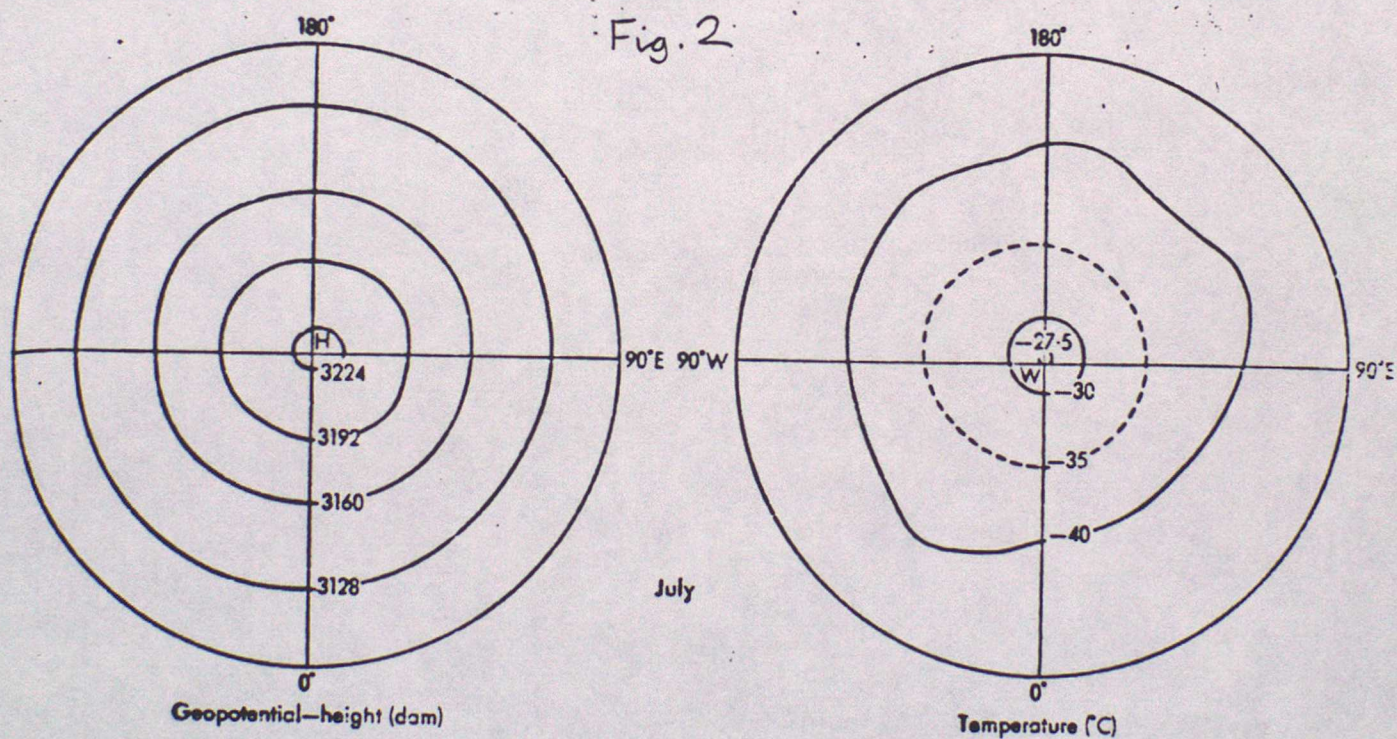


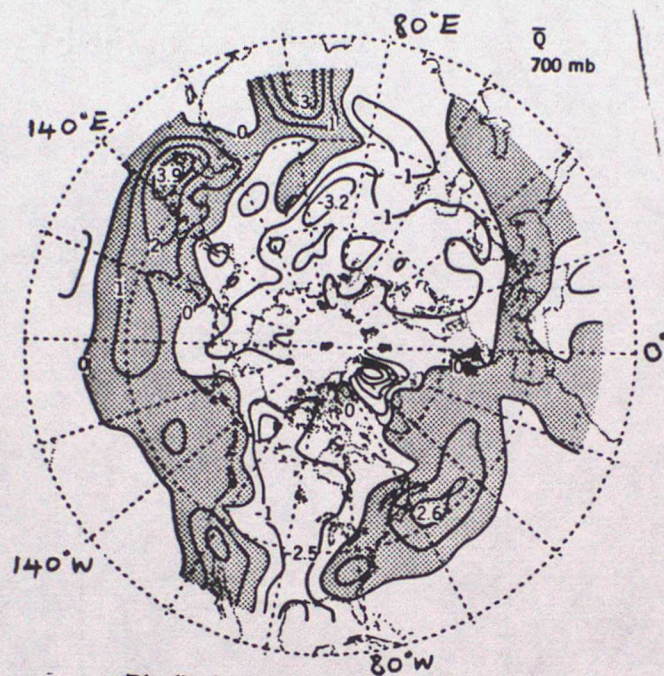
Fig. 2



Synoptic charts at 10 mb for the Northern Hemisphere during winter and summer showing fields of geopotential—height (dam) and temperature (°C) taken as averages over several years (from Met. Abhand., Band 100/Heft 4, Freie University of Berlin).



Fig. 3



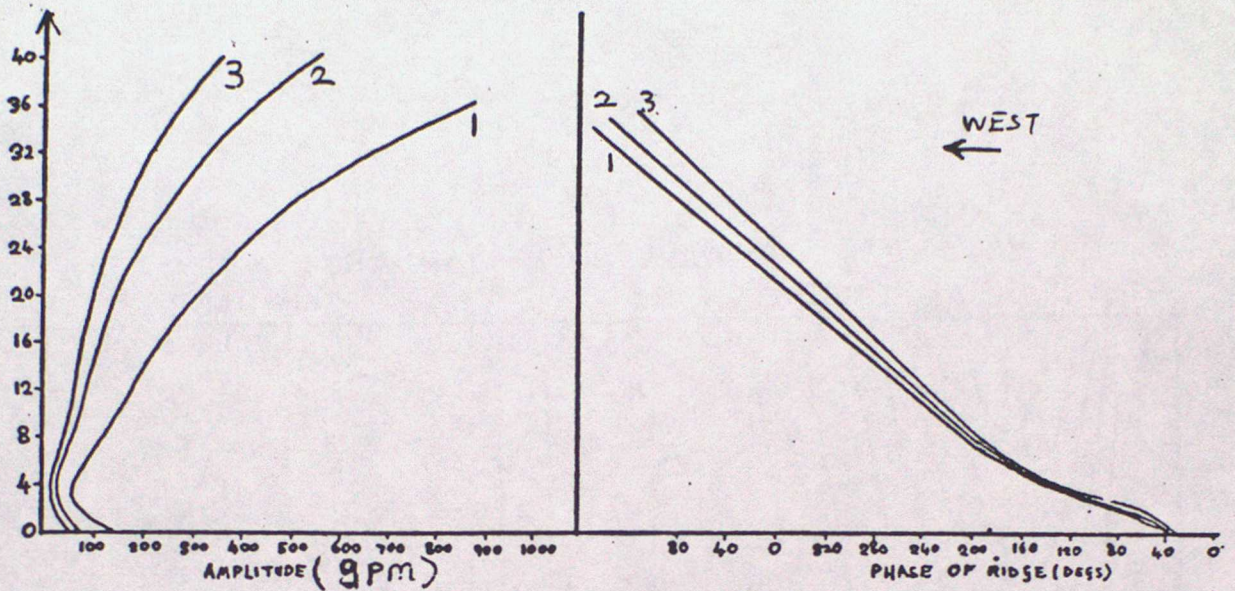
Distribution of diabatic heating rate  $\bar{Q}$  at 700 mb.  
Contour interval  $1^{\circ}\text{C day}^{-1}$ .



Fig. 4

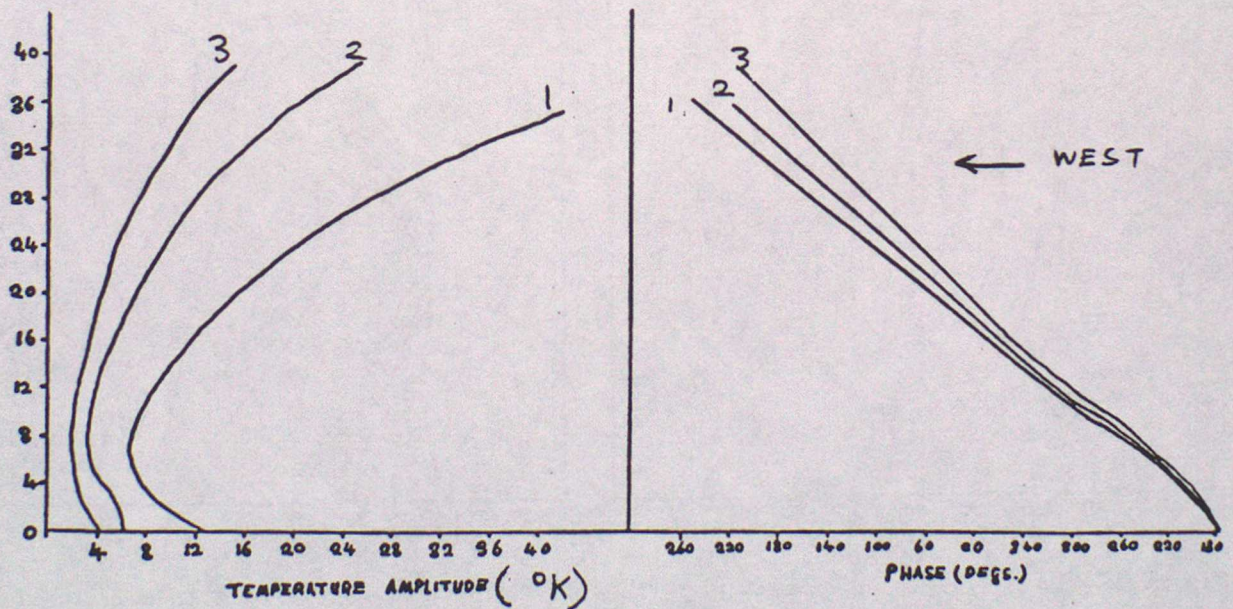
(a)

HEIGHT (Km)



GEOPOTENTIAL HEIGHT FIELD

(b)



TEMPERATURE FIELD

$$B = 3.0 \times 10^{-5} \text{ m}^{-1}, \quad S_0(z) = \left( \frac{3.0^\circ\text{C/DAY}}{260^\circ\text{K}} \right) \exp\left(-\frac{z}{4 \text{ KM.}}\right)$$

$$\text{AND } \bar{u} = 10 \text{ ms}^{-1}$$



Fig. 5

WAVE NO. 1 - JANUARY

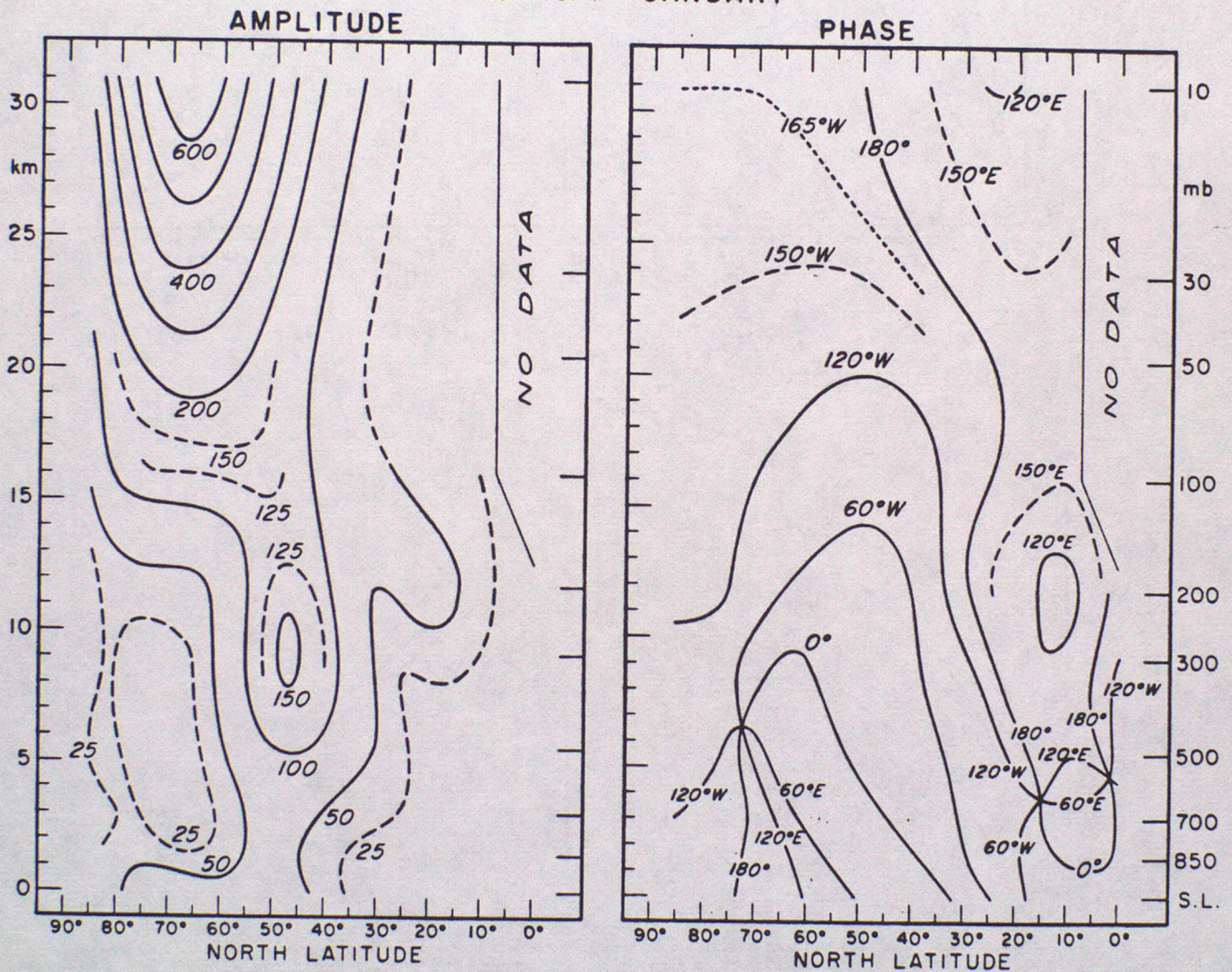
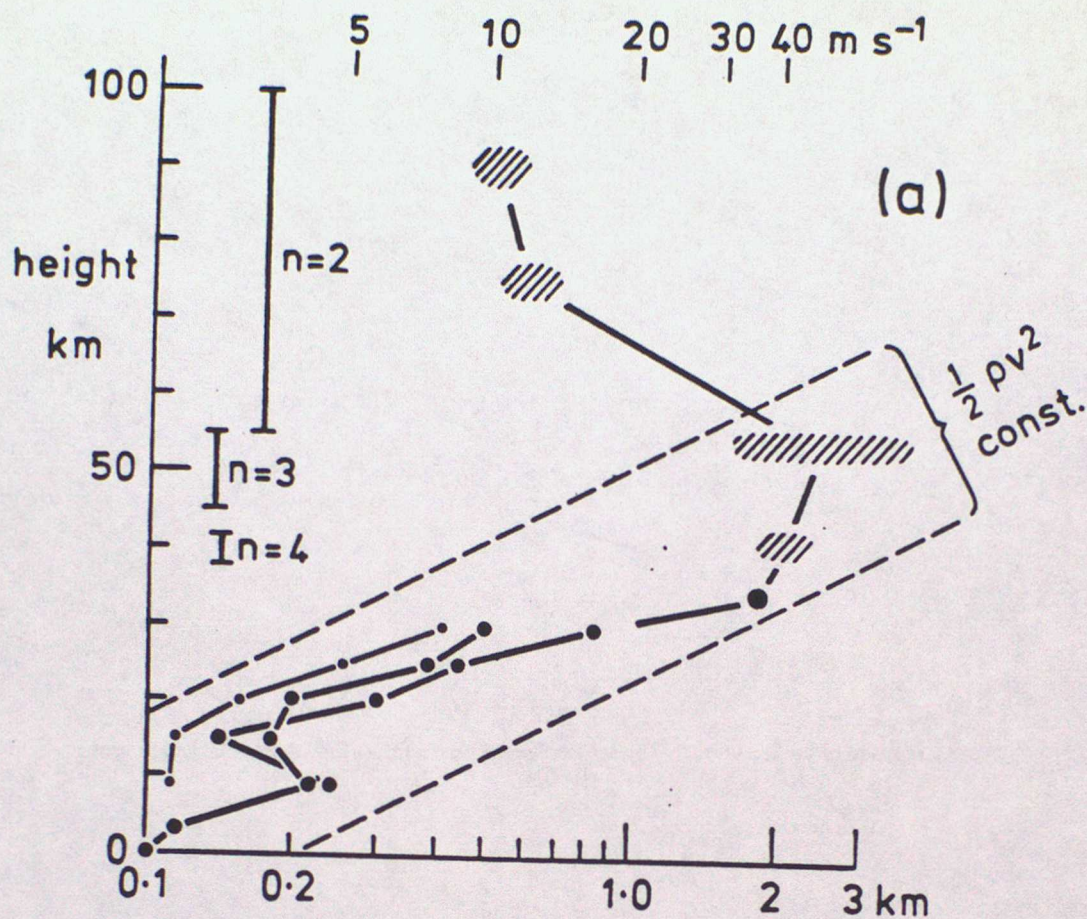


Figure 1 - Long-term January mean amplitude (metres) and phase (longitude of amplitude) (metres) and phase (longitude of ridge) or zonal harmonic  $m = 1$  for northern hemisphere (van Loon et al., 1973).



Fig. 6



$$[\delta p / \rho g]_{\min}^{\max} = [\delta z]_{\min}^{\max}$$

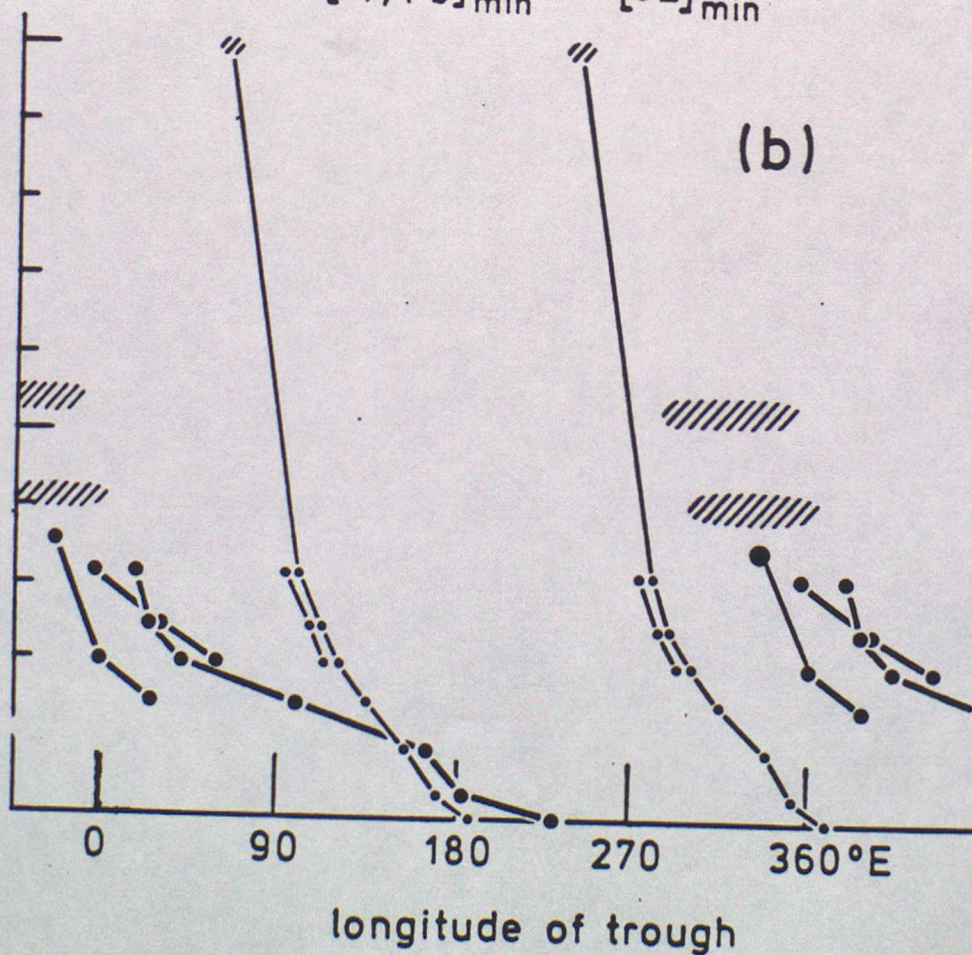
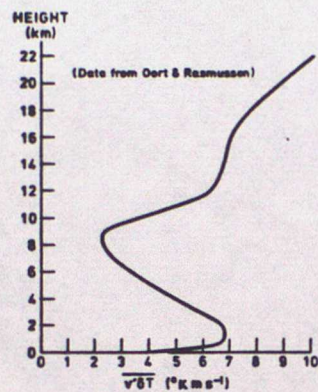




Fig. 7



Vertical section of the latitudinally averaged poleward 'temperature flux' due to stationary waves for January 1963.



## Lecture 2    Persistent Anomalous Circulation and Blocking

The study of blocking underwent a resurgence of interest in the late 1970s with the appearance of some new(?) theoretical ideas and with the greater availability of high quality global datasets. Since then many of the properties of blocking known to forecasters have found expression in highly simplified models of the atmosphere and are better quantified in terms of new diagnostics. Nevertheless it is probably also true to say that our ability to forecast blocking in the extended range sense (eg 7 days - 1 month) has not benefitted noticeably from these studies.

There are two particular types of anomalous circulation that I would like to emphasise in this Lecture. The first and most important type is the familiar regional blocking for which the anomalous circulation is predominantly confined to a certain longitude sector and occurs in geographically preferred regions. It typically has a timescale of the order of two weeks and tends to be most frequent at certain times of the year (eg western Europe in Spring). The second type is what I shall refer to as the 'severe winter pattern'. It is epitomised by the northern hemispheric circulation patterns of winters such as 1947 and 1962/63 when the axes of the major jetstreams were much further south than normal and low wavenumber planetary waves were of very large amplitude. These anomaly patterns are even more persistent than blocking and, as in the 1962/63 winter last longer than two months.

Instead of giving a review of the many theories of blocking that have been put forward in the last forty years we shall concentrate on three recent models. Before that a brief sketch of the phenomenon itself will be presented.



(i) The Blocked flow type

Blocking 'highs' are characterised by a region of warm air with higher than ambient pressure which extends upwards from the surface to the lower stratosphere. Within them the winds are generally light and the tropopause is higher than average. They are usually accompanied by a somewhat smaller region of low pressure with the opposite properties. This combined 'dipole' pattern is embedded in a diffluent flow field and tends to fluctuate in amplitude and phase (longitude) with the passage of travelling weather systems (Fig 1). There is often a tendency for high pressure cells to collapse only to rebuild further to the west causing an overall westward translation of the pattern. A dynamically significant aspect of the blocked flow field is the reversed potential vorticity gradient (from the normal poleward gradient) as is clearly portrayed by isentropic analyses of Ertel potential vorticity, (Hoskins, McIntyre and Robertson, Shutts (1986).) Potential vorticity within the blocking anticyclone is low relative to the ambient flow but high in the accompanying cut-off low further south. (Fig. 2.)

(ii) Free-mode model

One frequently gets the impression from studying sequences of synoptic charts that changes in weather type are often accompanied by an abrupt change in the configuration of the planetary scale flow and a new quasi-equilibrium pattern set up. Such behaviour is characteristic of some idealised non-linear systems containing quasi-equilibrium or 'attractor' points. The free-mode approach to representing blocking flow patterns involves finding time-independent solutions to approximated forms of the equations of motion and examining their sensitivity to governing parameters.



Perhaps the simplest free-mode model with any relevance to blocking is the vortex doublet of classical hydrodynamics embedded in a uniform flow. For a purely barotropic, incompressible and two-dimensional fluid on an  $f$ -plane (the 'dishpan' case) fluid parcels conserve their vorticity. The vorticity distribution associated with a point vortex at a position  $\underline{r}_0$  in the  $(x,y)$  plane <sup>is</sup> proportional to  $\delta(\underline{r}-\underline{r}_0)$  where  $\delta$  denotes the Dirac delta function. The tangential velocity associated with such a vortex is inversely proportional to the distance from the vortex core. Two point vortices of opposite sign though equal circulation strength self-induce a translational movement of the vortex pair in a direction at right angles to their dipole axis and with a speed inversely proportional to their separation. The doublet can be rendered stationary by adding to this solution a uniform opposing current. (Fig. 3.)

This solution is restricted to systems with no spatial variation in background rotation. (ie no planetary beta effect.) Stern (1975) showed how dipole solutions (named Modons) could be constructed for the beta-plane case and McWilliams (1980) used the equivalent barotropic equations to obtain a stationary Modon solution which serves as a model of blocking, (Fig. 4). Various extensions of these barotropic models to the baroclinic case have been made though, as yet, no primitive equation solutions have been found. Of course, real atmospheric blocking is never time-independent and these solutions should at best be regarded as a zero-order description (in the language of perturbation theory) of the phenomenon.



(iii) Resonance theories

The idea that blocking may be a manifestation of some kind of internal resonance is old and difficult to trace back to the originator. As a simple example of the principle, consider the barotropic absolute vorticity equation:

$$\frac{D}{Dt} (\zeta + f) = F \quad (1)$$

where  $F$ , is some unspecified source of vorticity due, for instance, to vortex compression associated with flow over mountains. In terms of the non-divergent streamfunction  $\psi$  defined such that  $u = -\frac{\partial \psi}{\partial y}$  and  $v = \frac{\partial \psi}{\partial x}$  then eq. (1) becomes:

$$\left( \frac{\partial}{\partial t} + \frac{\partial \psi}{\partial x} \frac{\partial}{\partial y} - \frac{\partial \psi}{\partial y} \frac{\partial}{\partial x} \right) \left( \frac{\partial^2 \psi}{\partial x^2} + \frac{\partial^2 \psi}{\partial y^2} \right) + \beta \frac{\partial \psi}{\partial x} = F \quad (2)$$

where  $\beta = \frac{df}{dy}$  is assumed constant. Now choose a purely sinusoidal forcing function  $F$  such that:

$$F = F_0 \sin kx \cos \mu y$$

where  $k$  and  $\mu$  are wavenumber vector components. Now look for stationary solutions for  $\psi$  involving a zonal flow component with:

$$\psi = -Uy + A \cos kx \cos \mu y$$

and where  $A$  is a constant. It can be shown that the nonlinear terms (terms in  $A^2$ ) cancel and that:



$$A = \frac{F_0}{k[U(k^2 + \mu^2) - \beta]} \quad - (3)$$

From eq. 3, it can be seen that waves satisfying Rossby's stationary wave formula:

$$k^2 + \mu^2 = \beta/U \quad - (4)$$

will be resonant in the sense that the inviscid theory predicts an infinite amplitude response.

Accepting the assumptions of this model, it is difficult to see why the atmosphere is not perpetually resonant since the Fourier spectrum of  $F$  will always contain some contribution near to the stationary wavenumber. The analysis is complicated in general by the non-uniform spatial variation of the background wind in height as well as horizontally. The existence of resonant modes then hinges crucially on whether or not Rossby wave energy can be dynamically 'contained' by, for instance, strong westerly winds in the stratosphere. (Lecture 1.) Lateral containment is more difficult to realise since stationary Rossby waves have 'critical lines' (where  $U=0$ ) in the sub-tropics.

When the flow is not precisely uniform, the non-linear terms do not cancel and a perturbation analysis is required to establish the relationship between  $A$  and  $U$  given  $k$  and  $\mu$ . It turns out that the equation to be solved for this non-linear case is analogous to that of the anharmonic oscillator, (Buzzi and Trevison, 1980). The resonance curve ( $A$



against  $U$ ) now folds over and no finite value of  $U$  gives an unbounded response, (Fig. 5). Instead, for a range of values of  $U$ , high and low amplitude responses are possible. There is an interesting analogy here between the dynamics of the finite amplitude pendulum and these weakly non-linear flows when  $Uk$  is interpreted as an angular frequency of oscillation, (ie  $2\pi/(\text{oscillation period experienced by a parcel})$ ).

(iv) Transient eddy-forced models

The characteristic diffluence and jetstream splitting associated with blocking causes transient baroclinic waves to become deformed immediately upstream of the block. The resulting anomalous local fluxes of vorticity and heat

lead to a time-mean dipole vorticity source oriented so as to reinforce the block dipole pressure pattern, (Shutts, 1983, Fig. 6). Although this conceptual model is incomplete in the sense that it only describes the nature of the time-averaged forcing function of, for instance, eq. 2.2, it can be studied in the context of a time-dependent barotropic model. There is a growing consensus of opinion that the resonant forcing of local non-linear free-mode patterns by their interaction with transient eddies is the essential mechanism at work in blocking. The geographical distribution of blocking is then controlled by the long quasi-stationary wave pattern forced by orographic and land/sea thermal influences.

A particular problem with the conceptual eddy forcing model is that no clear distinction between eddy and block can be defined in practice. During the life-time of a single blocking episode, only two or three eddy 'events' may contribute to the forcing of the block. The definition of 'eddy' as the deviation from a time-mean value is barely useful and is frustrated by the movement of the blocking pattern during the period. The



alternative is to dispense with the block/eddy decomposition of the fields of motion and take a Lagrangian view for which trajectories of air parcels are the main interest. On the timescale of a few days, the adiabatic assumption is not grossly in error for upper tropospheric flow and isentropic analysis provides a useful tool for studying air movement. Two conserved quantities (for adiabatic, inviscid flow) are useful to plot on isentropic surfaces: Ertel potential vorticity and mixing ratio. Since potential vorticity is a key quantity in dynamical theory (Hoskins et al, 1985) it represents much more than a tracer of air motions. By looking at sequences of potential vorticity maps plotted on a chosen isentropic surface, the injection of high or low potential vorticity air into the block by transient eddies can be seen. Ideally, the block would be characterised by an inner region where air is trapped as a pair of counter-rotating cells of high and low potential vorticity, (eg the Modon). The slow spin-down of this dipole by surface friction coupled with radiative cooling would be offset by the intermittent injection of 'fresh' high and low potential vorticity brought about by transient eddies. This can be seen to happen in the sequence Figs 7 (a-h). For a full account and diagnostic analysis of this blocking episode see Shutts (1986).

(v) The 'severe winter' pattern

In contrast to the usual concept of blocking, the 'severe winter pattern' is a hemispheric circulation anomaly with a strong zonally-averaged component. Figs 8 (a) and (b) show the sea-level pressure and 500 mb height anomalies over the Northern Hemisphere for the February of 1947. This shows the characteristic dominance of anomalous high pressure in latitudes north of 50°N with a ridge into the mid-west of the United States and with anomalously low pressure extending across the North



Pacific and Atlantic. The implied geostrophic wind anomaly is easterly almost everywhere between 50° and 60°N and Siberian air extends well into Europe. Compare this pattern with that of January 1977. (Fig. 9.) A brief perusal of the sea-level pressure anomaly charts stored in Met 0 13 show that this hemispheric pattern tends to occur quite frequently though is not necessarily associated with severe winter conditions in the British Isles due to minor local differences. Furthermore, empirical orthogonal analyses of real data and a 15 year general circulation model integration have both revealed this pattern to dominate the interannual variation at sea-level and 500 mb (Lau, 1981).

Since this type of anomaly is hemispheric, fairly zonal and of long timescale (1-2 months) it should be regarded as a change in the modus operandi of the general circulation. As for normal circulation types, transient eddies probably play an important role in maintaining this type of anomalous flow. Changes in the distribution and intensity of the major atmospheric heat sources (Palmer and Owen, 1986) could also play an important part in supporting an anomalous pattern such as this though it would be difficult to distinguish cause and effect.



## References

- Buzzi, A. and Trevisan, A. (1980) 'Stationary response of barotropic weakly non-linear waves to quasi-resonant orographic forcing'. J. Atmos. Sci., 37, 947-957.
- Hoskins, B.J., (1985) 'On the significance of isentropic potential vorticity maps'. Quart. J. Roy. Met. Soc., 111, 877-946.
- McIntyre, M.E. and Robertson, A.W.
- Lau, N-C. (1981) 'A diagnostic study of recurrent meteorological anomalies appearing in a 15 year simulation with a GFDL general circulation model'. Mon. Wea. Rev., 109, 2287-2311.
- McWilliams, J.C. (1980) 'An application of equivalent modons to atmospheric blocking'. Dyn. Atmos. Oceans, 5, 43-66.
- Palmer, T.N. and Owen, J.A. (1986) 'A possible relationship between some 'severe' winters in North America and enhanced convective activity over the tropical west Pacific'. Mon. Wea. Rev., 114, 648-651.
- Shutts, G.J. (1983) 'The propagation of eddies in diffluent jetstreams: eddy vorticity forcing of 'blocking' flow fields'. Quart. J. Roy. Met. Soc., 109, 737-761.



- Shutts, G.J. (1986) 'A case study of eddy forcing during an Atlantic blocking episode'.  
Adv. in Geophys., 29, (to appear).
- Stern, M. (1975) 'Minimal properties of planetary eddies'.  
J. Mar. Res., 33, 1-13.



## Legends

- Fig. 1 Sea-level pressure field (top) and height contours of the 500 mb surface (bottom) for 15 February, 12Z, 1983.
- Fig. 2 Contours of the Ertel potential vorticity calculated on the 320°K isentropic surface on 15 February, 12Z, 1983. The contour interval is variable so as to enhance the detail in the potential vorticity field where gradients are small. The shaded regions are of high potential vorticity and represent stratospheric air.
- Fig. 3 Streamlines of a stationary vortex doublet embedded in uniform flow.
- Fig. 4 Streamlines of a stationary equivalent barotropic 'Mödon' taken from McWilliams (1980).
- Fig. 5 The steady state amplitude of a disturbance forced by barotropic flow over orography plotted against the uniform speed of the current,  $U$ . The solid curve indicates the linear response when the orography is sinusoidal and the basic flow has uniform speed. The dashed curve is the modified response when certain non-linear terms are included.
- Fig. 6 A schematic picture of the deformation of meridionally elongated eddies as they propagate into a split jetstream region upstream of a blocking dipole. The associated sense of time-mean eddy vorticity forcing is indicated by the black arrows.
- Figs 7 A daily sequence (Feb 9-16 12Z) of Ertel potential vorticity maps (a)-(h) for the northern hemisphere plotted on the 320°K isentropic surface.

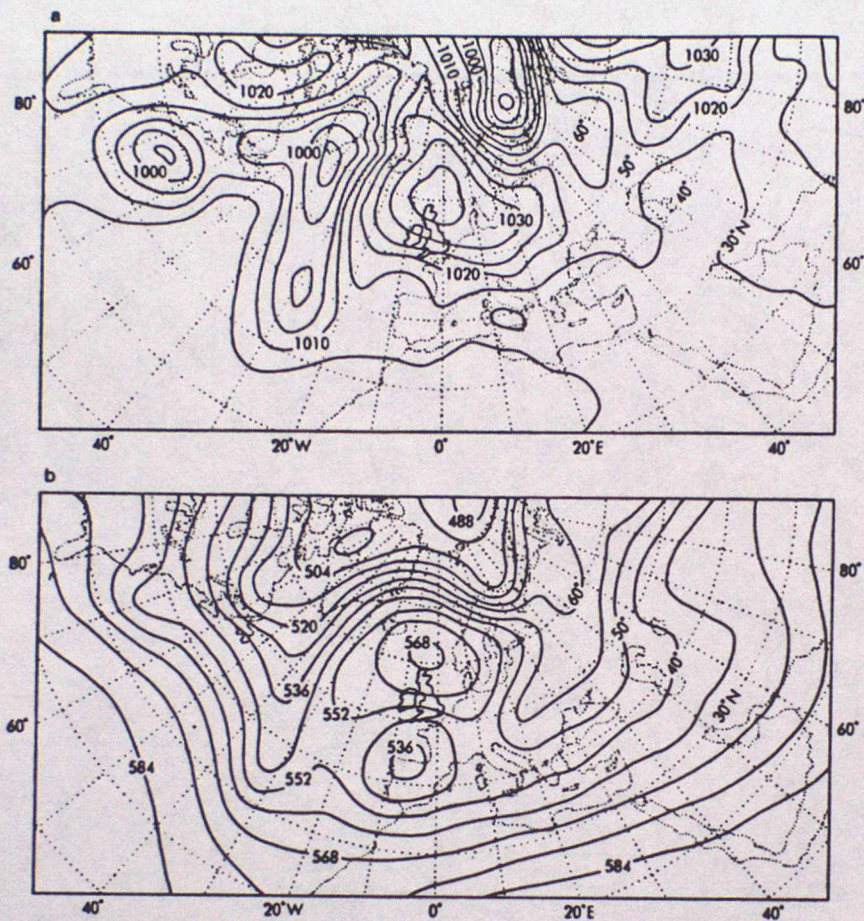


Figs 8 Sea-level pressure and 500 mb geopotential height anomalies for  
(a)-(b) northern hemisphere during February 1947. Contour intervals:  
4 mb and 6 dam respectively.

Fig. 9 Sea-level pressure anomaly for the northern hemisphere during  
January 1977. Contour interval: 4 mb.



Fig. 1



(a) Mean sea level pressure field for 15 February, 12Z. Contour interval: 5 mbar. (b) Height contours of the 500-mbar surface for 15 February, 12Z. Contour interval: 8 dam.

1983







Fig. 3

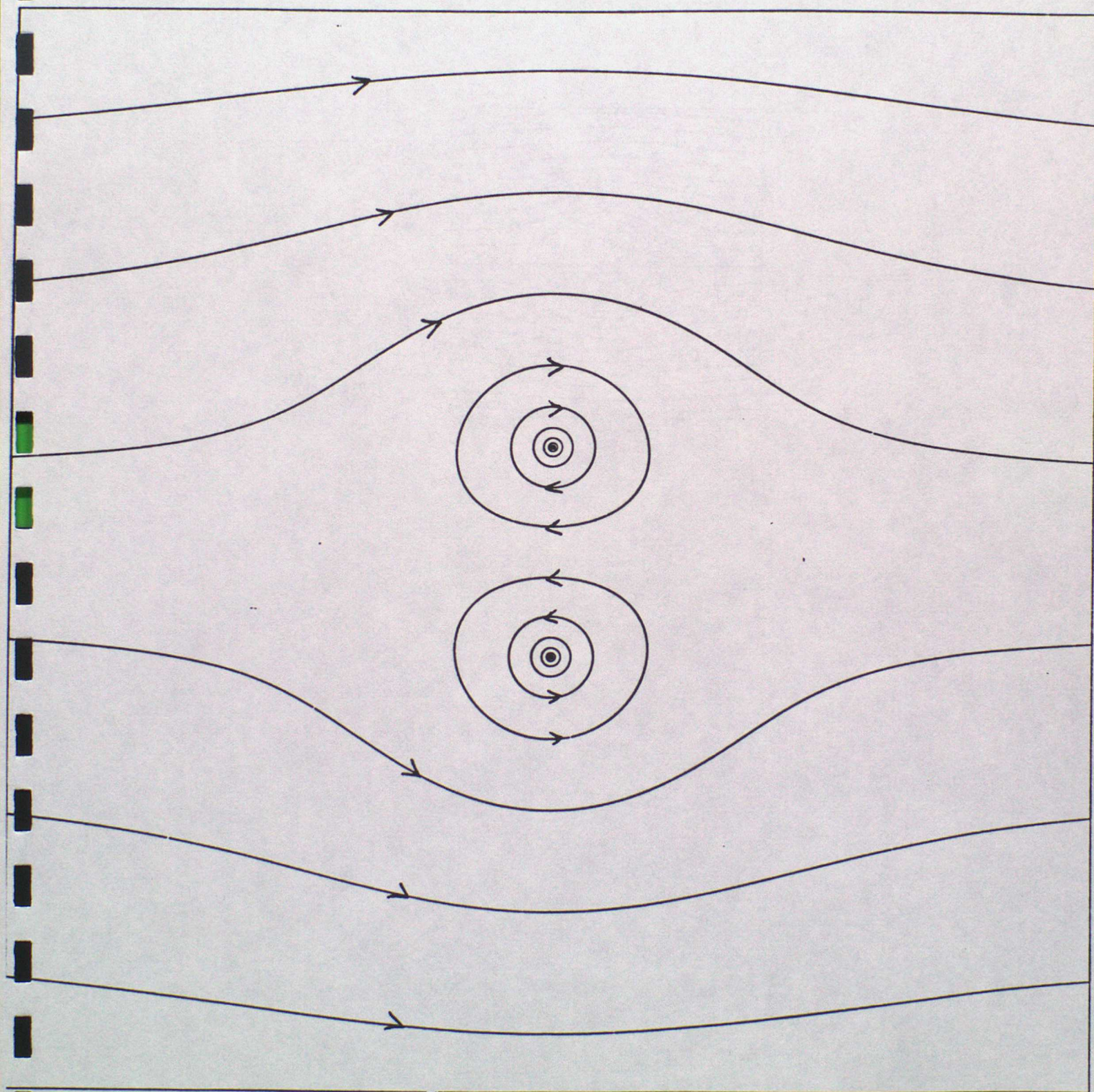




Fig. 4

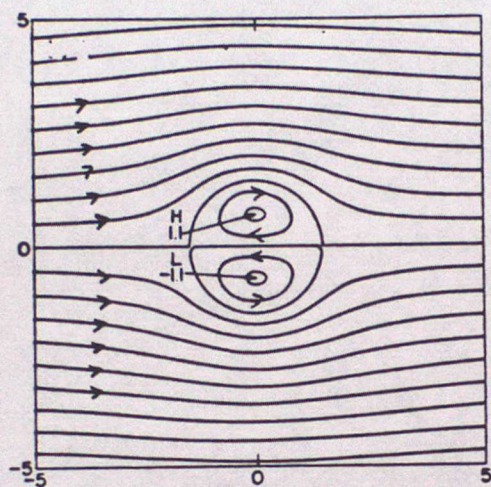




Fig. 5

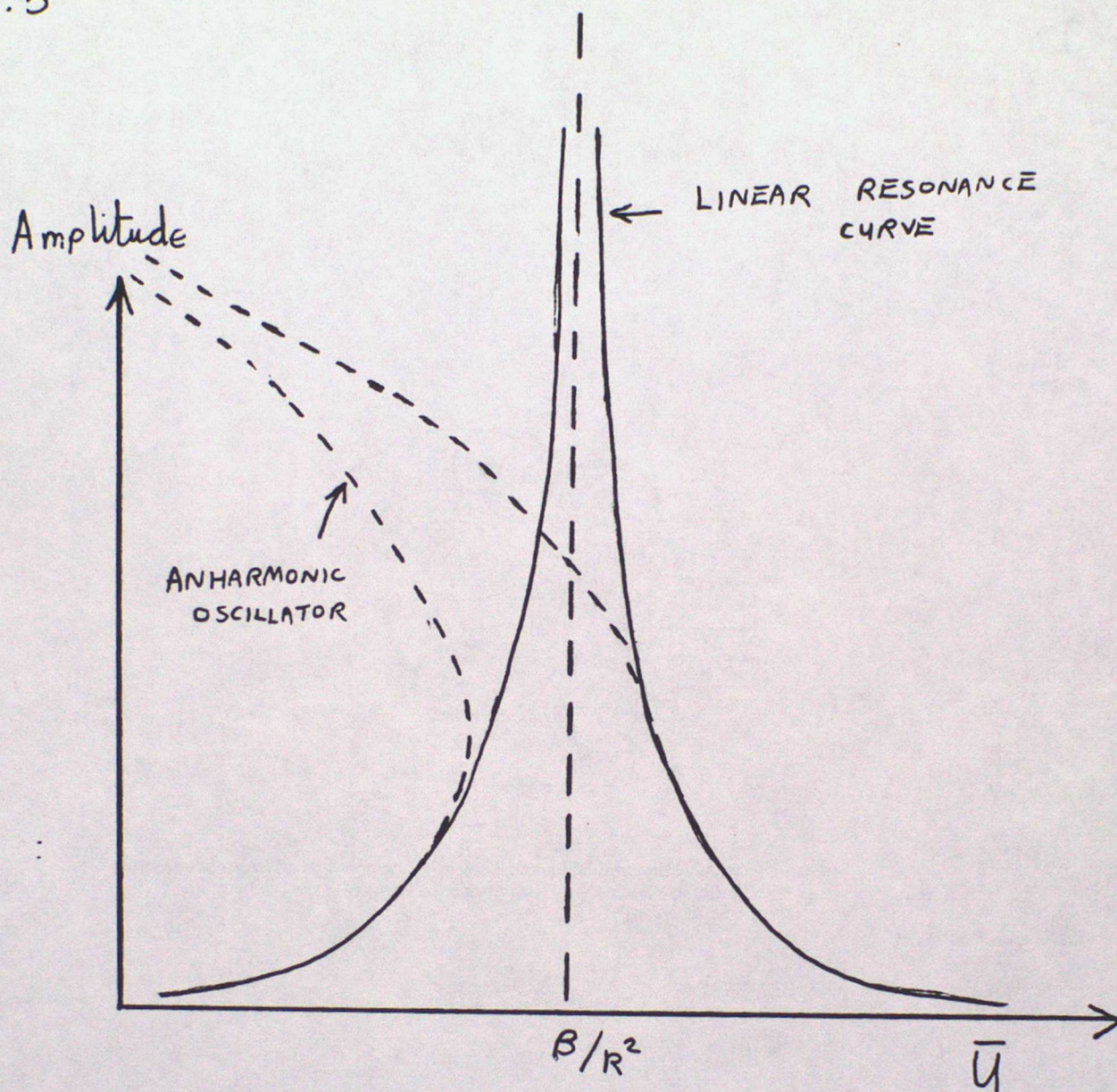
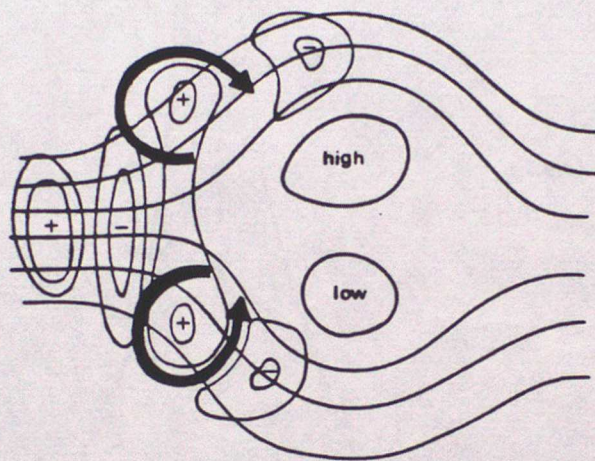




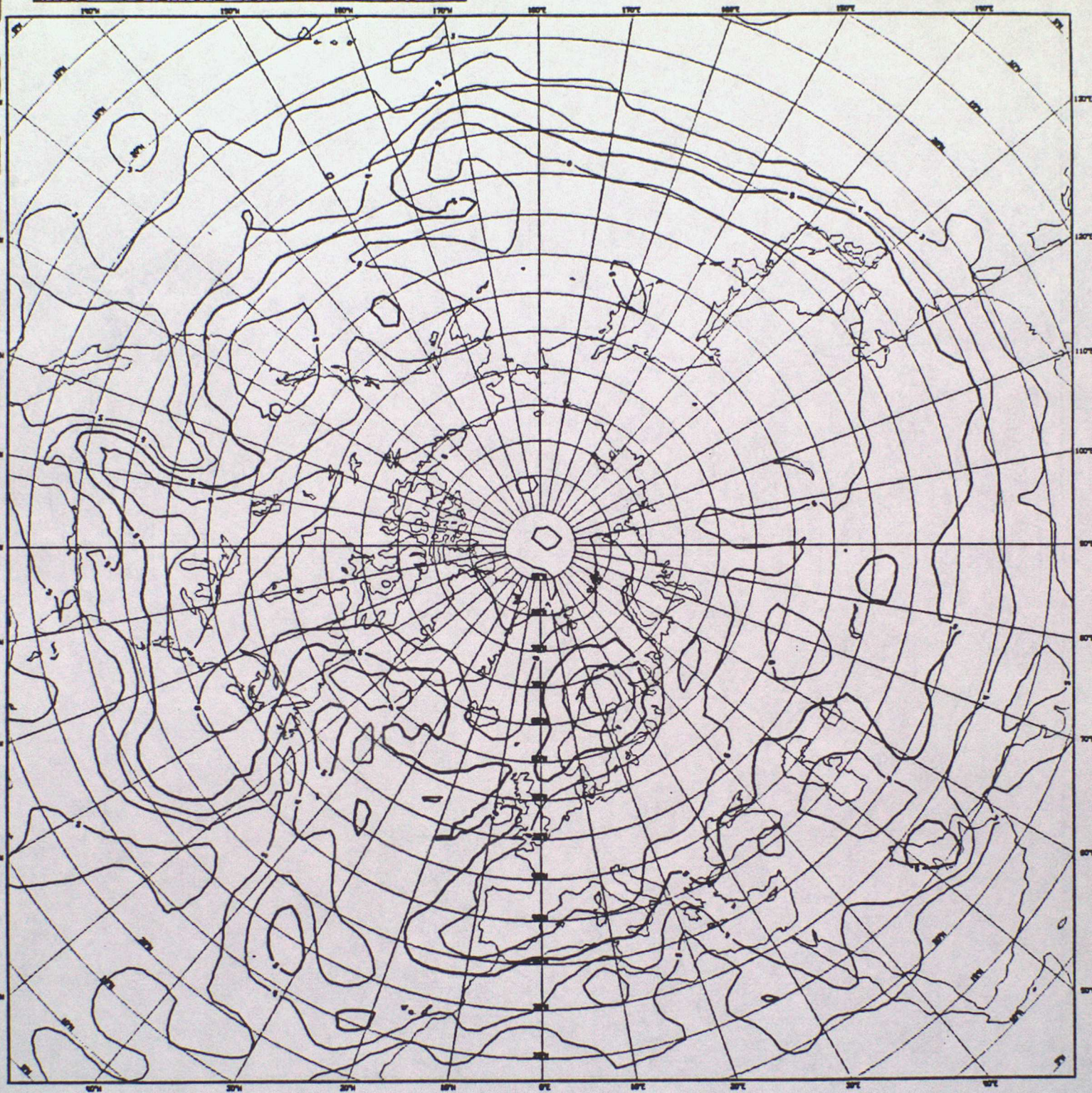
Fig. 6



Schematic picture of the production and subsequent deformation of eddies propagating into a split jetstream together with their associated vorticity forcing pattern.



ERTEL POTENTIAL VORTICITY AT 320 K

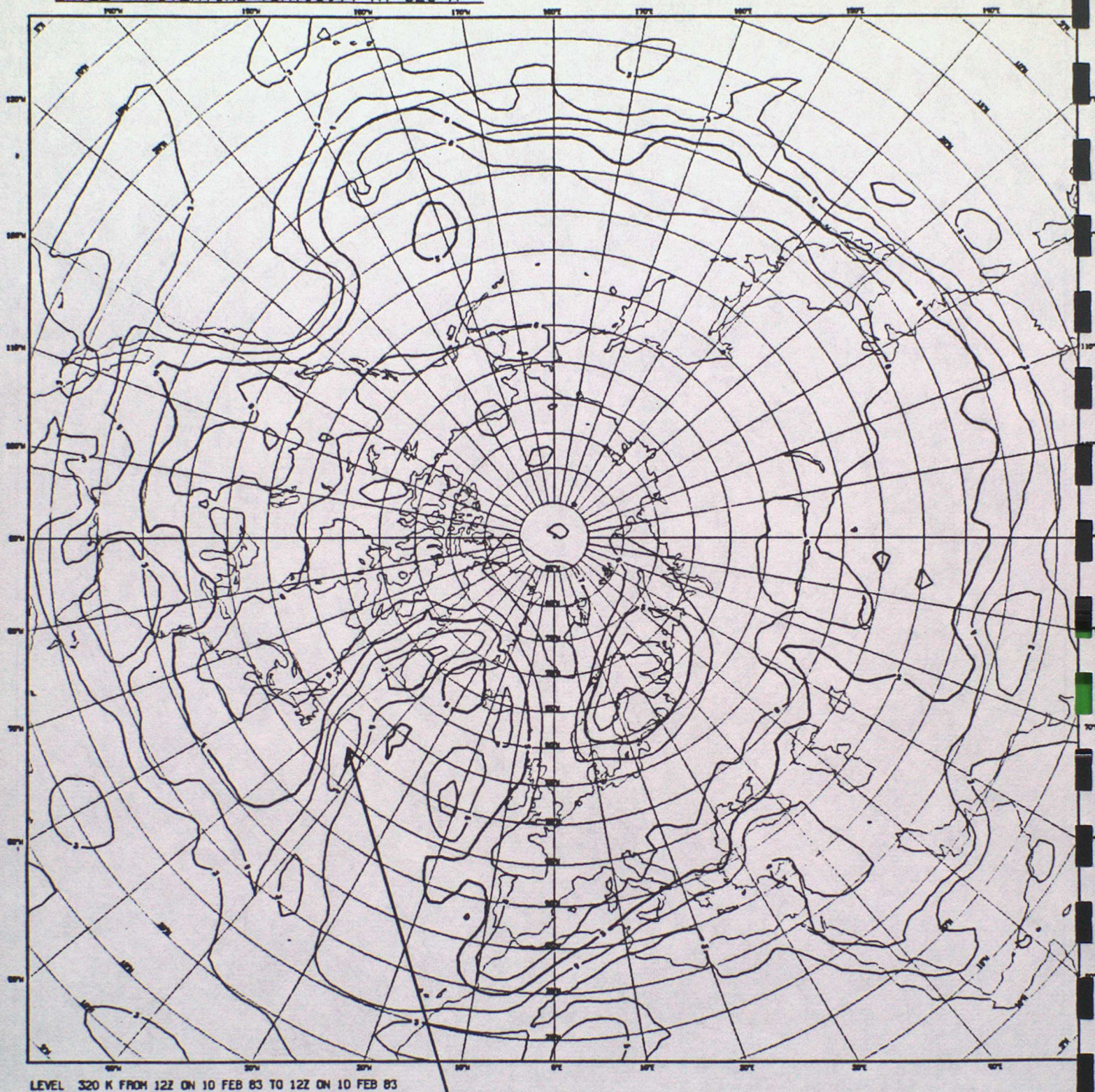


LEVEL 320 K FROM 12Z ON 9 FEB 83 TO 12Z ON 9 FEB 83

Fig. 7(a)



ERTEL POTENTIAL VORTICITY AT 320 K



LOW POTENTIAL VORTICITY 'TONGUE'

Fig. 7 (b)



ERTEL POTENTIAL VORTICITY AT 320 K



Fig. 7(c)



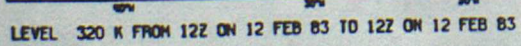
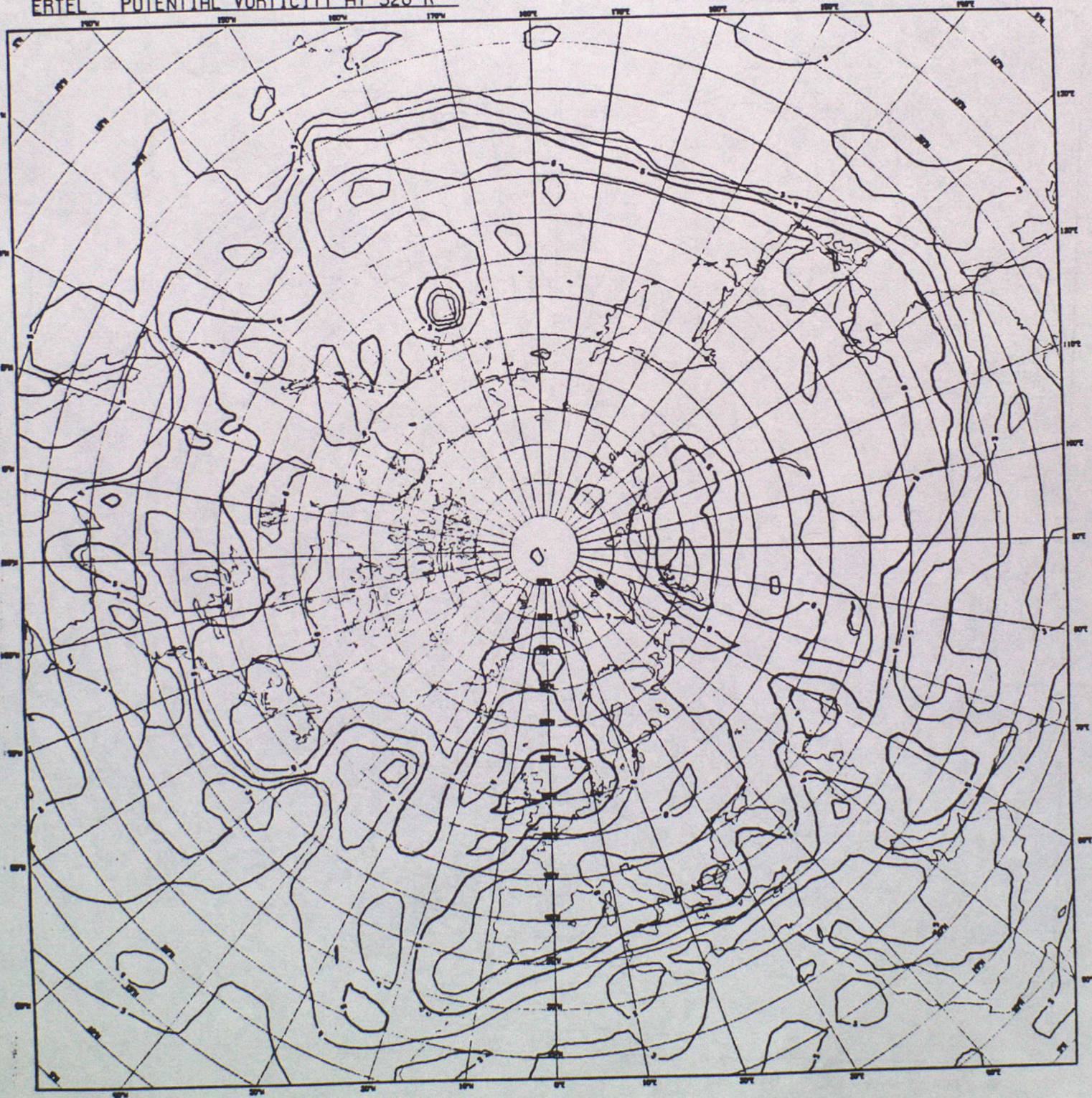




Fig. 7(e)

ERTEL POTENTIAL VORTICITY AT 320 K

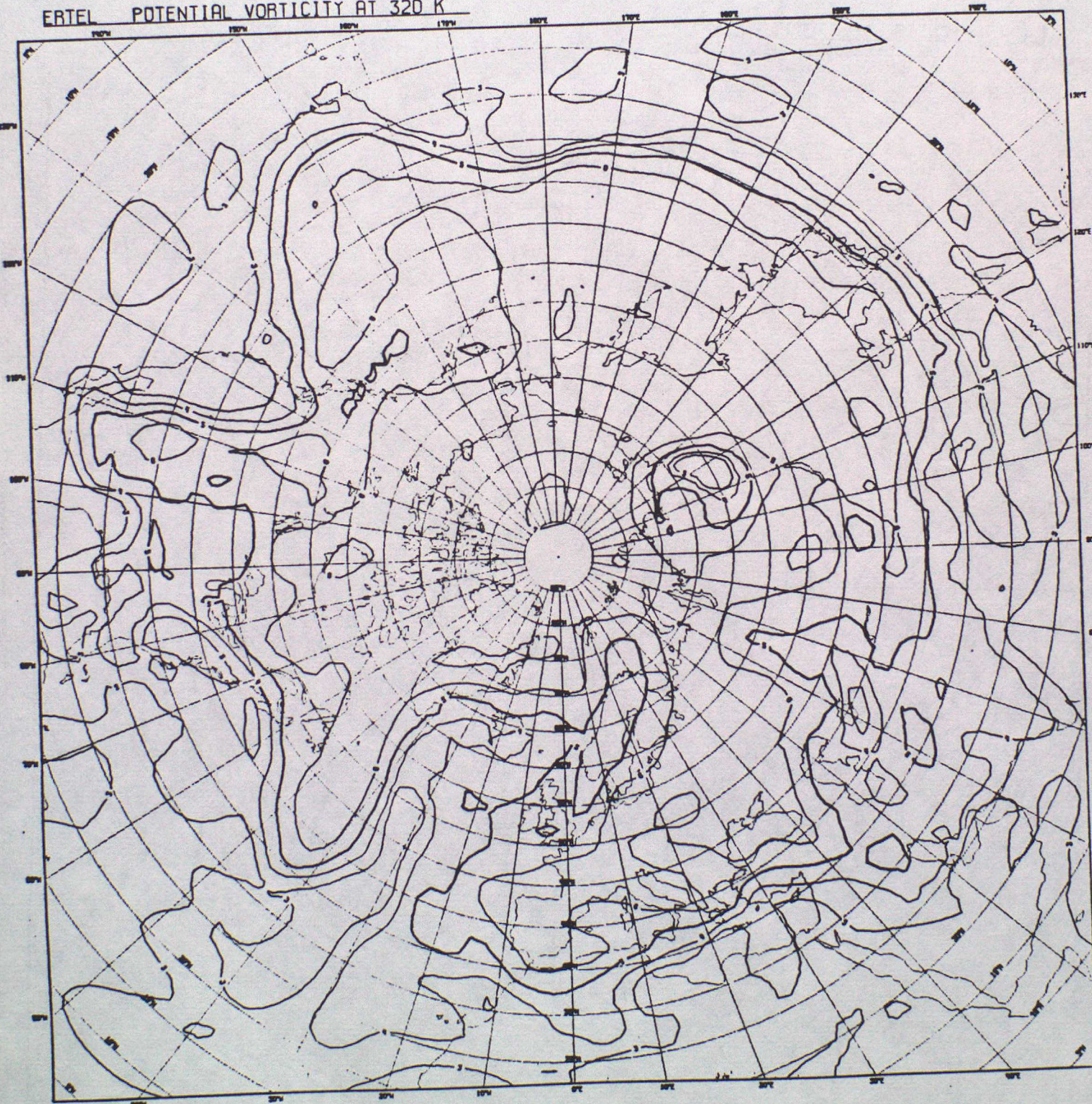


LEVEL 320 K FROM 12Z ON 13 FEB 83 TO 12Z ON 13 FEB 83



Fig. 7(f)

ERTEL POTENTIAL VORTICITY AT 320 K

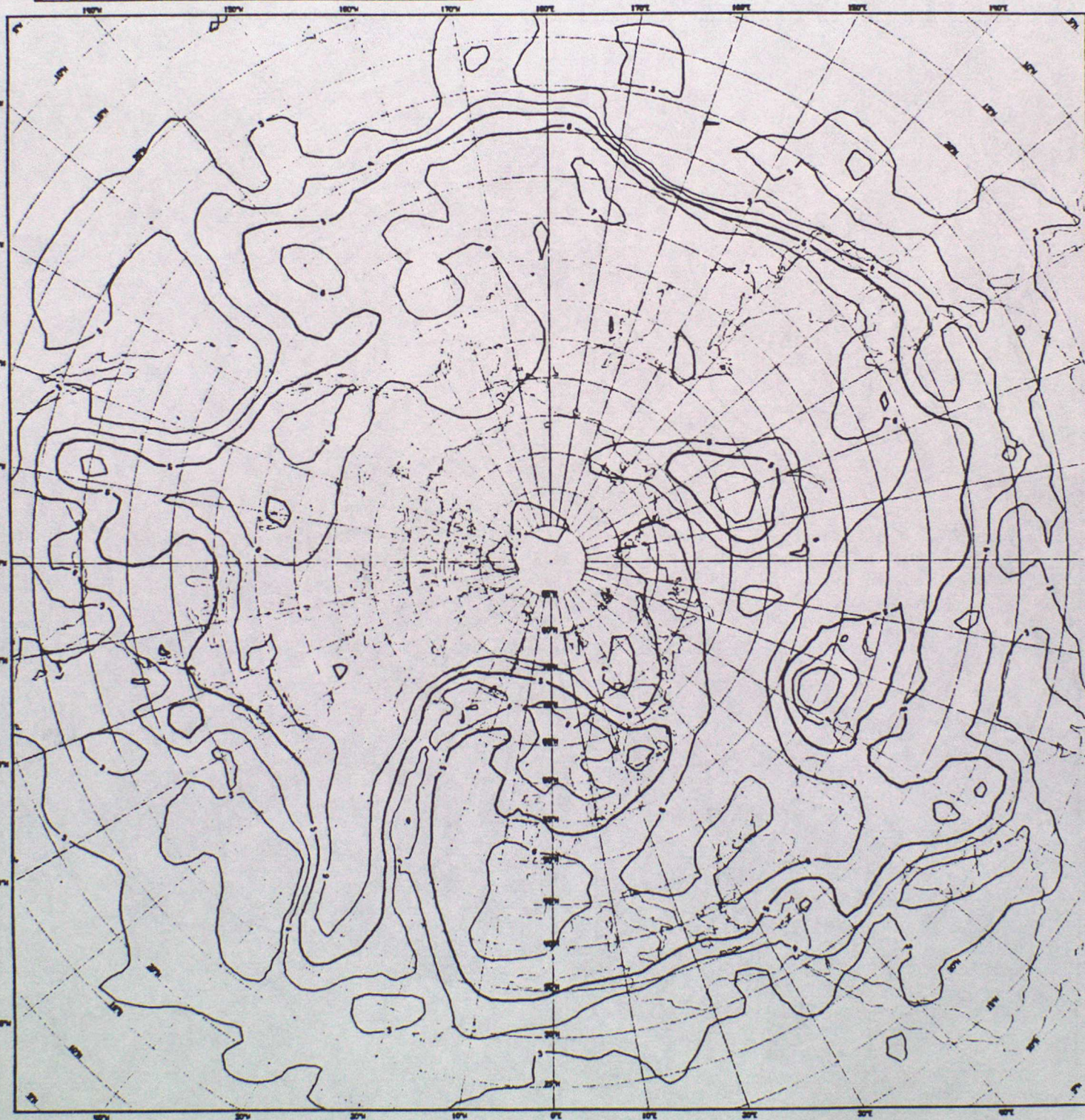


LEVEL 320 K FROM 12Z ON 14 FEB 83 TO 12Z ON 14 FEB 83



Fig. 7(g)

ERTEL POTENTIAL VORTICITY AT 320 K

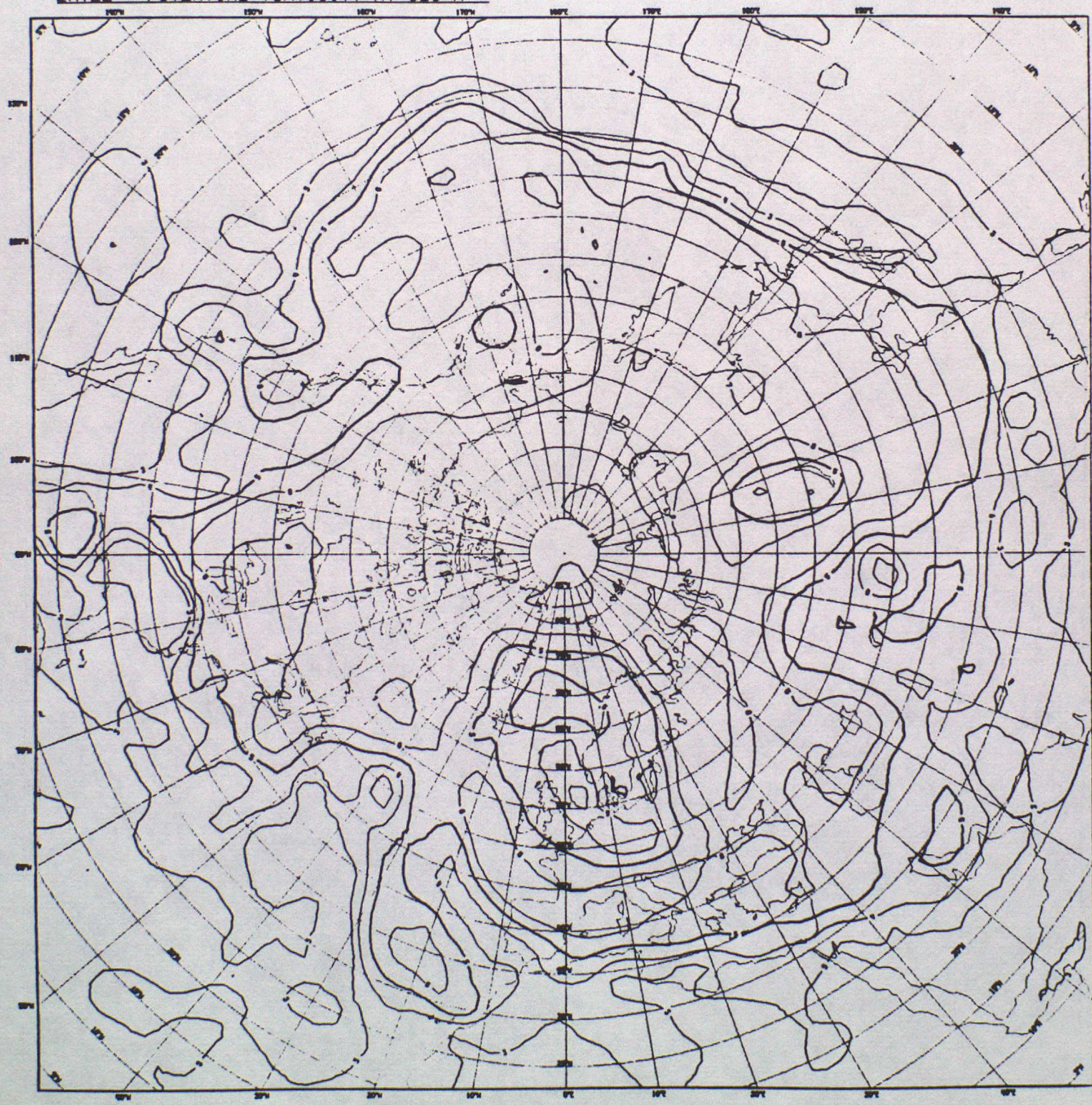


LEVEL 320 K FROM 12Z ON 15 FEB 83 TO 12Z ON 15 FEB 83



Fig. 7(h)

ERTEL POTENTIAL VORTICITY AT 320 K



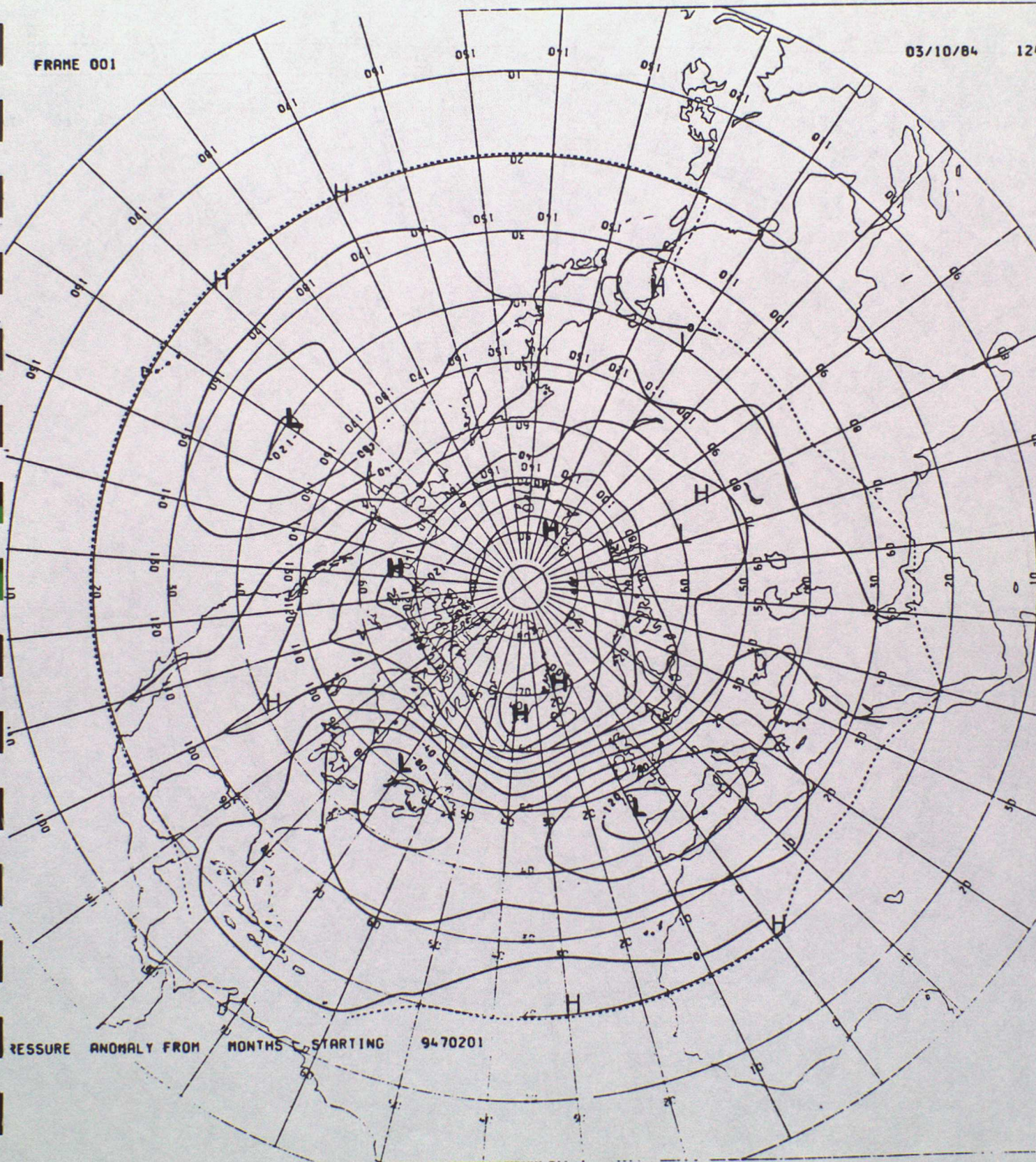
LEVEL 320 K FROM 12Z ON 16 FEB 83 TO 12Z ON 16 FEB 83



Fig. 8 (a)

FRAME 001

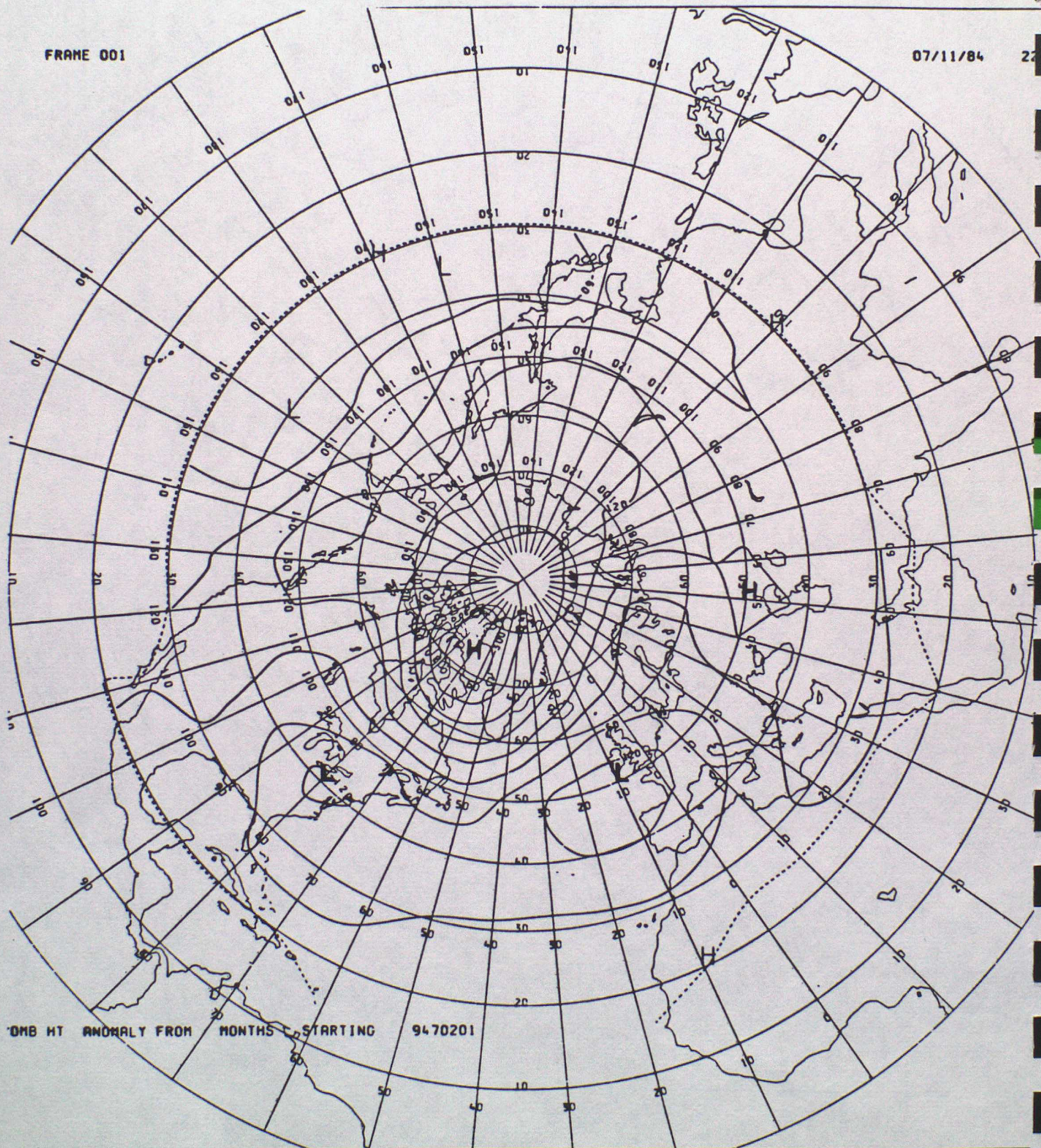
03/10/84 121



PRESSURE ANOMALY FROM MONTHS STARTING 9470201



Fig. 8 (b)

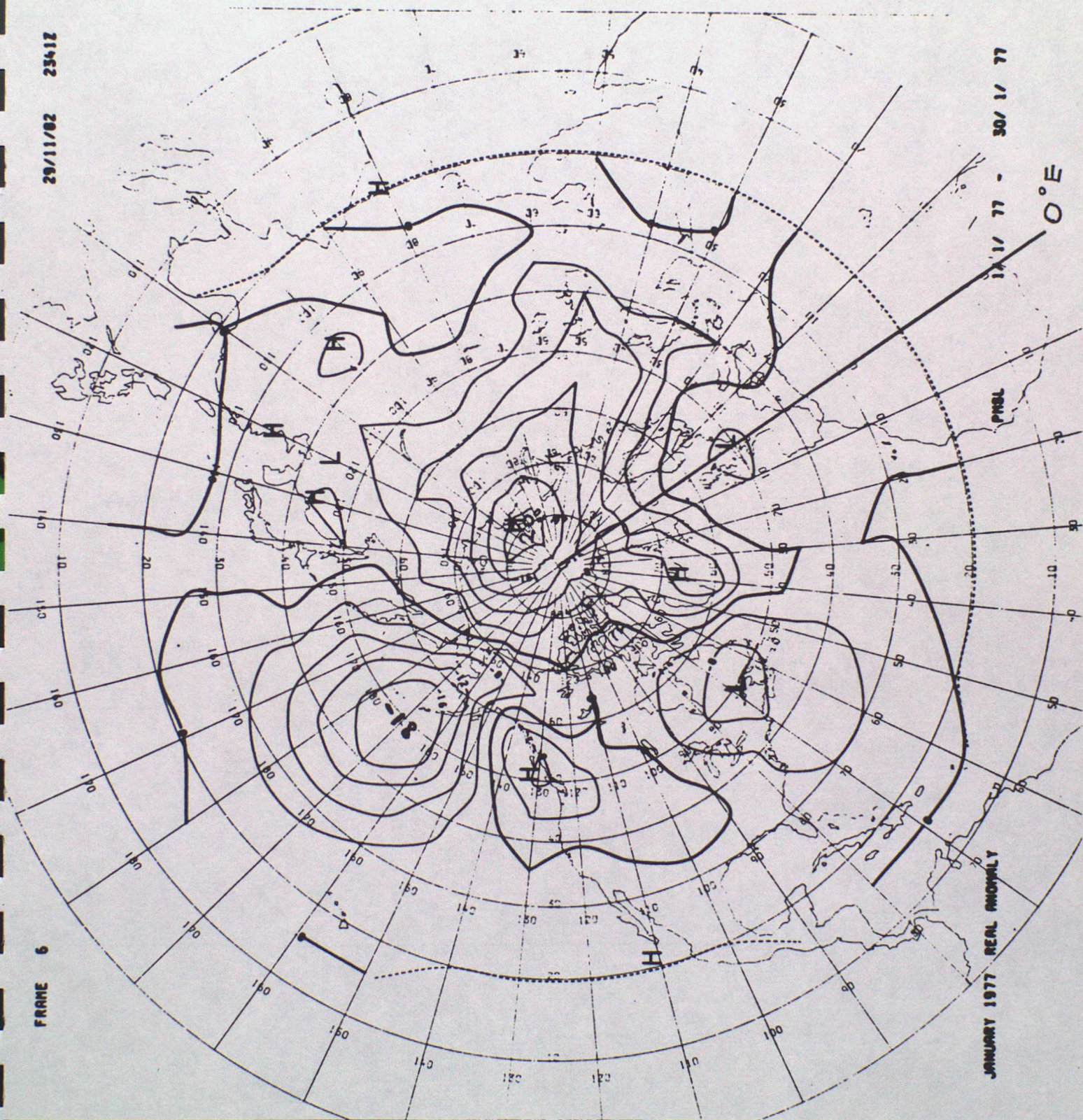




FRAME 6

29/11/82 2341Z

Fig. 9



JANUARY 1977 REAL ANOMALY

17/1/77 - 30/1/77

0°E



### Lecture 3    Dynamics of the monthly-mean climate

We consider one month to be the smallest averaging time interval that could be used for a local (in space) definition of climate to make sense. Implicit in this choice is the need to average over many baroclinic wave life cycles (life cycle time scale  $\sim 7$  days). Ideally, one would like to explain all of the major time-averaged synoptic features such as the Icelandic low and Siberian anticyclone in winter and the Azores High and Indian monsoon in summer together with the positions of the major storm tracks. A physical understanding of the principal dynamical factors involved in determining the strength and position of these phenomena might then allow their inter-annual variability to be forecast. Whilst this is a rather ambitious goal the idealised theoretical models developed along the way provide one with a dynamical framework with respect to which one can develop and interpret diagnostics, (eg  $\underline{Q}$  - vectors, Hoskins, et al (1978)). The classical approach has been to try to understand features of the zonally-averaged climate (eg three-cell mean meridional circulation) and relate them to heat and momentum budget requirements. Since the zonally-averaged climatic fields represent much of the observed variation across the globe it is important to have a dynamically-consistent picture of the underlying mechanics which determines them.

#### (a) Heat transfer

The latitudinal imbalance of net heating in vertical columns (extending into the ground/sea and throughout the atmosphere) is determined primarily by the geometrically-controlled variation of insolation and the weak latitudinal dependence of outgoing infra-red radiation. The latter is at least partly due to the dominance of water vapour amongst the other infra-red radiating tri-atomic molecules and the fact that the uppermost



optically black layer of water vapour occurs at a temperature fixed by freezing and precipitation ( $\sim -18^{\circ}\text{C}$ ). Much of the heat energy surplus in the tropics is not immediately available since solar radiation over large regions is absorbed into the upper few metres of the oceans. It is subsequently released to the atmosphere mainly through evaporation into the Trade Winds and ultimately converted to sensible heat energy through condensation on ascent in deep tropical convection. The warming influence of this latent heat release is transmitted to tropical regions distant from the convection by forced subsidence in association with the radiation of inertia-gravity waves but particularly Kelvin and Rossby-gravity modes, (Gill, 1982).

Heat energy is removed from the subtropics in the familiar organised baroclinic weather systems of synoptic charts and quasi-stationary planetary wave systems, (Lecture 1). This type of large-scale 'sloping' convection (Green 1979) transfers heat polewards and upwards so as to balance the radiative sink in higher latitudes. During autumn and winter the middle latitude oceans give up much heat energy stored in them during the summer providing depressions with considerable latent heat energy which can be organised and released in 'explosive cyclogenesis'.

A simple zonally-averaged climate model much loved by the climatologist requires the tropospheric, depth-averaged temperature to be determined given fixed or parametrized heat sources and sinks. From this temperature distribution, the thermal wind equation can be invoked to find a consistent wind field provided that some assumption is made about the surface wind (eg no flow). In these models, poleward heat transport is usually represented by a non-linear diffusion law where the eddy diffusion



or transfer coefficient (Green, 1970) is a function of the poleward temperature gradient. In fact, Green gives theoretical and observational support for the existence of a heat transfer law of the form:

$$\overline{v\phi} = 5.5 \times 10^{-3} \left( \frac{g}{B} \right)^{1/2} \Delta\phi^2$$

where the overbar refers to a zonal, height and time average,  $g$  is the acceleration due to gravity,  $B$  is a mean static stability,  $\phi$  is the logarithm of potential temperature and  $\Delta\phi$  is the pole-equator difference in  $\phi$ . In spite of being cast in the form of a diffusion law, Green's transfer theory is independent of mixing ideas.

Stone (1978) takes a very different viewpoint and suggests that baroclinic instability is super-efficient at transporting heat for temperature gradients in excess of a certain critical gradient, defined in accordance with two-level quasi-geostrophic theory on a beta-plane. He argues that the observed poleward temperature gradient will never be far from this critical value since smaller gradients lead to very weak baroclinic instability which is unable to satisfy the global heat budget requirement and a slightly larger temperature gradient causes too much heat to be transported. This critical temperature gradient turns out to be proportional to the cotangent of latitude and the static stability. Observational evidence is given in Stone's paper to support this 'baroclinic adjustment' hypothesis in middle latitudes.

Another interesting hypothesis concerning the zonal-mean temperature is that of maximum available potential energy generation. (Lorenz, 1960; Paltridge, 1978 and Shutts, 1981.) Given heat sources and sinks which are themselves some function of temperature, it is hypothesized that the time



and zonal-mean temperature is such that the available potential energy (APE) generation rate is a maximum. If for instance we could write the time-mean diabatic heating rate  $Q(y)$  as:

$$Q(y) = -\gamma (\delta T(y) - \delta T_*(y))$$

where  $y$  is latitude,  $\gamma^{-1}$  is a time constant,  $\delta T$  is the temperature perturbation about some mean and  $\delta T_*$  is some known equilibrium temperature perturbation such that the mean of  $Q$  is zero, then the APE generation rate is proportional to:

$$\int Q \delta T dy = -\gamma \int (\delta T - \delta T_*) \delta T dy$$

which is a maximum if  $\delta T = 1/2 \delta T_*(y)$ . Of course in practice  $Q$  is not merely a function of  $\delta T$  and the detailed physics (eg cloud albedo) cannot be ignored.

(b) Momentum transfer

A theory which predicts the latitudinal distribution of temperature is of very limited use since it fails to tell us anything about the sense of the winds at the surface and by inference, the frictionally-induced mean meridional circulation. What we require is a dynamical model which can account for the time-mean surface westerlies of middle latitudes and easterlies in the sub-tropics. Since there are no internal atmospheric sources or sinks of momentum in the zonally-averaged sense, frictional stress and wave drag at the surface can only be balanced by the height-integrated flux convergence of momentum. Of course, the surface wind pattern exists because of the momentum transport though observations



alone do not tell us this. The poleward momentum transport required to maintain the mid-latitude surface westerlies is brought about almost entirely by large-scale eddies (quasi-stationary forced planetary waves and baroclinic instabilities) and only in the tropics is the mean meridional circulation important. Even then the very existence of the observed 'Hadley circulation' relies on the presence of large-scale eddy momentum transport and it is incorrect to think of it as an independent agency for transporting heat and momentum. The often quoted notion of the Hadley circulation as the 'flywheel of the general circulation' is misleading. It is simply an ageostrophic response resulting from the destruction of the zonally-averaged thermal wind balance by:

- (a) diabatic heating in equatorial cumulonimbus
- (b) frictional deceleration of the Trades
- (c) a net upper tropospheric sink of westerly momentum due to the poleward transport by large-scale eddies. This causes the Trades and therefore (b).
- (d) radiational cooling in non-precipitating regions throughout the tropics.

The principal reason that eddy transport of momentum dominates the total height-integrated poleward momentum transport is that the net Coriolis torque  $\int_D \rho f v dx dz$  vanishes at any latitude since there must be no long-term mass flux polewards. (D refers to the region of the longitude/height plane above the surface.) The term  $\int \rho \bar{v} \frac{\partial \bar{u}}{\partial y} dz$  which represents the poleward flux of relative momentum due to the mean meridional circulation is small except in the tropics, ( $\bar{\phantom{x}}$  denotes the zonal average.) Figs 1 (a, b) show latitude-height cross-sections of the poleward momentum transport split into transient and stationary wave



contributions for January 1979 based on FGGE data. Note that the transient eddies transport momentum polewards except north of  $60^{\circ}\text{N}$  whereas the stationary waves have a pronounced equatorward component near  $60^{\circ}\text{N}$ . In general, eddy momentum transfer is vertically coherent with a strong peak near the tropopause. The height-integrated momentum flux convergence from these pictures implies a westerly momentum sink at the surface between  $30^{\circ}$  and  $60^{\circ}\text{N}$  (in the time-mean) and an easterly sink between the equator and  $30^{\circ}\text{N}$ . The pattern of zonal winds observed in that month (Fig. 2) were consistent with this required surface momentum exchange - representing as they do the normal climatological picture.

The zonally-averaged pressure field consistent with this distribution of zonal winds (through geostrophy) implies a low pressure belt at  $60^{\circ}\text{N}$  and sub-tropical anticyclone belt at  $30^{\circ}\text{N}$ . Frictionally-induced ageostrophic motion at the surface then suggests that the former regions will be cloudy and wet and the latter clear and dry.

The transport of momentum by large-scale eddies is therefore crucial to the determination of the mean state of the atmosphere. The question that dynamical meteorologists have tried to address for at least forty years is, 'What dynamical principles govern the sense of the momentum transport?' Many different ways of interpreting the tendency of baroclinic waves to transport momentum polewards have been proposed - all of which seem perfectly plausible. Most depend upon the existence of a 'beta-effect' ie variation of the Coriolis parameter with latitude. It can be shown that disturbances forced in mid-latitudes will tend to propagate as Rossby waves towards the equator and in the process exhibit a marked NE-SW orientation - the signature of poleward momentum transfer, (Hoskins, Simmons and Andrew (1977)). Baroclinic instability can, to some extent, be



regarded as an initial rapid disturbance energy growth phase associated with the conversion of zonal to eddy available potential energy followed in the mature phase by upward and equatorward Rossby wave radiation, (Edmon et al, 1980).

The polar easterlies north of  $60^{\circ}\text{N}$  are not a very important aspect of the general circulation since they only occupy a small area of the earth's surface and are highly variable from month to month. Even so, they appear to be consistent with the observed equatorward flux of momentum in high latitudes particularly by the stationary waves.

In summary, the zonally-averaged mean state of the troposphere can be thought of as being governed by two eddy transport properties:

- 1) The height-integrated poleward momentum flux which determines the surface winds.
  - 2) The height-integrated poleward heat flux which gives, through the thermal wind relation, the mean vertical wind shear
- though parametrized relations between the surface stress and wind and the temperature and heat source are required to complete the description.

Longitudinal variations of eddy heat and momentum transport are currently thought to contribute strongly to the zonal asymmetry of the mean circulation in addition to the topographical forcing functions discussed in Lecture 1.



## References

- Edmon, H.J., Hoskins, B.J. (1980) 'Eliassen-Palm cross-sections for the troposphere'.  
J. Atmos. Sci., 37, 2600-2616.
- Gill, A.E. (1982) 'Atmosphere-Ocean Dynamics'  
Academic Press, International  
Geophysics Series, Vol. 30.
- Green, J.S.A. (1970) 'Transfer properties of the  
large-scale eddies and the general  
circulation of the atmosphere'.  
Quart. J. Roy. Met. Soc., 96,  
157-185.
- Green, J.S.A. (1979) 'Topics in dynamical meteorology: 8.  
Trough-ridge systems as slantwise  
convection'.  
Weather, 34, 2-10.
- Hoskins, B.J., Draghici, I. (1978) 'A new look at the  $\omega$ -Equation'.  
and Davies, H.C. Quart. J. Roy. Met. Soc., 104,  
31-38.
- Hoskins, B.J., Simmons, A.J. (1977) 'Energy dispersion in a barotropic  
and Andrews, D.G. atmosphere'.  
Quart. J. Roy. Met. Soc., 103,  
553-567.

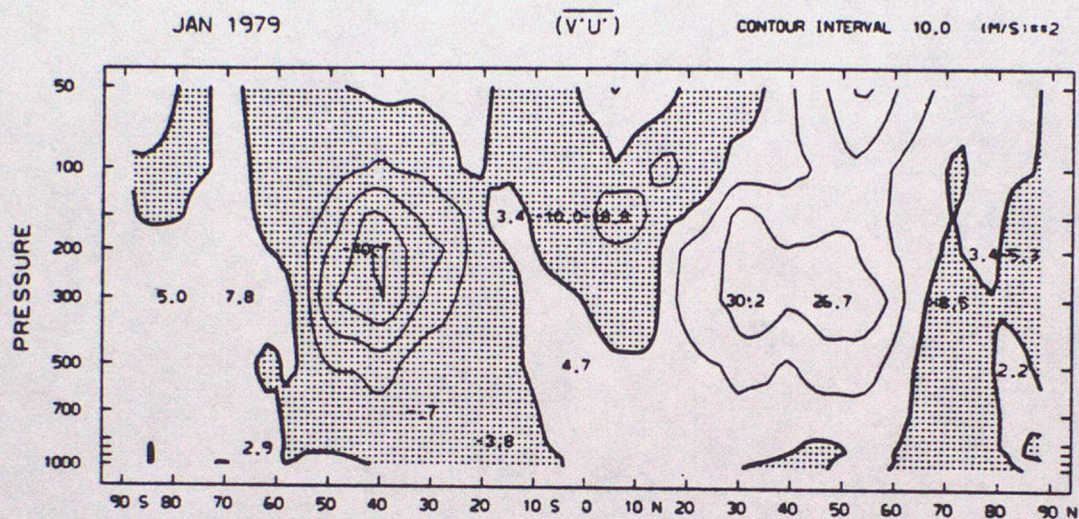


- Lorenz, E.N. (1960) 'Generation of available potential energy and the intensity of the general circulation'. Dynamics of Climate, R.L. Pfeffer, Ed., Pergamon Press, 86-92.
- Paltridge, G.W. (1978) 'The steady state format of global climate'. Quart. J. Roy. Met. Soc., 104, 927-945.
- Shutts, G.J. (1981) 'Maximum entropy production states in quasi-geostrophic dynamical models'. Quart. J. Roy. Met. Soc., 107, 503-520.
- Stone, P.H. (1978) 'Baroclinic adjustment'. J. Atmos. Sci., 35, 561-571.

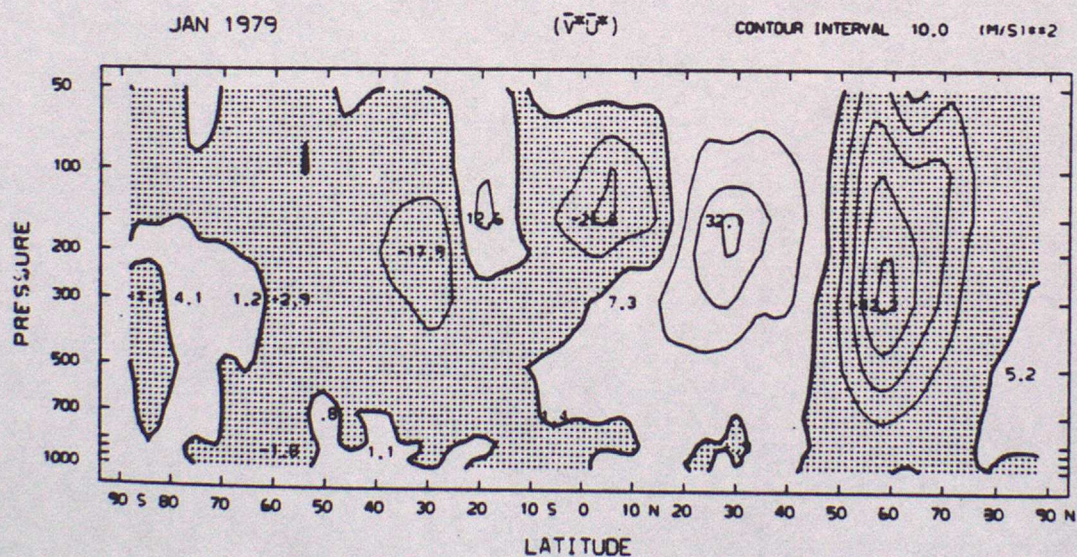


Fig. 1

(a)



(b)



Poleward flux of westerly momentum due to (a) transient eddies, (b) stationary eddies during January 1979 based on GFDL analyses of FGGE data.



## Lecture 4 - Semi-geostrophic frontogenesis

### (a) Symmetrically stable parallel flows

A natural class of time-independent solutions of the full equations of motion in a rotating system are those representing rectilinear flow in geostrophic and hydrostatic balance. To show this and demonstrate semi-geostrophic theory in its simplest terms we will use the Boussinesq equation system put forward by Hoskins and Bretherton (1972) namely:

$$\frac{Du}{Dt} - fv + \frac{\partial \phi}{\partial x} = 0 \quad (1)$$

$$\frac{Dv}{Dt} + fu + \frac{\partial \phi}{\partial y} = 0 \quad (2)$$

$$\frac{\partial u}{\partial x} + \frac{\partial v}{\partial y} + \frac{\partial w}{\partial z} = 0 \quad (3)$$

$$\frac{D\theta}{Dt} = 0 \quad (4)$$

$$\frac{\partial \phi}{\partial z} = g\theta/\theta_0 \quad (5)$$

noting that  $z$  is a pseudo-height coordinate given by:

$$z = \left[ 1 - \left( \frac{p}{p_0} \right)^{(\gamma-1)/\gamma} \right] \frac{\gamma H_s}{\gamma-1}$$

with:  $p$  = pressure

$p_0$  = a reference pressure

$\gamma$  = ratio of specific heats

$H_s$  = density scale height



$\phi$  = geopotential

$\theta_0$  = a constant reference value of  $\theta$

and other symbols have their usual meaning.

An exact solution to these equations is:

$$u = 0$$

$$V = V(x, z)$$

$$w = 0$$

$$\theta = \theta(x, z)$$

$$\phi = \phi(x, z)$$

such that:

$$fV = \frac{\partial \phi}{\partial x} = f v_g \quad (\text{geostrophic balance}) \quad (6)$$

$$\frac{g\theta}{\theta_0} = \frac{\partial \phi}{\partial z} \quad (\text{hydrostatic balance}) \quad (7)$$

implying a thermal wind equation:

$$f \frac{\partial v_g}{\partial z} = \frac{g}{\theta_0} \frac{\partial \theta}{\partial x} \quad (8)$$

Clearly, one can choose any potential temperature distribution  $\theta(x, z)$  and use (8) to find a consistent  $v_g$ , though the stability of the resulting flow could not be guaranteed. For instance, any flow field for which  $\frac{\partial \theta}{\partial z} < 0$  locally would obviously not be stable. It can be shown that even if  $\frac{\partial \theta}{\partial z} > 0$  everywhere the flow is not necessarily stable to two-dimensional perturbations. Before giving a heuristic argument to explain the stability of parallel flow we must introduce the concept of absolute momentum, M.



Considering perturbations to the basic state given by Eqs (6) and (7) which are two-dimensional and oriented in the y-direction then Eq (2) can be written as:

$$\frac{D}{Dt}(v + fx) = \frac{DM}{Dt} = 0 \quad (9)$$

since  $\frac{\partial}{\partial y} \equiv 0$ . The absolute momentum  $M = fx + v$  can be considered to be the rectilinear analogue of angular momentum which is conserved following displacements in circular flow. Let us now examine the forces exerted on a two-dimensional parcel as it is displaced from its equilibrium position. Fig. 1(a) represents the local disposition of  $M$  and  $\theta$  surfaces corresponding to a particular rectilinear flow field. A parcel at point A with absolute momentum  $M_0$  and potential temperature  $\theta_0$  is moved along the  $M_0$  surface of the undisturbed field of motion. Since  $M$  is conserved, the  $v$ -component of the parcel will be equal to that of its environment and therefore in geostrophic balance. At point B the parcel will be potentially cooler than the environment by  $\Delta\theta$  and so will experience a downward acceleration of  $g\Delta\theta/\theta_0$ . Since this has a component directed from B to A, work will be required to move the parcel in this direction. Moving the parcel from A to C generates no excess buoyancy but it now has an excess absolute momentum (and  $v$ -component) of  $\Delta M$  which leads to a Coriolis force acting in the  $x$ -direction. Again, work is required to move the parcel from A to C. It can be shown that this follows for a parcel displacement in any direction and so the flow is stable. On the other hand, the orientations of  $\theta$  and  $M$  surfaces in Fig. 1(b) causes corresponding forces in the opposite directions and the system is unstable. These two cases may be distinguished by the sign of the scalar product



$-(\underline{j} \wedge \nabla M) \cdot \nabla \theta$  (c.f. Figs 1(a) and (b)). Now  $-\underline{j} \wedge \nabla M$   
 ( $\underline{j}$  is the unit vector into the plane of Figs 1(a) & (b))

may be written as:

$$\underline{k} \left( f + \frac{\partial v_g}{\partial x} \right) - \underline{i} \frac{\partial v_g}{\partial z}$$

which is the absolute vorticity vector  $\underline{\zeta}_a$  and so:

$$q = \underline{\zeta}_a \cdot \nabla \theta$$

must be positive for stability.

$q$  is the Ertel potential vorticity for incompressible flow.

If the configuration of Fig. 1(a) were turned upside down  $q$  would not be altered but the resulting flow would obviously be unstable with  $\frac{\partial \theta}{\partial z} < 0$ . Stability may be ensured by requiring both  $q$  and  $\frac{\partial \theta}{\partial z} > 0$  or both  $q$  and  $\frac{\partial M}{\partial x} > 0$ .

Another way of expressing this stability condition is that the matrix

$$\begin{pmatrix} M_x & M_z \\ \theta_x & \theta_z \end{pmatrix} \quad M_x = \frac{\partial M}{\partial x} \text{ etc.}$$

should be positive-definite (ie has no negative eigenvalues).

In general therefore, rectilinear flows in geostrophic and hydrostatic balance are in stable equilibrium with respect to 2D perturbations when  $q > 0$  and when  $M$  and  $\theta$  increase monotonically with respect to  $x$  and  $z$ .



(b) Slow evolution under deformation

Exact rectilinear motion is not very interesting in its own right since it is time independent. However, if the flow is forced slowly by irreversible physical processes (eg diabatic heating or friction) or dynamically (eg geostrophic deformation) it may evolve to form fronts. If the time scale of this forcing is long compared to  $f^{-1}$  then we may consider the flow to be geostrophic in the y-direction at all times.

Under these conditions we may make the semi-geostrophic assumption and write Eqs (1) and (2) as:

$$\frac{Du_g}{Dt} - fv + \frac{\partial \phi}{\partial x} = 0 \quad (10)$$

$$\frac{Dv_g}{Dt} + fu + \frac{\partial \phi}{\partial y} = 0 \quad (11)$$

which implies that  $\left| \frac{D}{Dt} \right| \ll f$  :

Gradients of  $\theta$  may be concentrated near  $x=0$  under the influence of a pure geostrophic deformation field:

$$\begin{aligned} u_g &= -\alpha x \\ v_g &= \alpha y \end{aligned}$$

where  $\alpha \ll f$  . If such a deformation field is superimposed on a rectilinear flow in the y-direction then Eqs (10) and (11) may be approximated to:

$$fv_g = \frac{\partial \phi}{\partial x}$$

$$\text{and} \quad \frac{Dv_g}{Dt_2} + \alpha v_g + fu = -f\alpha x \quad (12)$$

$$\text{where} \quad \frac{D}{Dt_2} = \frac{\partial}{\partial t} + u \frac{\partial}{\partial x} + w \frac{\partial}{\partial z} \quad \text{and} \quad \frac{\partial \phi}{\partial y} = -fu_g = f\alpha x$$



have been used. Eq (12) can then be written in the simplified form:

$$\frac{DM}{Dt} = -\alpha M \quad (13)$$

Eqs (4) and (13) tell us that if we follow a parcel of fluid then  $\theta$  is conserved and  $M = M(t=0) e^{-\alpha t}$ . The fluid as a whole will continually adjust to maintain thermal wind balance through an ageostrophic cross-frontal circulation. The essential mechanics of frontal formation is very clearly portrayed by the zero potential vorticity model in which  $\theta = \theta(M)$  ie ( $\theta$  and  $M$  surfaces coincide).

We may further simplify the analysis of this problem by considering the fluid to be composed of a finite number of elements each with uniform  $M$  and  $\theta$ . Consider the situation in Fig. 2 in which two elements reside in a rectangular region in the  $(x,z)$  plane. Stability is only possible if the element with the higher  $M$  and  $\theta$  occupies the upper right-hand corner of the rectangle so that effectively  $\frac{\partial \theta}{\partial z}, \frac{\partial M}{\partial x} > 0$ .

Now Margules' classic formula for the slope of a frontal discontinuity can be written as:

$$\frac{dz}{dx} = - \frac{f [M]}{g [\theta/\theta_0]} \quad (14)$$

where  $[ ]$  indicates the difference across the discontinuity. In other words the slope of the interface between elements 1 and 2 in Fig. 2 is constant (in space) and given by  $-f[M_1-M_2]\theta_0/g[\theta_1-\theta_2]$ . Since the volumes (or areas in this case) of the elements are known there is a unique



stable configuration for the elements. If a deformation flow field is imposed as described above then the area, potential temperature and absolute momentum of each element are given by:

$$\begin{aligned} A_i &= A_i(t=0) e^{-\alpha t} \\ \theta_i &= \theta_i(t=0) \\ M_i &= M_i(t=0) e^{-\alpha t} \end{aligned} \quad i=1, 2.$$

The rectangle of fluid will shrink in the x-direction and, according to (14), the slope of the interface will decrease exponentially in time.

Now consider the three element arrangement depicted in Fig. 3(a) which could be thought of as a piecewise constant approximation of  $M$  and  $\theta$  to real continuous data. As deformation is applied the two element interfaces rotate in accordance with (14) at different rates and collide at the lower boundary (Fig. 3(b)). This point corresponds to the formation of a boundary discontinuity when the continuous problem is solved. At later times, element 2 is lifted clear of the lower boundary and we say that the surface discontinuity has propagated into the fluid (Fig. 3(c)). Of course, this element model already contains discontinuities in  $M$  and  $\theta$  at interfaces. The newly created interface between element 1 and 3 can be regarded as a higher order discontinuity by virtue of its bigger jump in  $M$  and  $\theta$ . With a larger number of elements the tendency to form an intruding discontinuity is much more obvious. Figs. 4(a), (b) and (c) show the evolution of the frontal discontinuity in a 28 element generalization of the previous example, (Cullen, 1983 and Chynoweth, 1984).



Element models may be built without the zero potential vorticity restriction  $\theta = \theta(M)$ . Given elements with characteristic values of  $A_i$ ,  $\theta_i$  and  $M_i$ , there exists a unique stable arrangement in a convex domain such as the rectangle (Cullen and Purser, 1984). Elements then have irregular though convex polygonal geometry which will evolve in time under the action of a deformation flow field. Figs. 5(a) and (b) show a non-zero potential vorticity solution at two different times.



## References

- Chynoweth, S (1984) 'Geometric solutions to the Lagrangian semi-geostrophic equations'.  
Met O 11, Tech. Note No. 182.
- Cullen, M J P (1983) 'Solutions to a model of a front forced by deformation'.  
Quart. J. Roy. Met. Soc., 109, 565-573.
- Cullen, M J P and Purser, R J (1984) 'An extended Lagrangian theory of semi-geostrophic frontogenesis'.  
J. Atmos. Sci., 41, 1477-1497.
- Hoskins, B J and Bretherton, F P (1972) 'Atmospheric frontogenesis models: mathematical formulation and solution'.  
J. Atmos. Sci., 29, 11-37.



## Legends

- Fig. 1 (a)  $M$  and  $\theta$  contours for a symmetrically stable rectilinear flow.  
(b) As for (a) except for an unstable flow.
- Fig. 2 A two-element rectilinear flow (the Margules front) showing the initial configuration (solid lines) and after deformation (dashed lines).
- Fig. 3 (a)-(c) Three stages in the deformation of a rectilinear flow composed of three elements.
- Fig. 4 (a)-(c) Three stages in the deformation of 28 element frontal flow with zero potential vorticity. The initial state of (a) shows the instant at which the solution has a discontinuity at the upper and lower boundaries. Two discontinuity lines grow into the fluid at later times (b) and (c) (from Chynoweth, 1984).
- Fig. 5 (a)-(b) Two stages in the deformation of a non-zero potential vorticity flow using the element method.



Fig. 1 (a)

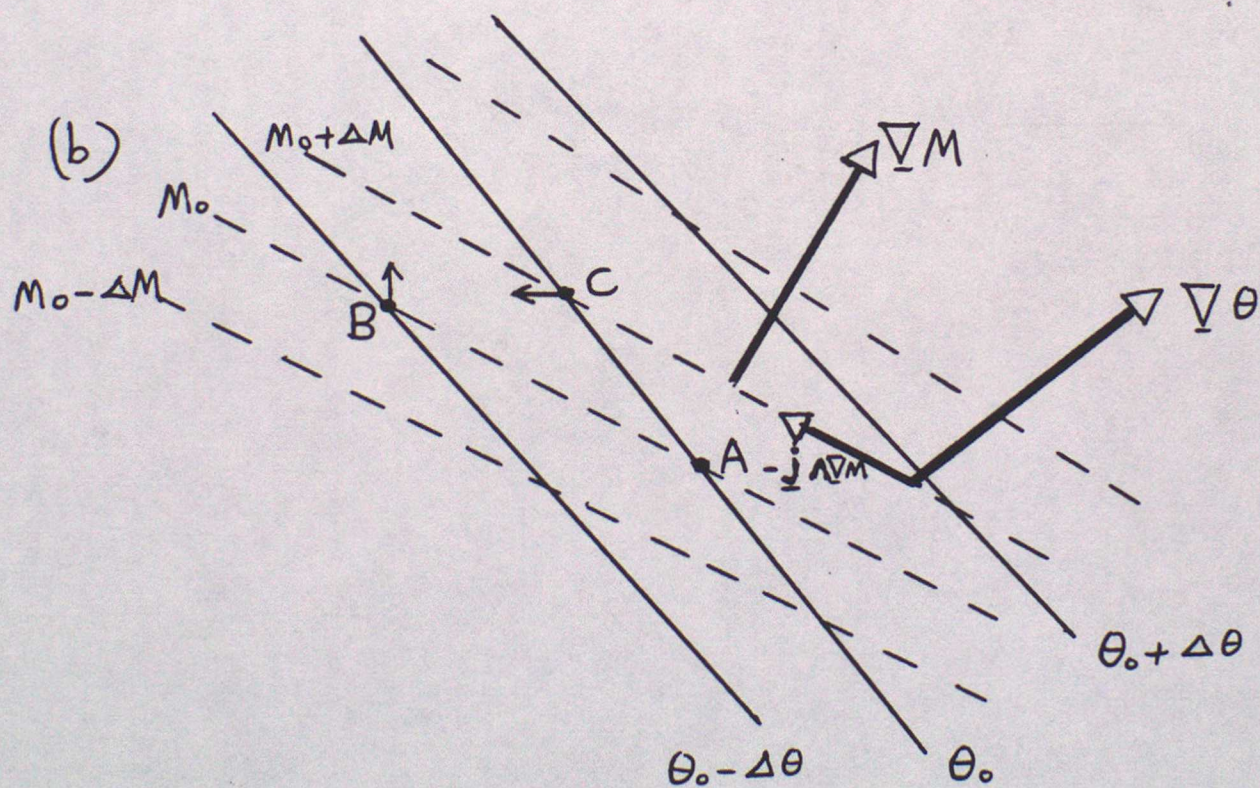
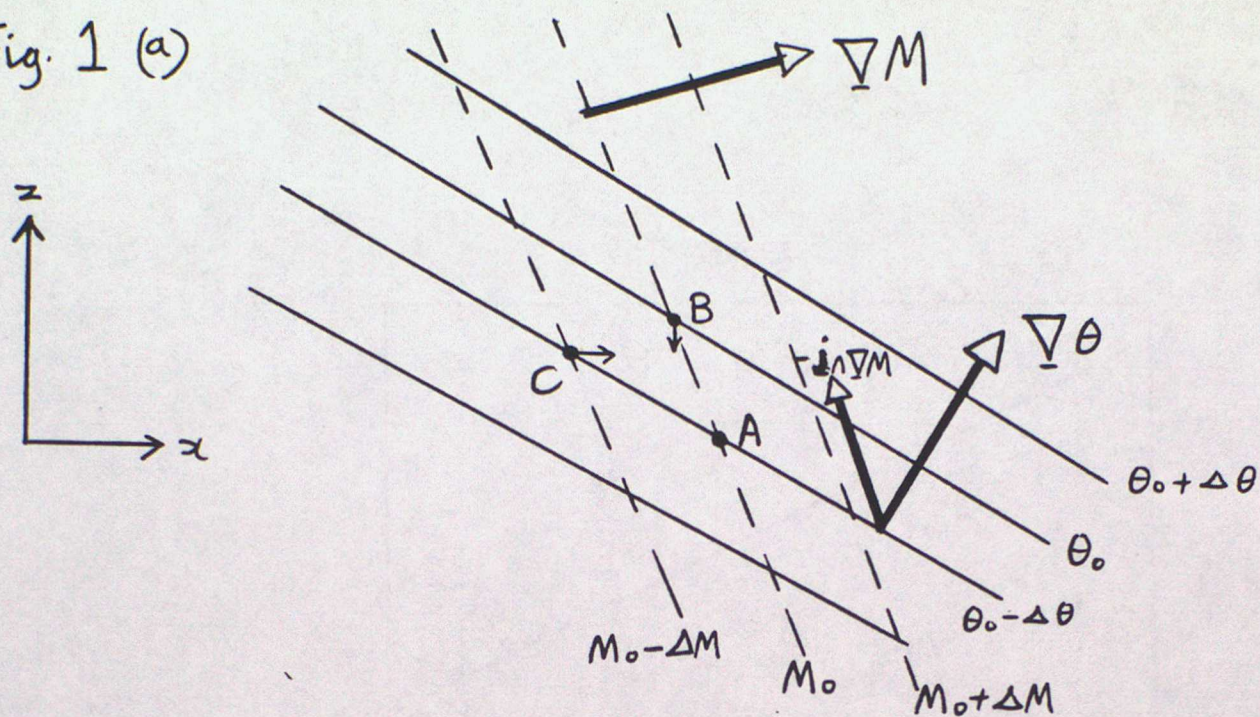
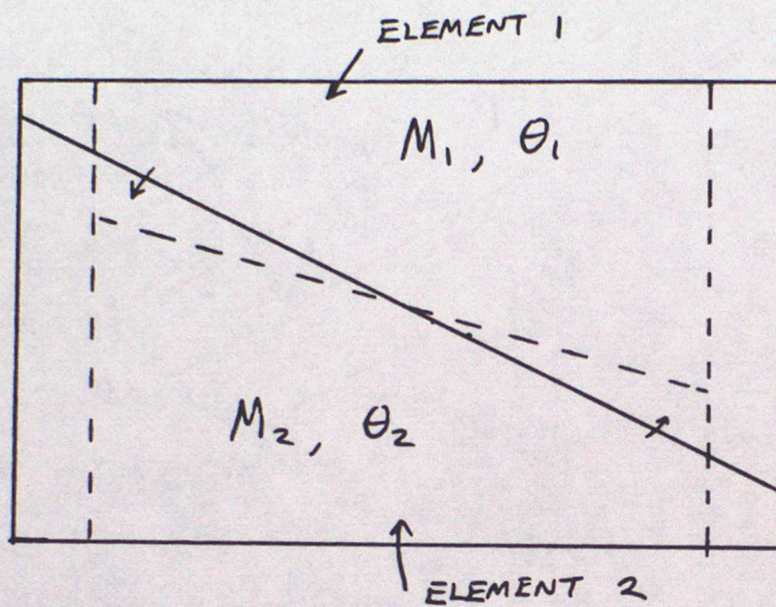




Fig. 2

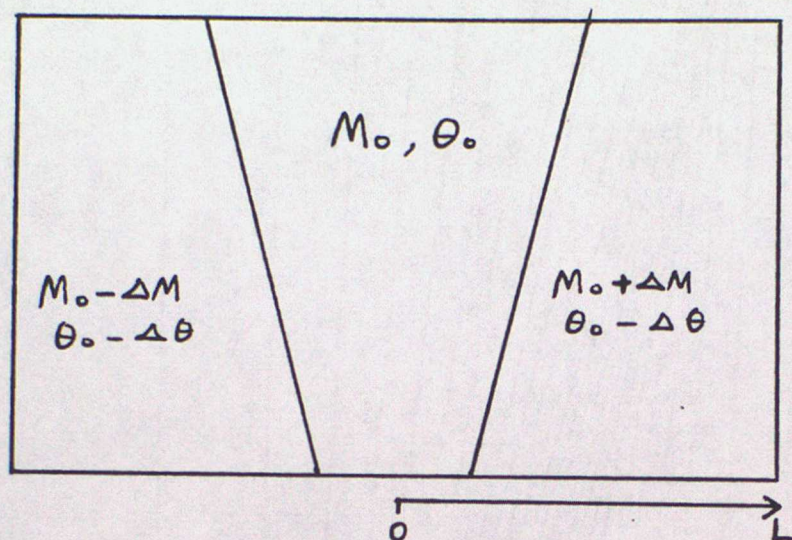


—— Initial Configuration  
- - - - After deformation.



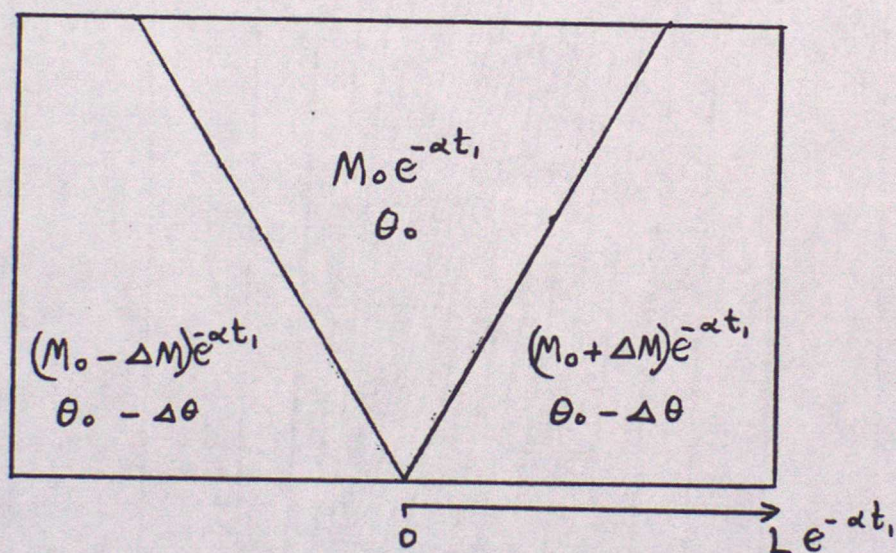
Fig. 3

(a)



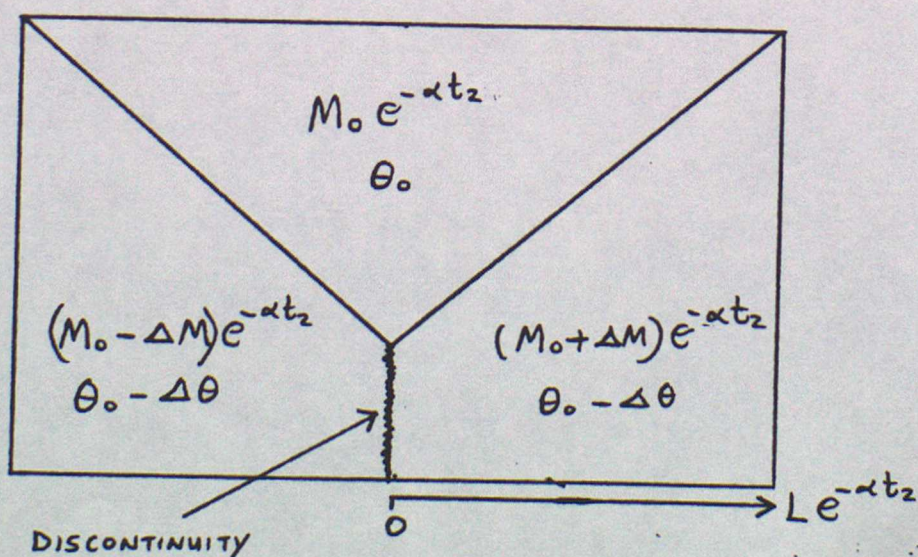
$t = 0$

(b)



$t = t_1$

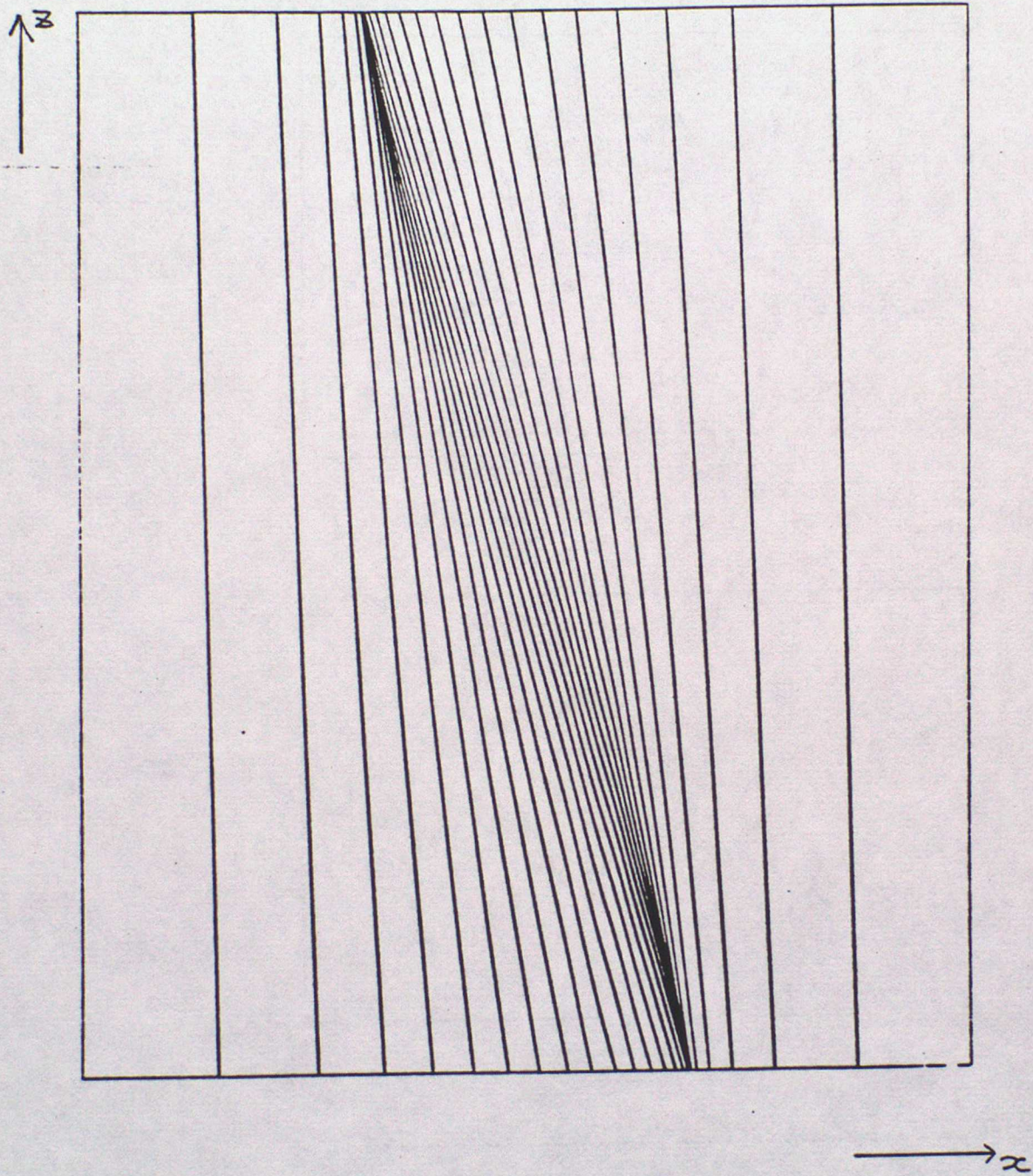
(c)



$t = t_2$



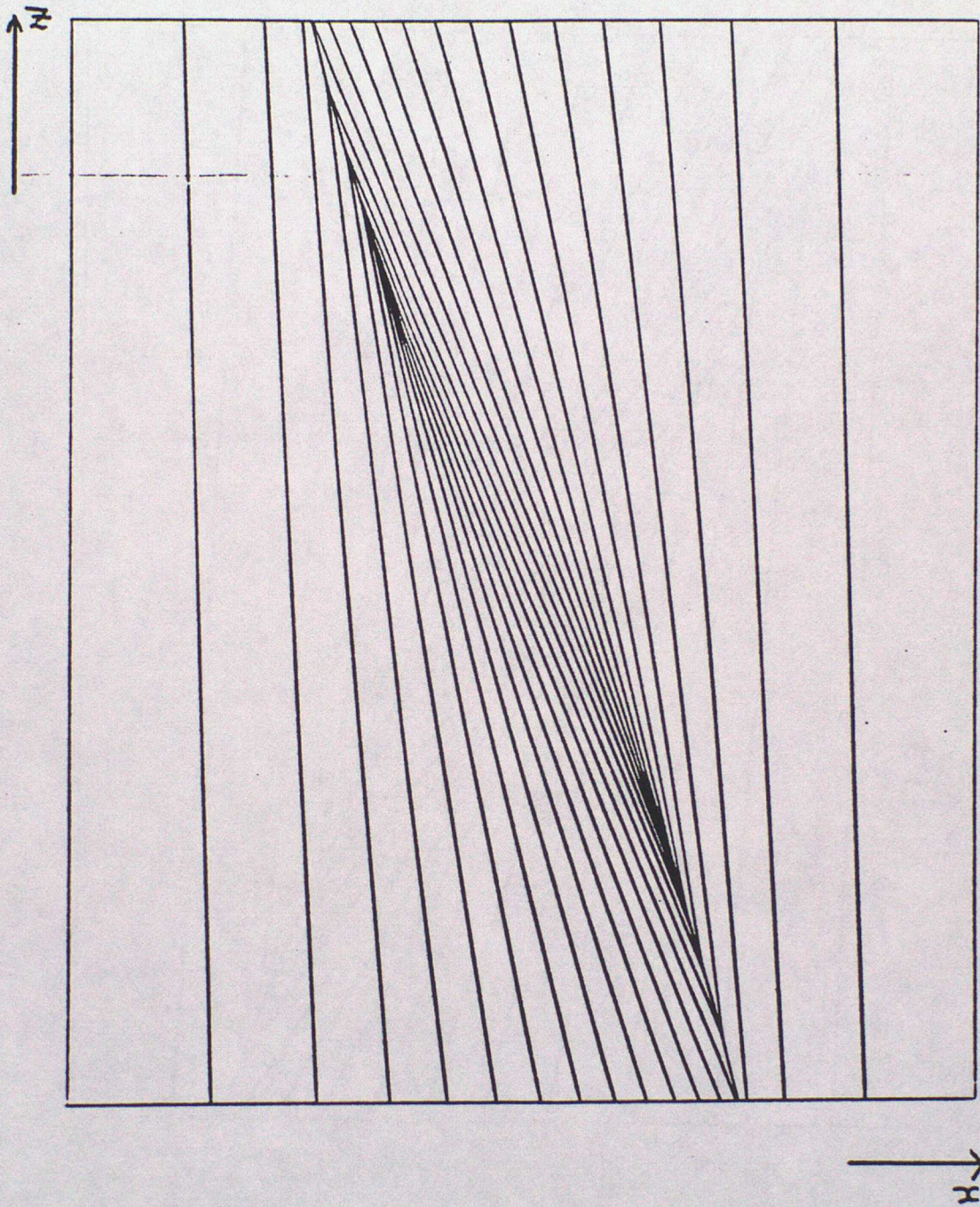
Fig. 4 (a)



Time = 0 Secs.



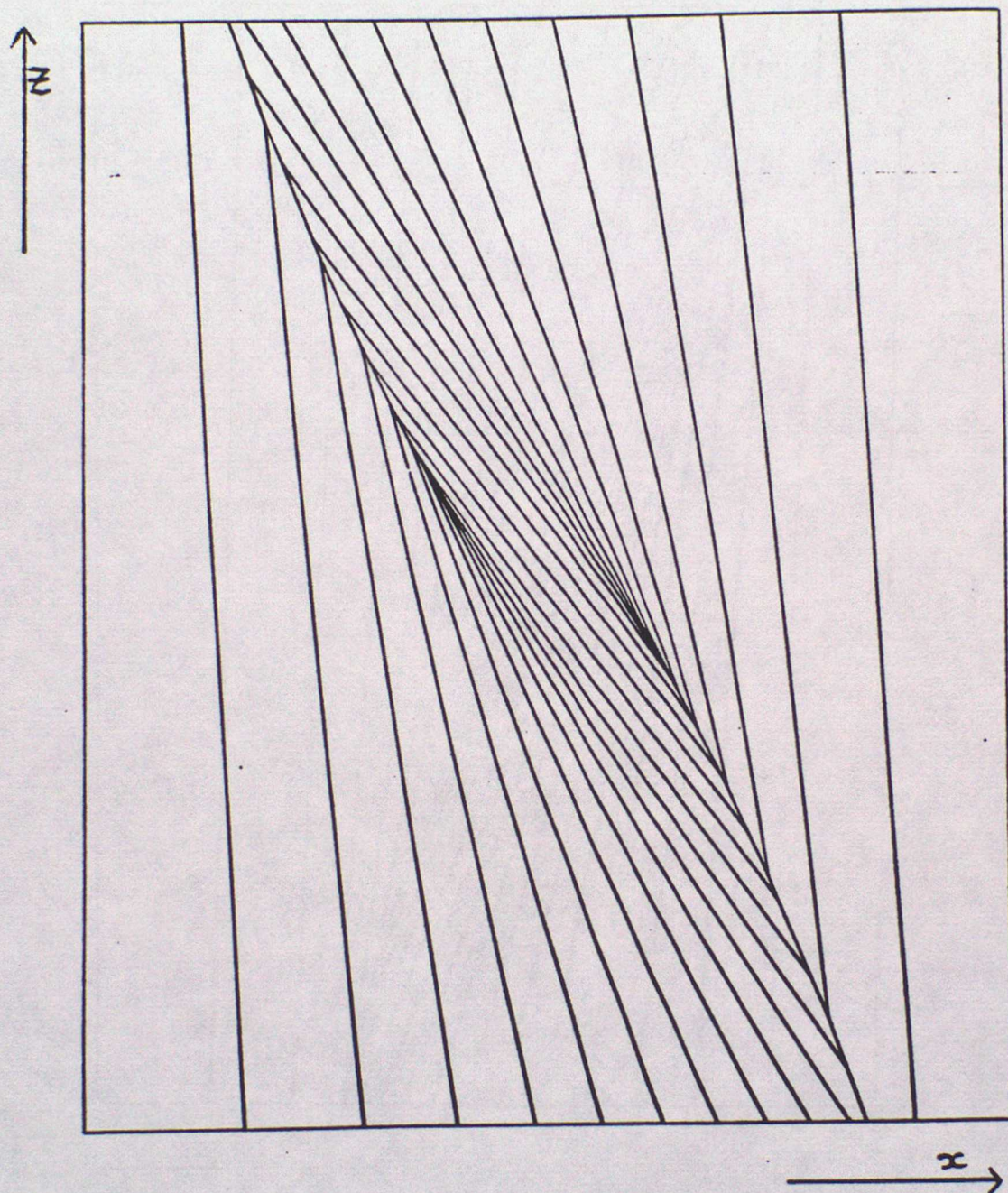
Fig. 4(b)



Time = 20,000 SECS.



Fig. 4 (c)



Time = 50,000 SECS.



Fig. 5(a)

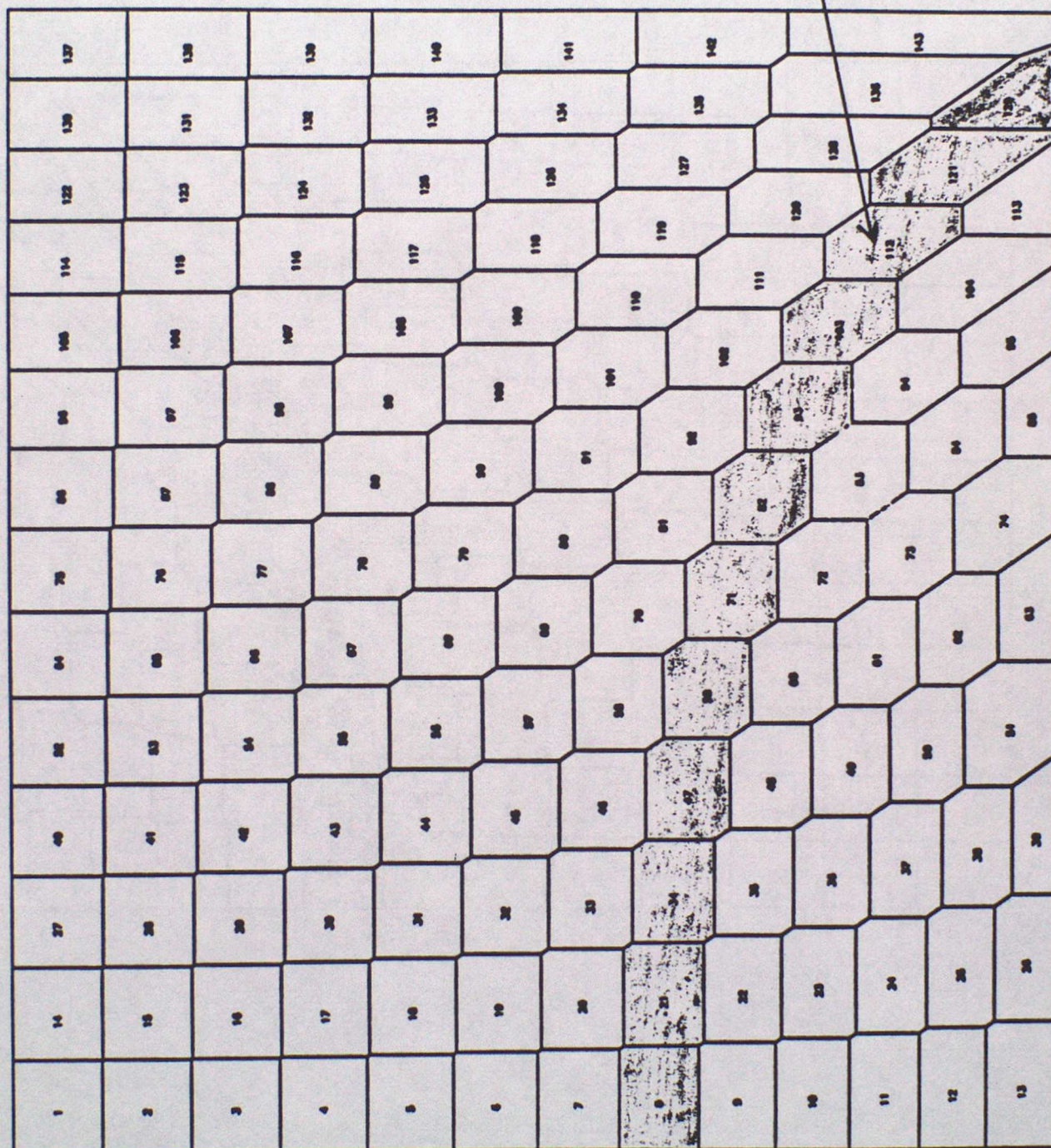
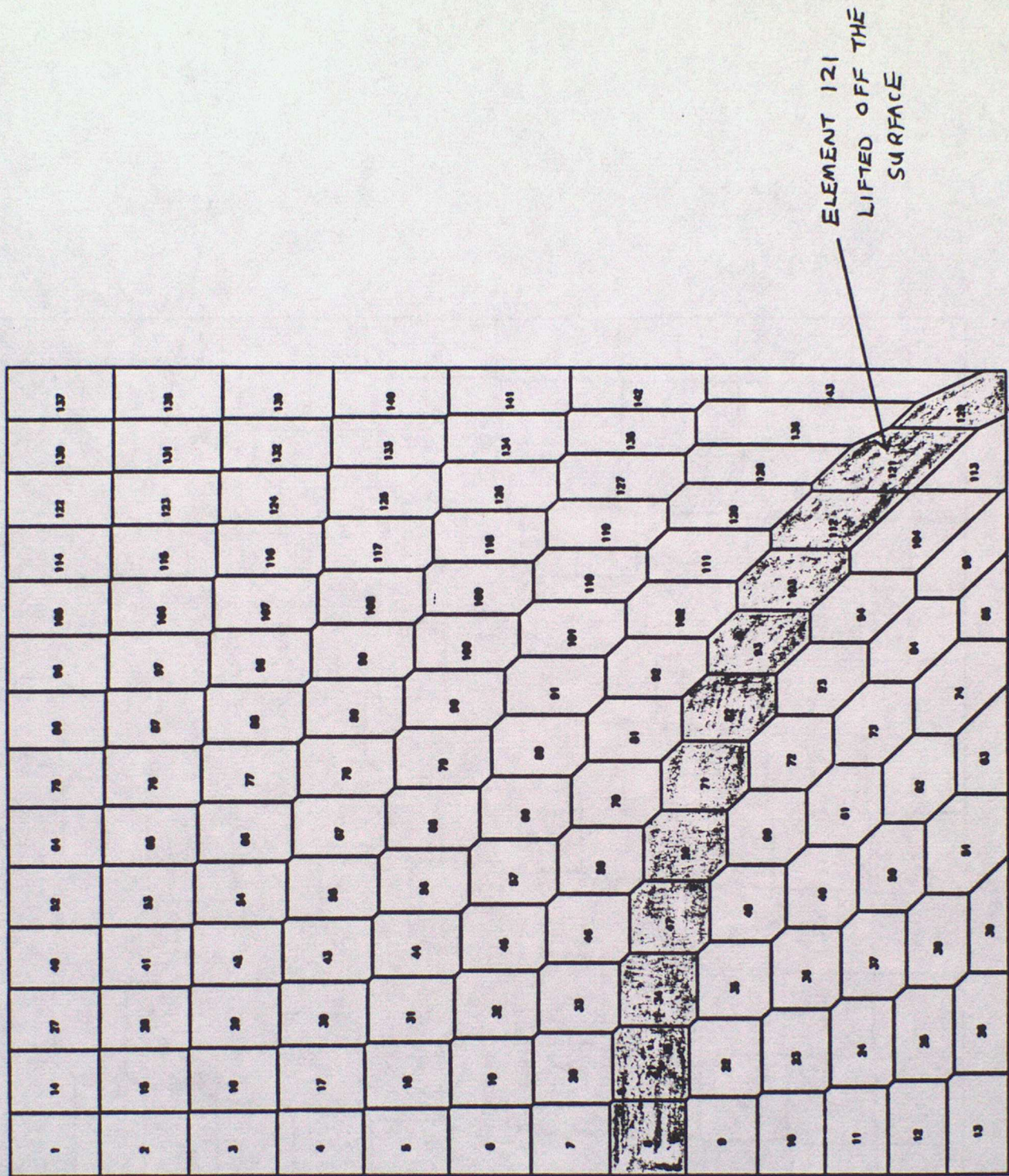




Fig. 5 (b)





## Lecture 5 - Flow over mountains

### (a) Non-rotating, non-hydrostatic flow

There is a vast literature on the influence of orography on atmospheric flow. A comprehensive review has been written by Smith (1979) and is highly recommended additional reading for this course. An excellent summary of mountain wave flow solutions is also given in Gill (1982) whose notation we shall follow.

Consider firstly the linearised equations of motion for incompressible, nonrotating stratified flow given in Table 8.1 of Gill (1982) pg 261:

$$\frac{\partial^2}{\partial t^2} \left( \frac{\partial^2 w}{\partial x^2} + \frac{\partial^2 w}{\partial y^2} + \frac{\partial^2 w}{\partial z^2} \right) + N^2 \left( \frac{\partial^2 w}{\partial x^2} + \frac{\partial^2 w}{\partial y^2} \right) = 0 \quad (1)$$

where  $w$  is the vertical velocity and  $N$  the Brunt-Vaisala frequency. If the steady two-dimensional response to orography of a uniform airstream with speed  $U$  is sought, then set  $\frac{\partial}{\partial y} \equiv 0$  and  $\frac{\partial}{\partial t} = U \frac{\partial}{\partial x}$  so that:

$$U^2 \frac{\partial^2}{\partial x^2} \left( \frac{\partial^2 w}{\partial x^2} + \frac{\partial^2 w}{\partial z^2} \right) + N^2 \frac{\partial^2 w}{\partial x^2} = 0 \quad (2)$$

Sinusoidal solutions of general form  $\exp[i(kx + \gamma z)]$  satisfy Eq (2) subject to the dispersion relation:

$$-(k^2 + \gamma^2) + \frac{N^2}{U^2} = 0$$

or

$$\gamma^2 = \left( \frac{N}{U} \right)^2 - k^2 \quad (3)$$



Suppose that  $R > \frac{N}{U}$  implying that  $\gamma = \pm i|\gamma|$ , then solutions periodic in  $x$  are of the form:

$$w = \text{Real} \left\{ e^{ikx} (A e^{-|\gamma|z} + B e^{|\gamma|z}) \right\}.$$

If the fluid is unbounded above and forced by sinusoidal orography with elevation  $h(x)$  given by:

$$h = h_m \sin kx$$

then  $B = 0$  (finite energy condition) and  $A$  is determined by the condition:

$$w|_{z=0} = U \frac{\partial h}{\partial x} = U k h_m \cos kx \quad (4)$$

so that:

$$A = U k h_m.$$

The vertical velocity field is therefore given by:

$$w = U k h_m \exp[-|\gamma|z] \cos kx \quad (5)$$

where  $|\gamma| = [k^2 - (\frac{N}{U})^2]^{1/2}$  and takes the form of sinusoidal wave field decaying with height without phase tilt. As  $k \rightarrow \infty$  (short horizontal wavelengths) the solution represented by Eq (5) tends to the potential flow solution  $e^{-kz} \cos kx$ . Note that the vertical displacement of material surfaces  $\eta$  is given in linear theory by:



$$w = U \frac{\partial \eta}{\partial x}$$

and so:  $\eta(x, z) = h_m \sin kx \exp[-|v|z]$

Substituting eq (5) into the continuity equation:

$$\frac{\partial u}{\partial x} + \frac{\partial w}{\partial z} = 0$$

for  $w$  implies that:

$$u = U \left( 1 + h_m |v| \exp[-|v|z] \sin kx \right)$$

showing that the cross-ridge flow at the mountain top is greater than the undisturbed flow by the factor  $(1 + h_m |v|)$ .

This type of evanescent response occurs when:

$$k > \frac{N}{U} \quad \text{or} \quad L_x < \frac{2\pi U}{N} = L_N$$

where  $L_x$  is the horizontal wavelength. (Taking  $U \sim 10 \text{ ms}^{-1}$  and  $N \sim 10^{-2} \text{ s}^{-1}$  suggests that  $L_x \leq 6 \text{ km}$ ). In reality the flow response at such small scales will be complicated by boundary layer processes and the model should not be regarded as accurate.

If  $k < \frac{N}{U}$  then the vertical wavenumber  $v$  is real and solutions will be of the general form:

$$w = \text{Real} \left\{ A e^{i(kx + vz)} + B e^{i(kx - vz)} \right\} \quad (6)$$



As before, eq (4) can be used as a lower boundary condition but now the finite energy condition does not suffice to eliminate one of the solution modes. Since disturbance energy may be transmitted in this parameter range we must decide what is the appropriate upper boundary condition.

If the atmosphere had a 'lid' at some height then one might expect energy to be reflected and a sort of standing wave set up. Of course there are no naturally occurring lids - not even the tropopause which only acts as a lid for amplifying baroclinic waves. If  $N$  or  $U$  vary with respect to height in such a way that  $v^2$  becomes negative above a certain height then wave energy will be trapped below this level. In a compressible atmosphere disturbances will amplify with height due to the 'whiplash effect' and eventually attain a critical amplitude above which they become dynamically unstable. Wave energy may be partially reflected in this process though in general it is safe to assume that all the energy would be dissipated in a manner analogous to surface waves breaking in gently shoaling coastal waters.

We require, therefore, a boundary condition that will select a solution with pure upward energy radiation. This may be obtained from the sense of the group velocity associated with waves of the form  $\exp i(kx + \gamma z - \sigma t)$  where  $\sigma$  is the angular frequency. The dispersion relation for such travelling waves is given by eq (3) but with  $U$  replaced with  $U - \frac{\sigma}{k}$  ie

$$\gamma^2 = \frac{N^2 k^2}{(kU - \sigma)^2} - k^2$$

or



$$(kU - \sigma)^2 = \frac{N^2 k^2}{\gamma^2 + k^2} \quad - \quad (7)$$

The vertical component of the group velocity vector  $C_{gz}$  is given by:

$$C_{gz} = \frac{\partial \sigma}{\partial \gamma} = \frac{(kU - \sigma)\gamma}{\gamma^2 + k^2} \quad \text{using eq (7)}$$

For stationary waves ( $\sigma = 0$ ) and the group velocity is upward if  $\gamma > 0$  and so  $B$  must be set equal to zero in eq (6). In other words, waves which tilt upstream with height have upward energy propagation as in the case of stationary planetary waves in westerly flow (Lecture 1). The full solution for uniform flow over sinusoidal orography when  $\kappa < N/U$  is easily seen to be:

$$w = U k h_m \cos(kx + \gamma z) \quad (8)$$

and using the continuity equation the horizontal flow speed is given by:

$$u = U \left( 1 - \gamma h_m \cos(kx + \gamma z) \right) \quad (9)$$

In this case the 'mountain top' wind speed,  $u(kx = \frac{\pi}{2}, z = 0)$  is equal to  $U$  and the wind speed maximum occurs on the lee-side of the orographic peaks.

The horizontally-averaged momentum flux  $\overline{uw}$  obtained from eqs (8) and (9) is easily shown to be:



$$\overline{uw} = -\frac{1}{2} U^2 k \lambda h_m^2$$

which for hydrostatic waves with  $\kappa^2 \ll \nu^2$  simplifies to:

$$\overline{uw} = -\frac{1}{2} U k N h_m^2 \quad (10)$$

The pressure perturbation can be obtained from the x-component of the linearised momentum equation ie

$$\rho_0 U \frac{\partial u'}{\partial x} + \frac{\partial p'}{\partial x} = 0 \quad (\rho_0(z) \text{ is the basic state density})$$

which for sinusoidal perturbations integrates to give:

$$p' = -\rho_0 U u' \quad (11)$$

The pressure drag (D) on the orography (per wavelength) is given by:

$$D = \int_0^{2\pi/k} p'(x, h) \frac{\partial h}{\partial x} dx$$

and may be linearized to:

$$D = \int_0^{2\pi/k} p'(x, 0) \frac{\partial h}{\partial x} dx$$

Using eqs (4) and (11), this can be re-expressed as:



$$D = \int_0^{2\pi/k} -\rho_0 [u w]_{z=0} d\alpha$$

so that the drag force per unit length  $Dk/2\pi$  is given by:

$$\frac{Dk}{2\pi} = -\rho_0 \overline{u w}$$

It can be seen that the upward energy radiating gravity wave represented by eq (8) is consistent with momentum transfer from atmosphere to 'earth' through the action of pressure forces on the orography. Since  $\rho_0 \overline{u w}$  is height-independent, the flow is not apparently decelerated anywhere! Of course in the real atmosphere  $\rho_0 \overline{u w}$  cannot be independent of height as  $z \rightarrow \infty$  and waves frequently 'break' in the lower stratosphere. Fig. 1 shows the vertical momentum flux  $\rho_0 \overline{u w}$  measured from aircraft flying over the Rocky mountains on 17th February 1970, (Lilly and Kennedy, 1973). The momentum flux is (relatively) height-independent up to 15 km above which it rapidly falls to zero in a highly turbulent layer. Effectively, the drag force exerted by the orography on the atmosphere is communicated via the wave system to the lower stratosphere where the flow is strongly decelerated.

(b) Rotating, hydrostatic flow

The linearised w-equation for hydrostatic flow at scales large enough for rotation to be important is:

$$\left( \frac{\partial^2}{\partial t^2} + f^2 \right) \frac{\partial^2 w}{\partial z^2} + N^2 \left( \frac{\partial^2 w}{\partial x^2} + \frac{\partial^2 w}{\partial y^2} \right) = 0 \quad (12)$$



for a basic state atmosphere at rest, (see Table 8.1 of Gill (1982)). For an atmosphere with basic flow  $U$  replace  $\frac{\partial}{\partial t}$  by  $\frac{\partial}{\partial t} + U \frac{\partial}{\partial x}$ . The dispersion relation corresponding to eq (7) is then given by:

$$\left. \begin{aligned} &[(Uk - \sigma)^2 - f^2] \gamma^2 = N^2 k^2 \\ \text{or } &\gamma = \frac{Nk}{[(Uk - \sigma)^2 - f^2]^{1/2}} \end{aligned} \right\} \quad (13)$$

Energy radiating solutions are now only possible if:

$$|Uk - \sigma| > f$$

or for stationary waves  $k > \frac{f}{U}$ . We can define a critical wavelength  $L_f = \frac{2\pi U}{f}$  such that  $L_x < L_f$  for radiation of inertia-gravity waves. Taking  $U = 10 \text{ ms}^{-1}$  and  $f = 10^{-4} \text{ s}^{-1}$  gives  $L_f \sim 600 \text{ km}$  and so if sinusoidal orography is to generate radiating inertia-gravity waves:

$$L_N < L_x < L_f$$

which, for a  $10 \text{ ms}^{-1}$  wind, means that:

$$6 \text{ km} \lesssim L_x \lesssim 600 \text{ km}.$$



Note that the boundary between radiating and evanescent solutions at  $L_x = L_f$  corresponds to the Rossby number  $R_o = \frac{Uk}{f} = 1$ . As  $R_o \rightarrow 0$  this evanescent inertial-gravity wave response tends to the non-radiating, quasi-geostrophic  $f$ -plane response with  $w$ -equation:

$$f^2 \frac{\partial^2 w}{\partial z^2} + N^2 \left( \frac{\partial^2 w}{\partial x^2} + \frac{\partial^2 w}{\partial y^2} \right) = 0 \quad (\text{cf eq (12)}) \quad (14)$$

In this case the flow response to sinusoidal orography can readily be seen to be:

$$w = Uk h_m \exp \left[ -\frac{Nkz}{f} \right] \cos kx$$

which is identical to the potential flow solution of very large  $k$  when the vertical co-ordinate is stretched by the factor  $\frac{N}{f}$ .

So far we have only considered flow over sinusoidal orography though by expressing the response as a Fourier transform we may obtain the solution for flow over any orographic profile. An isolated hill is made up of a continuous spectrum of wavelengths some of which will propagate others which will not. Figs 2(a) and (b) show some standard solutions for flow ( $U = 10 \text{ ms}^{-1}$ ,  $N = 10^{-2} \text{ s}^{-1}$ ) over a two-dimensional ridge of bell-shaped cross-section ie

$$h(x) = \frac{h_m}{1 + (x/a)^2}$$



where  $a$  is the half width. The Swiss Alps have a half width of about 50 km. Notice that even when  $a = 100$  km there is considerable wave radiation with wavelengths  $\sim 300$  km. The diagram below Fig. 2(b) shows the meridional displacement of trajectories based on  $h_m = 1$  km.

(c) Semi-geostrophic solutions

The quasi-geostrophic  $w$ -equation may be written as:

$$\frac{f^2}{N^2} \frac{\partial^2 \theta}{\partial z^2} + \frac{\partial^2 \theta}{\partial x^2} = 0 \quad (15)$$

for the two-dimensional case since the thermodynamic equation relates  $w$  and  $\theta$  through:

$$U \frac{\partial}{\partial x} (\theta / \theta_0) + w \frac{N^2}{g} = 0$$

It can be shown (Hoskins and Bretherton, 1972 Eq 3.47) that the equivalent equation underlying uniform semi-geostrophic flow is:

$$\frac{f^2}{N^2} \frac{\partial^2 \theta}{\partial Z^2} + \frac{\partial^2 \theta}{\partial X^2} = 0 \quad (16)$$

where  $X = M/f = x + v_g/f$  (see Lecture 4) and  $Z = z$  so that  $\frac{\partial}{\partial Z} = \frac{\partial}{\partial z}$  holding  $X$  constant. Stretching the  $z$  coordinate by the factor  $N/f$  reduces eq (16) to Laplace's equation which admits simple solutions of the type found in the theory of potential flow around isolated obstacles. In these solutions  $\theta$  is required to be constant on the surface of the orography. No linearization of the lower boundary condition is required



and the geostrophic momentum co-ordinate transformation  $(x, z) \rightarrow (X, Z)$  has allowed ageostrophic advection (a non-linear process) to be represented even though the governing equations are linear.

Figs. 3(a) and (b) show the  $\theta$  and  $v_g$  contours respectively for flow over an elliptical mountain whose major axis is twice as long as its minor axis in the space  $(x, Nz/f)$ . As in the evanescent solutions discussed earlier, the flow component across the mountain is stronger than the basic flow over the summit in association with the squeezing together of isentropic surfaces. If the basic flow is westerly then a southerly develops ahead of the ridge and a northerly on the lee-side. When the ridge has semi-circular cross-section in  $(x, Nz/f)$  space, the squeezing together of isentropic surfaces above the mountain summit becomes intense and it can be shown that  $u, \frac{\partial \theta}{\partial z} \rightarrow \infty$  actually at the summit, (Fig. 4(a)). It can also be shown that the absolute vorticity measured on the mountain surface  $(f + \frac{\partial v_g}{\partial x})|_{z=h}$  is zero with strong along-ridge jets at the foot of the ridge, (Fig. 4(b)). For mountains of aspect ratio  $\geq \frac{f}{N}$  the geostrophic momentum co-ordinate transformation breaks down, as the mountain is unable to sustain an isentropic surface (NB isentropic mountains are cold). Semi-geostrophic solutions can, however, be constructed by the element method mentioned in lecture 4. In these, the mountain top is potentially warmer than its lower slopes if there is no cross-mountain flow).

Finally, we show some semi-geostrophic solutions for flow over a rectangular block mountain which could not be obtained using the geostrophic momentum co-ordinate transformation. Fig. 5(a) shows a triangular wedge of cold air with uniform potential temperature  $\theta_0 - \Delta\theta$  supported by a rectangular block mountain and in geostrophic and



hydrostatic balance. The atmosphere above is effectively infinite and of uniform  $\theta_0$  so that the cold air interface is essentially a Margules front. Each of the elements characterizing the wedge has a uniform absolute momentum  $M_i$  which satisfies the semi-geostrophic evolution equation:

$$\frac{dM_i}{dt} = fU$$

where  $U$  is a basic state geostrophic wind directed across the mountain ridge and affecting all of the fluid. Therefore each element has an absolute momentum known for all time and given by:

$$M_i(t) = M_i(t=0) + fUt$$

$v_g$  in the environment atmosphere above can be shown to be zero for all time and so the absolute momentum there will equal  $fx$ . Margules' formula for the slope of the cold air interface then reads:

$$\frac{dz}{dx} = \frac{f[M_i(t) - fx]}{g \Delta\theta/\theta_0} \quad (\text{see Lecture 4}) \quad (17)$$

Area conservation of elements together with eq (17) uniquely determines a sequence of equilibrium configurations. Fig. 5(b) and (c) show the cold air geometry at later times.  $\frac{dz}{dx}$  increases because the  $x$  position of each element is not free to increase due to the blocking influence of the mountain. Eventually (Fig. 5(c)) the cold air reaches the mountain top and the area conservation requirement of the element next to the mountain must be relaxed to allow it to cross over. The cold air which has crossed the mountain then piles up as a dome downstream, (Figs. 5(d) and (e) (for full



details see Shutts (1986)). The different pressure forces exerted on the mountain from the windward and lee-sides due to the different weights of cold air imply a net drag force. Unlike the analytic solutions discussed earlier the mountain surface is never isentropic in this model. Cold air released from the mountain top instantaneously jumps to a new equilibrium position downstream corresponding in reality to a strong downslope current/weir. In practice, air tends to go around mountain ridges of finite length since large values of  $v_g$  develop immediately upstream.

(d) Mountain drag

The ability of orography to extract momentum from atmospheric flow through pressure forces is arguably its most important influence on the general circulation. Palmer et al (1986) have made a case for the parametrization of gravity wave drag in numerical weather prediction models based on observational momentum budget studies and the nature of systematic errors. Back-of-the-envelope calculations using linear theory suggest that the drag on orography with length scales between 20 and 150 km should be comparable with surface frictional stress.

For example the surface stress  $\tau_s$  based on eq (10) is given by:

$$\tau_s = \frac{1}{2} \rho_s U \kappa N h_m^2$$

where  $\rho_s$  is the surface density. If we take  $\frac{1}{2} h_m^2$  to be equivalent to the mean (over land) sub-grid scale orographic variance of the current operational coarse mesh model ( $\sim (200 \text{ m})^2$ ),  $\kappa = 2\pi/60 \text{ km}$ ,  $\rho_s = 1 \text{ kg m}^{-3}$ ,  $U = 5 \text{ ms}^{-1}$  and  $N = 10^{-2} \text{ s}^{-1}$  then:



$$\tau_s \approx 0.2 \text{ Nm}^{-2}$$

compared to a 'typical' surface frictional stress  $\sim 0.1 \text{ Nm}^{-2}$ . At larger horizontal length scales rotation becomes important and tends to suppress wave radiation or at least reduce the group velocity of the associated wave system. Inviscid quasi-geostrophic theory gives no drag for synoptic scale mountains on an f-plane, however semi-geostrophic theory gives 'weir-like' solutions for steep barrier orography.

The net pressure force acting on the rectangular block in Fig. 5(e) is given by:

$$D = \int_0^{h_m} \Delta p \, dz = \frac{1}{2} \rho_0 g \frac{\Delta \theta}{\theta_0} h_m^2 \quad (18)$$

since the pressure difference  $\Delta p$  across the block is given by:

$\Delta p = \rho_0 g \frac{\Delta \theta}{\theta_0} h_m \left(1 - \frac{z}{h_m}\right)$ , ( $\rho_0$  is a constant basic state density). Using  $\rho_0 = 1 \text{ kg m}^{-3}$ ,  $g = 10 \text{ ms}^{-2}$ ,  $\Delta \theta = 5^\circ \text{K}$ ,  $\theta_0 = 300^\circ \text{K}$  and  $h_m = 2 \text{ km}$  then eq (18) gives:

$$D = 3.4 \times 10^5 \text{ Nm}^{-1}$$

or a drag of  $3.4 \text{ Nm}^{-2}$  acting over 100 km! Notice that the net drag force is independent of  $U$ .



It is well known that comparably large forces act on the Swiss Alps during certain synoptic periods, (Davies and Phillips, 1985). The influence of such forces on synoptic evolution must be very powerful and there can be no doubt that current numerical weather prediction models have difficulty resolving such effects.



## References

- Davies, H C and Phillips, P D (1985) 'Mountain drag along the Gotthard Section during ALPEX'.  
J. Atmos. Sci., 42, 2093-2109.
- Gill, A E (1982) 'Atmosphere-Ocean Dynamics'.  
Academic Press.
- Hoskins, B J and (1972) 'Atmospheric frontogenesis models:  
Bretherton, F P Mathematical formulation and  
solution'.  
J. Atmos. Sci., 29, 11-37.
- Lilly, D K and Kennedy, P J (1973) Observations of a stationary  
mountain wave and its associated  
momentum flux and energy  
dissipation'.  
J. Atmos. Sci., 30, 1135-1152.
- Palmer, T N, Shutts, G J and (1986) 'Alleviation of a systematic  
Swinbank, R westerly bias in general  
circulation and numerical weather  
prediction models through an  
orographic gravity wave drag  
parametrization'.  
Quart. J. Roy. Met. Soc. (October).
- Shutts, G J (1986) 'The semi-geostrophic weir'.  
Met O 11 Technical Note No. 237.
- Smith, R B (1979) 'The influence of mountains on the  
atmosphere'.  
'Adv. in Geophys.', 21, 87-230.



### Legends

- Fig. 1 Mean observed profile of momentum flux over the Rocky mountains on 17th February 1970 as measured from aircraft (from Lilly and Kennedy, 1973).
- Fig. 2 Steady response of airstream of uniform speed as it passes over a two-dimensional ridge of bell-shaped cross-section. Figs. 2(a) and (b) correspond to mountain half-widths of 10 and 100 kms respectively. For further details, see Gill (1982).
- Fig. 3 Uniform potential vorticity solution for semi-geostrophic flow over a two-dimensional ridge with elliptical cross-section in  $(x, Nz/f)$  space.
- (a) Potential temperature field.
  - (b) Along-ridge wind, positive is into the picture.
- Fig. 4 (a)-(b) same as for Figs. 3(a) and (b) except for a ridge with semi-circular cross-section in  $(x, Nz/f)$  space).
- Fig. 5 (a)-(e) Five stages in the passage of a cold fluid across a rectangular block mountain.



Fig. 1

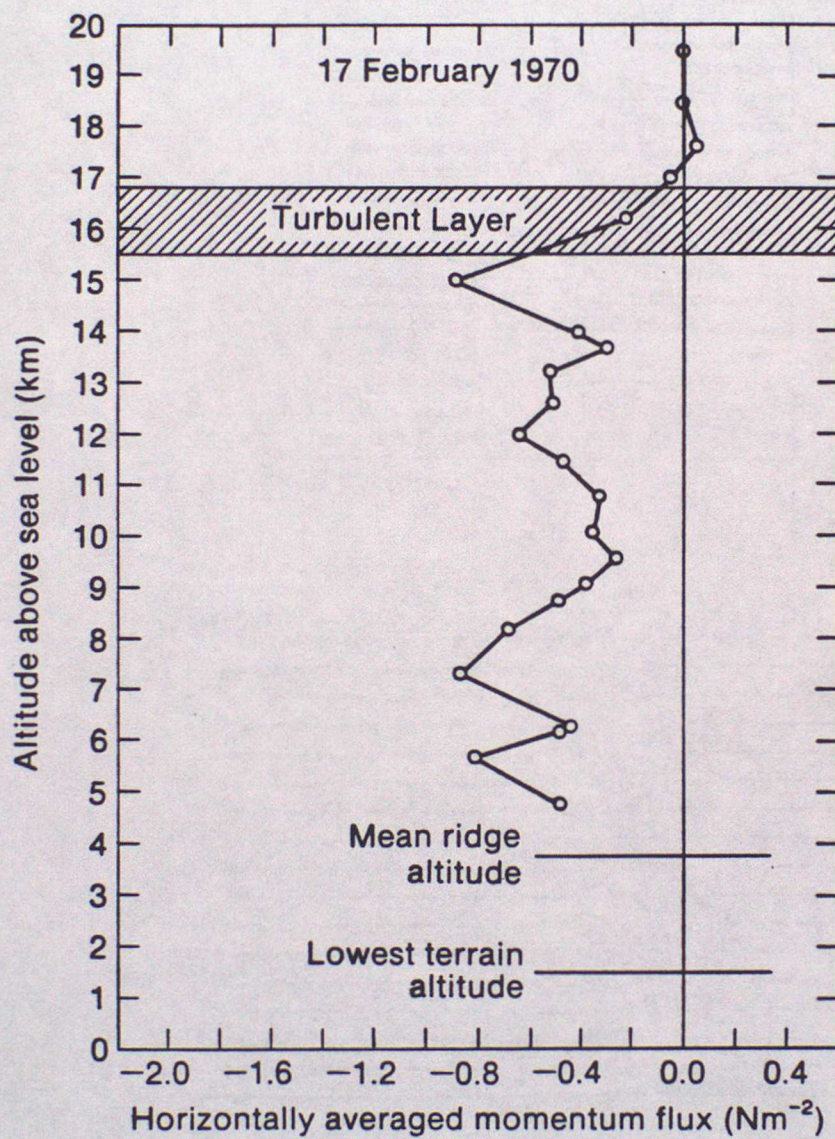




Fig. 2

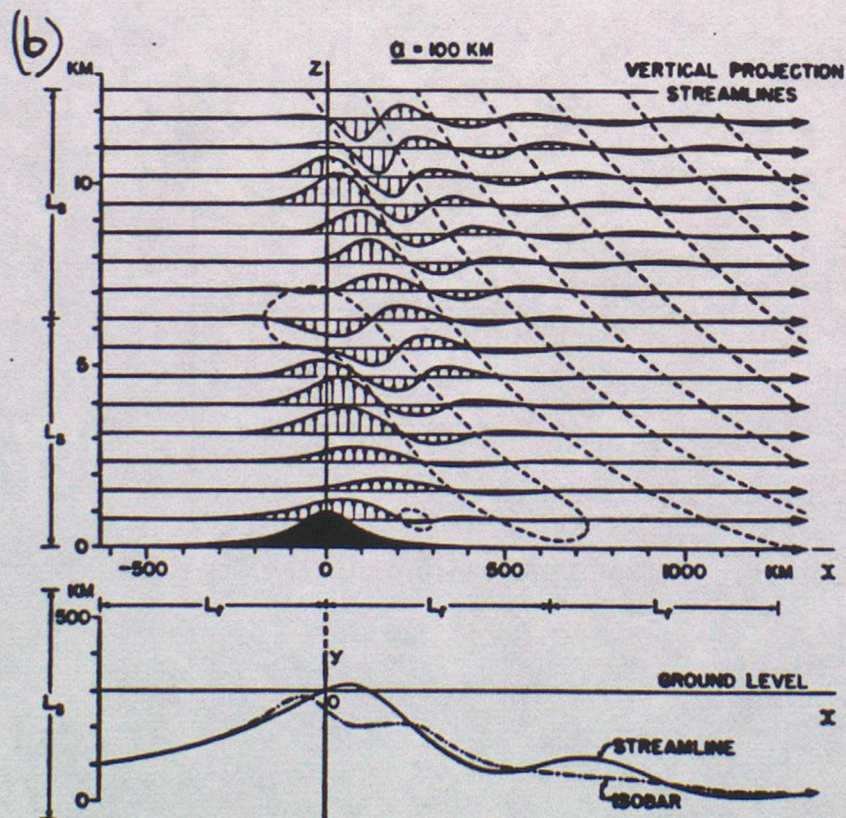
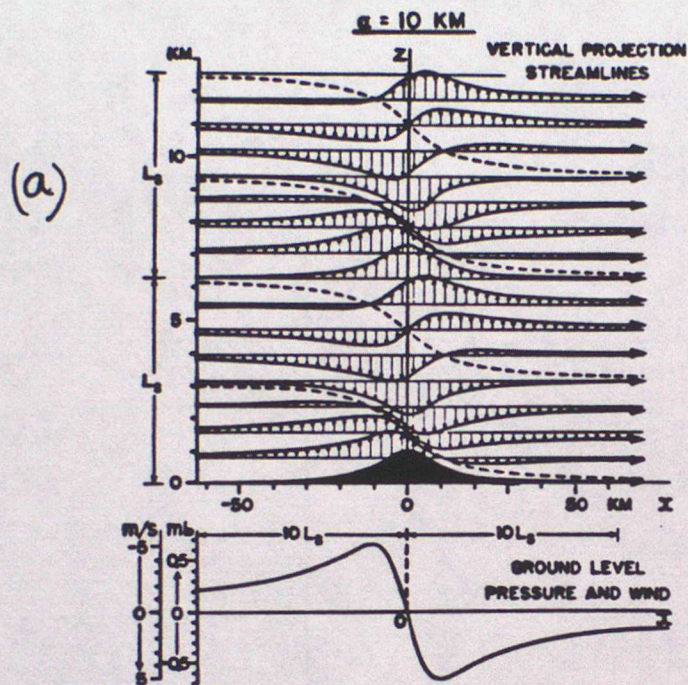




Fig. 3(a)

$\theta$





Fig. 3(b)

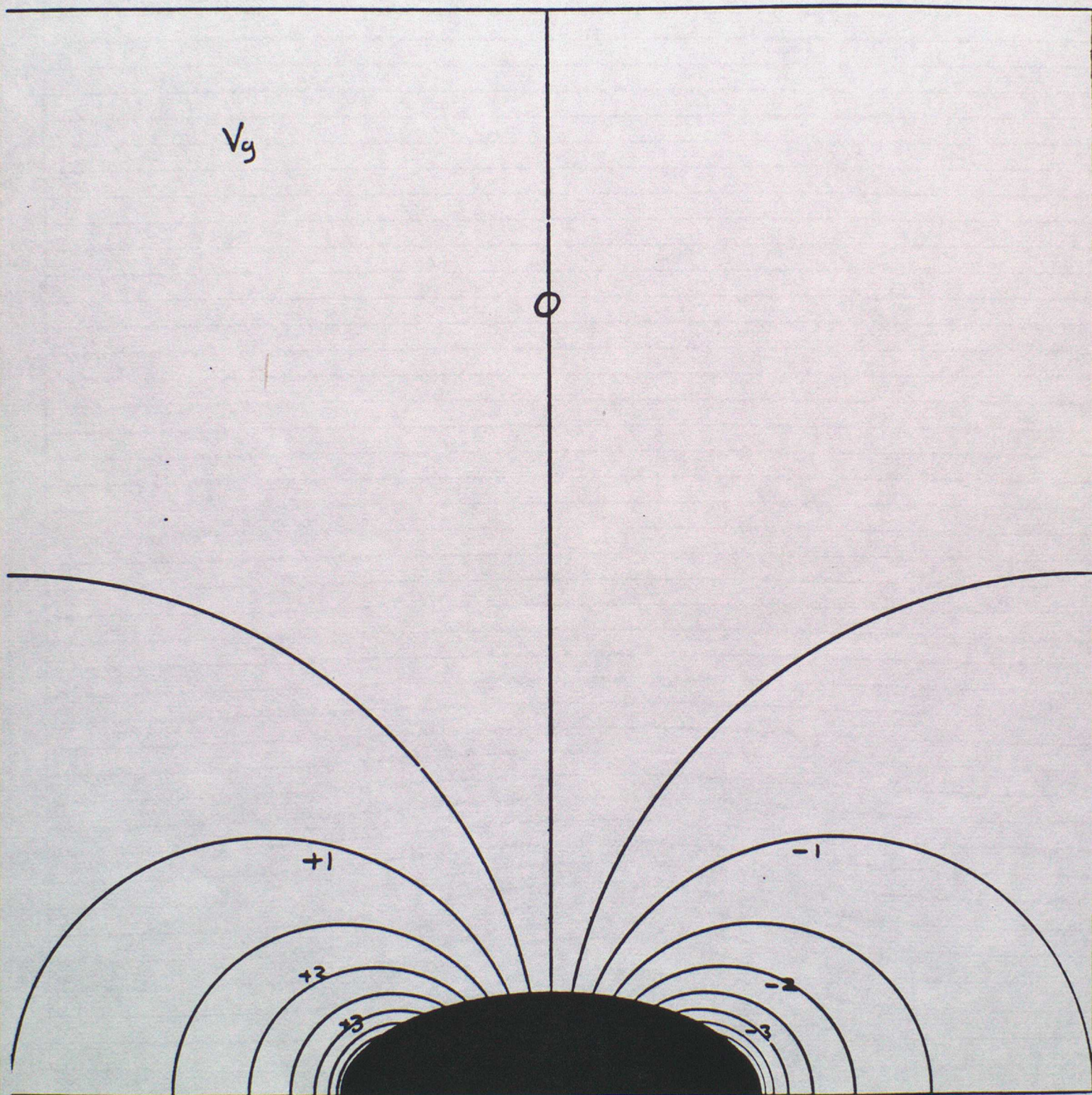




Fig. 4 (a)

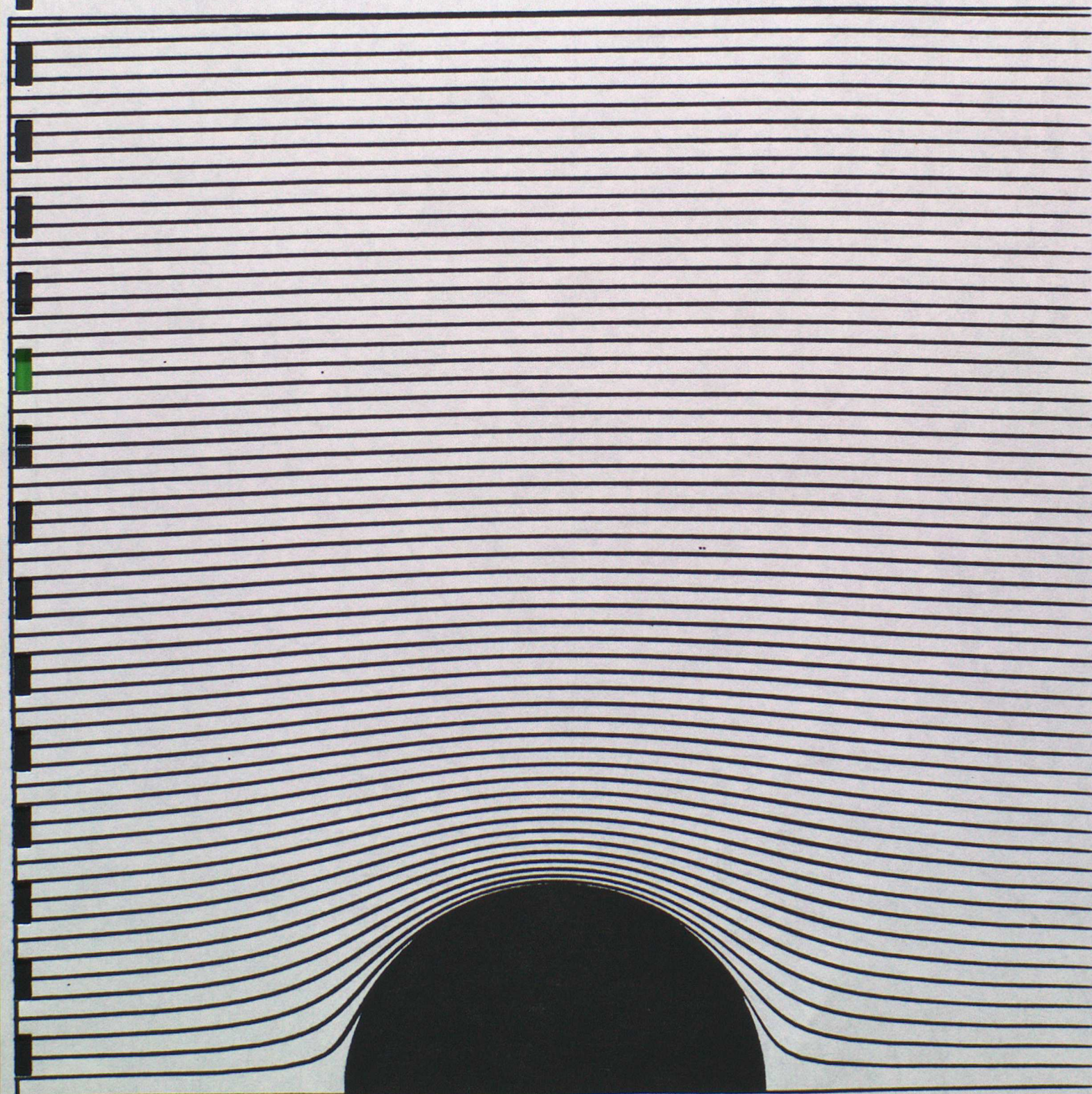




Fig. 4(b)

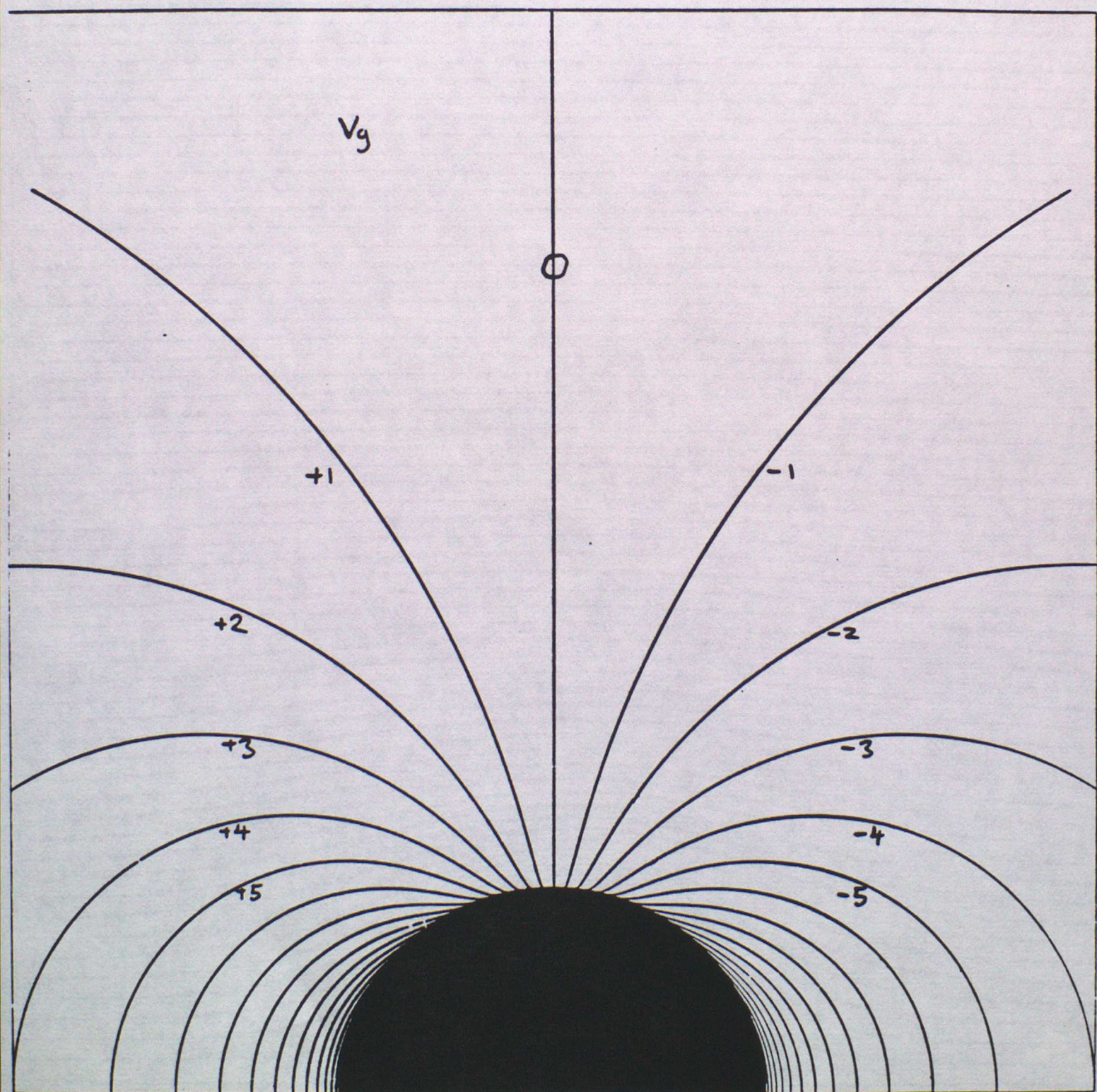




Fig. 5 (a)

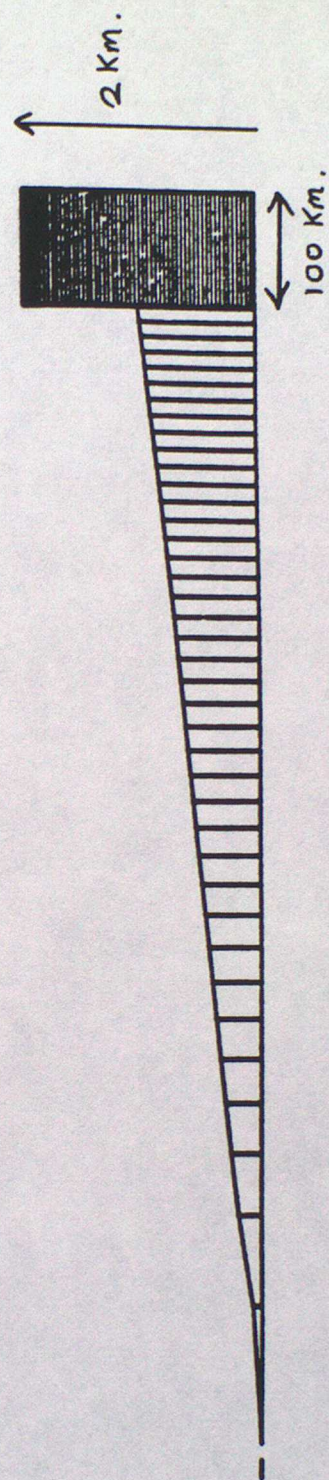




Fig. 5(b)

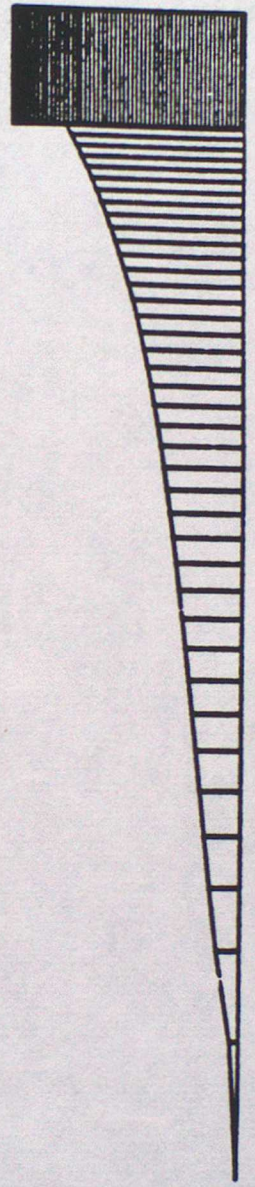




Fig. 5 (c)

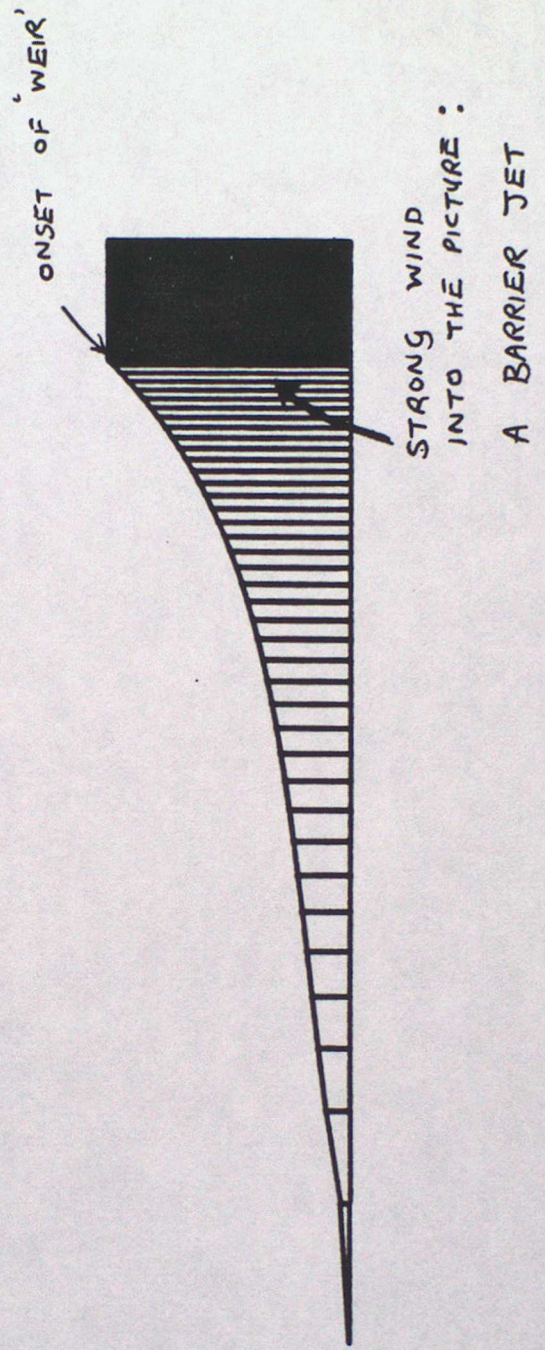




Fig. 5(d)

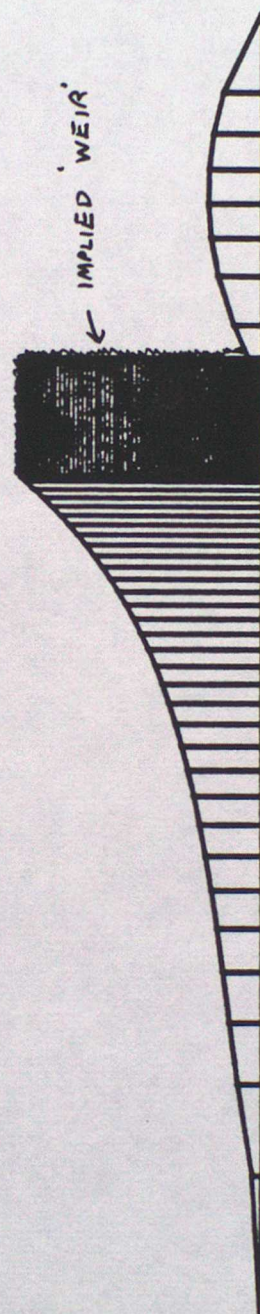




Fig. 5(e)

